



CANADIAN ASSOCIATION
OF PETROLEUM PRODUCERS

Canada's Oil and Natural Gas Producers

GUIDE

Influence of High Voltage DC Power Lines on Metallic Pipelines

October 2014

2014-0034

The Canadian Association of Petroleum Producers (CAPP) represents companies, large and small, that explore for, develop and produce natural gas and crude oil throughout Canada. CAPP's member companies produce about 90 per cent of Canada's natural gas and crude oil. CAPP's associate members provide a wide range of services that support the upstream crude oil and natural gas industry. Together CAPP's members and associate members are an important part of a national industry with revenues of about \$110 billion a year. CAPP's mission, on behalf of the Canadian upstream oil and gas industry, is to advocate for and enable economic competitiveness and safe, environmentally and socially responsible performance. Competitiveness, in North America and globally, is necessary so as to attract the capital necessary to grow production and expand markets to deliver value to the Canadian public and to our investors, Social License, from governments, Aboriginal peoples, the public, stakeholders and the communities in which we operate, will be determined by our collective performance and the effectiveness of our communication outreach.

Disclaimer

This publication was prepared for the Canadian Association of Petroleum Producers (CAPP) by HVDC Transmission Line Task Group composed of representatives from Pipeline, Telecommunications and Electrical Utilities operating in Alberta. While it is believed that the information contained herein is reliable under the conditions and subject to the limitations set out, CAPP and the HVDC Transmission Line Task Group do not guarantee its accuracy. The use of this report or any information contained will be at the user's sole risk, regardless of any fault or negligence of HVDC Transmission Line Task Group, CAPP or its co-funders.

2100, 350 – 7 Avenue S.W.
Calgary, Alberta
Canada T2P 3N9
Tel 403-267-1100
Fax 403-261-4622

1000, 275 Slater Street
Ottawa, Ontario
Canada K1P 5H9
Tel 613-288-2126
Fax 613- 236-4280

403, 235 Water Street
St. John's, Newfoundland and Labrador
Canada A1C 1B6
Tel 709-724-4200
Fax 709-724-4225

310, 1321 Blanshard Street
Victoria, British Columbia
Canada V8W 0B5
Tel 778-410-5000
Fax 778-410-5001

Overview

This guide provides members with a comprehensive resource to assist you in evaluating the electromagnetic influence on your pipelines presented by an adjacent HVDC power line. The guide introduces the operating principles of the HVDC system, contrasts it with AC system behaviors and introduces a screening guideline for gauging impact upon pipeline facilities.

Note 1: This version of the guideline applies ONLY to the two new HVDC transmission line projects in Alberta (ATCO Electric (EATL), and AltaLink (WATL)). Use in other situations, configurations, or projects is outside of the scope of this guideline.

Additional guidance and support for the use of this guideline by pipeline owners and their consultants is available from AltaLink and ATCO Electric, see below:

1. ATCO Electric – Shan Jiang, (780) 420-8047, shan.jiang@atcoelectric.com; Dinesh Sharma,(780) 420-5541, dinesh.sharma@atcoelectric.com
2. AltaLink- Liang Jiao, (404) 267-2175, liang.jiao@altalink.ca ;David Mildenberger (403) 267-3458, david.mildenberger@altalink.ca

Note 2: This document contains revisions from the original guideline. Please contact your applicable electrical utility and/or the CAPP HVDC Committee to ensure that the latest version of the guideline is being used.

Contents

1	Project Scope	1-1
1.1	Coupling Modes.....	1-2
1.1.1	Capacitive Coupling.....	1-2
1.1.2	Inductive Coupling.....	1-3
1.1.3	Conductive Coupling	1-3
1.2	Impacts to Pipeline.....	1-3
1.3	How to use this Guide.....	1-5
2	HVDC Fault Currents	2-1
2.1	HVDC System Description.....	2-1
2.2	Steady State Impacts	2-4
2.3	Fault Impacts.....	2-4
2.3.1	Fault Current Comparison AC versus DC	2-5
2.3.2	Response to Back Flashover Faults	2-9
2.3.3	Ground Current Distribution factors for Back Flashovers.....	2-10
2.3.4	Shielding Failures	2-11
2.3.5	Ground Current Distribution Factors for Shielding Failures	2-13
2.3.6	DMR out of Service	2-13
3	Inductive Coupling.....	3-14
3.1	DC Current.....	3-14
3.2	Distance to Pipeline	3-14
3.3	Exposure Length	3-15
4	Conductive Coupling	4-16
5	Application Example	5-20
6	Result Interpretation.....	6-23
6.1	Safety	6-23
6.1.1	IEEE Standard 80.....	6-23
6.1.2	IEC 60479 Parts 1&2	6-24
6.1.3	Application Example	6-27
6.2	Coating Stress	6-32
6.2.1	Holiday Test on Pipelines	6-32
6.2.2	NACE Standards.....	6-33
6.3	Damage to Metal.....	6-35
6.4	Damage to Insulating Flanges.....	6-35
6.5	Damage to Electrical Equipment connected to the Pipeline	6-35
6.6	Mitigation Methods.....	6-36
7	Screening Guidelines	7-36
7.1	Parameter Sensitivities.....	7-37
7.1.1	Impact of Pipe Diameter	7-37
7.1.2	Impact of Coating Resistance	7-39

7.1.3	Impact of Tower Footing Impedance.....	7-39
7.2	Maximum Parallels for Back Flashover Events.....	7-40
7.3	Minimum Crossing Angles for Back Flashover Events	7-42
7.4	Maximum Parallel for Shielding Failure Events	7-46
7.5	Minimum Crossing Angles for Shielding Failure Events.....	7-52
7.6	Preliminary Guidelines	7-59
7.6.1	Coating Integrity	7-59
7.6.2	Safety Criteria.....	7-61
7.6.3	Non-Metallic Pipelines with Tracer wires	7-63
7.6.4	Examples HVDC/Pipeline Geometries.....	7-64
8	Study Workflow.....	8-66
9	Information Interchange.....	9-67
9.1	Maps.....	9-67
9.2	Technical Data Pipeline	9-67
9.3	HVDC line	9-67
9.4	Common Data.....	9-68
10	Safety during Installation of Pipelines.....	10-68
11	References.....	11-69
A.1	HVDC Tower Shielding Angle.....	i
A.2	Background information Body Current Hazard Interpretation.....	ii

Figures

Figure 1	Pipeline/HVDC Line Interaction Project Process	1-6
Figure 2	Monopole Circuit HVDC project.....	2-2
Figure 3	EATL and WATL Tower Design.....	2-3
Figure 4	AC/DC Fault Current Comparison.....	2-5
Figure 5	AC/DC Fault Current Comparison (Detail)	2-6
Figure 6	Peak Fault Current versus Fault Distance for BF and SF Faults.....	2-7
Figure 7	Fault Duration versus Fault Distance for BF and SF faults.....	2-7
Figure 8	Positive Pole fault current for SF fault at different distances from Rectifier.....	2-8
Figure 9	Back flashover current paths	2-10
Figure 10	Fraction of fault current returning to Rectifier via DMR.....	2-11
Figure 11	Current Paths - Shielding Failure	2-13
Figure 12	Decrease in magnetic coupling factor with pipeline distance	3-15
Figure 13	Simplified Circuit: GPR transfer to Pipeline showing basic shock hazard.....	4-16
Figure 14	Normalized Potential Profiles from Reference [7] for Lattice Towers	4-18
Figure 15	Estimated HVDC Tower Footing Resistance.....	4-19
Figure 16	Pipeline/HVDC line geometry	5-20
Figure 17	SES CDEGS output compared to EMTPRV output.....	5-21
Figure 18	SES CDEGS output for example problem	5-22
Figure 19	IEC 60479/IEEE 80 Ventricular Fibrillation Thresholds.....	6-26

Figure 20 Induced Body Current at Tower 1 with BF at Tower 7.....	6-27
Figure 21 Exponential Envelope applied to absolute value of Body Current.....	6-28
Figure 22 Estimated Induced Body Current Profile along Pipeline (hand to hand path)	6-29
Figure 23 Induced Body Current (hand to hand path) with largest RMS value	6-30
Figure 24 Induced Body Current (hand to hand) with highest initial value	6-30
Figure 25 Comparison of NACE AC withstand limits with DC test voltages.....	6-34
Figure 26 Coating Capacitance Variation with thickness and pipe diameter	7-37
Figure 27 Variation in Coating Resistance with pipe diameter	7-38
Figure 28 Impact of pipe diameter upon coating voltage (BF).....	7-39
Figure 29 Impact of coating resistance - pipe diameter constant (BP).....	7-39
Figure 30 Peak Voltage Summary for Back Flashover Events.....	7-40
Figure 31 Tail Voltage Summary for Back Flashover Events.....	7-41
Figure 32 Crossing Geometry	7-43
Figure 33 Peak induced Voltages NPS 2.5 OD pipeline with different crossing angles	7-44
Figure 34 Peak tail voltages NPS 2.5 OD pipeline with different crossing angles	7-44
Figure 35 F_q (4 msec duration, hand to feet) profile along pipeline, 25° crossing for BF fault	7-45
Figure 36 Ground Current at Rectifier - Back Flashover Event.....	7-46
Figure 37 Ground Current at Rectifier - Shielding Failure.....	7-46
Figure 38 Tower Ground Currents - Shielding Failure.....	7-47
Figure 39 Coating Stress transient relative to low NACE AC limit.....	7-48
Figure 40 Pipeline voltage profile, Shielding Failure at Tower 7, 2253m parallel	7-49
Figure 41 Impulse stress for a fault mid parallel	7-51
Figure 42 Shock Current profile (Total Event, hand to feet), $t = 33$ msec, Shielding Failure at Tower 7.....	7-52
Figure 43 Voltage Profile along pipeline, fault at Tower 1 (origin), 25° crossing.....	7-53
Figure 44 Coating Voltage Stress across from Towers 1&2	7-54
Figure 45 Tower Ground Currents Towers 1&2.....	7-55
Figure 46 Voltage Profile along pipeline, fault at Tower 2, 25° crossing	7-55
Figure 47 Total Event Shock Current (hand to feet) at different pipeline points, fault at Tower 1, 25° crossing	7-56
Figure 48 Specific fibrillating Charge, F_q , (hand to feet) at different pipeline points, fault at Tower 1, 25° crossing.....	7-56
Figure 49 Voltage Profile along pipeline, fault at Tower 1, 15° crossing	7-57
Figure 50 Total Event Shock Current (hand to feet) at different pipeline points, SF fault Tower1, 15° crossing	7-58
Figure 51 Parallel conditions leading to coating integrity studies.....	7-60
Figure 52 Crossing conditions leading to coating integrity studies.....	7-60
Figure 53 Parallel conditions leading to Safety Studies	7-63
Figure 54 Crossing conditions leading to Safety Studies	7-63
Figure 55 Possible pipeline/HVDC line geometries for considering coating integrity	7-65
Figure 56 Study Workflow	8-66
Figure 57 Shielding Angle HVDC Tower showing arc paths	i
Figure 58 Simplified diagram for internal impedances of the human body [11].....	ii
Figure 59 Hypothetical Body Current with $Z_T = 450$ ohms (hand to feet path).....	iv
Figure 60 Exponential Envelope Construction.....	vi
Figure 61 Body Current (hand to hand) with transferred energy.....	ix

Figure 62 F_q trajectory for path hand to feet (Example 2)..... ix

Tables

Table 1 Nelson River Bipoles 1&2 Lightning Outages 1998-2000.....	2-12
Table 2 Ontario Hydro/AEP Lattice tower Footing Impedances.....	4-18
Table 3 Event Summary Shock Current across from Tower 1	6-28
Table 4 Body Currents for Crossing Results Hand to Hand path (Fault at Tower2).....	6-31
Table 5 Body Currents for Crossing Results Hand to Feet path (Fault at Tower 2).....	6-31
Table 6 Transient Withstand Criterion for HVDC Coating Stress Evaluation.....	6-35
Table 7 Shock Hazards (induced voltage) for BF events at different parallel lengths	7-42
Table 8 Attenuation Length, γ , in km for NPS 2.5 pipe	7-50
Table 9 Shock Hazards (induced voltage) for SF events at different parallel lengths.....	7-51
Table 10 Shock Hazards (induced voltage) for SF events at different crossing angles.....	7-58
Table 11 Conditions leading to Coating Integrity Studies.....	7-60
Table 12 Conditions Leading to Safety Studies.....	7-62
Table 13 Heart-Current factor F for different current paths (IEC 60479-1).....	iii

Revision History from June 2014 Edition:

1. Current pathway hand – feet specified for Figure 13.
2. Section 6.1.1 revised to reflect internal body impedance assumptions made in IEEE Standard 80.
3. Section 6.1.2 revised to be more in line with IEC 60479. Charge transfer integral (4 msec interval) replaced with IEC 60479 definitions for F_q and F_e for determination of initial fibrillation risk. Introduction of heart-current factor concept for different current pathways through body along with clarification of internal body impedance, Z_T to be used for different body pathways.
4. Section 6.1.3 application examples revised to reflect criterion changes in Section 6.1.2.
5. A new section on mitigation methods, 6.6.6 has been added.
6. Section 7.6.3 text has been replaced with a mitigation recommendation for non-metallic pipelines with tracer wires. The previous section 7.6.3 on HVDC/pipeline geometries is now section 7.6.4.
7. Section 7.2 revised with additional shock hazard evaluation based upon changes to Section 6.1.2.
8. Section 7.3 revised based upon changes to Section 6.1.2.
9. Section 7.4 revised based upon changes to Section 6.1.2. Exponential decay of voltage outside the induction zone discussed with simple criterion introduced to determine extent of possible safety risk outside the induction zone of the parallel.
10. Section 7.5 revised based upon changes to Section 6.1.2.
11. Section 7.6.2 “Safety Criteria” revised based upon changes to Section 6.1.2. Table 12 column 3 limits revised along with addition of revised estimation formulae for determining zone of influence with regard to appurtenances. Additional assumptions listed along with revised Figure 53 and Figure 54.
12. Appendix A.2 added to provide more background information on revised safety evaluation methodology.

1 Project Scope

The interaction between AC power lines and metallic pipelines is the subject of national standards [1] and guidelines [2] that together cover both analysis and mitigation issues. There appears to be no similar guideline for HVDC lines, especially those being proposed for the province of Alberta. This document is focused upon the EATL (Eastern Alberta Transmission Line) and WATL (Western Alberta Transmission Line) HVDC lines currently being constructed.

While the same electrical coupling mechanisms apply to both AC and HVDC lines, there are also significant response differences between them and by understanding steady state and fault phenomena that can arise within HVDC systems a proper approach to their analysis in the context of electrical coordination with metallic pipelines can be carried out. The purpose of this guide is to introduce HVDC systems with particular focus upon lines being built in Alberta, provide sufficient background information, and to provide users of this guide a systematic approach in dealing with analysis and mitigation aspects of HVDC system influences upon metallic pipelines. Both similarities and differences with AC lines are emphasized within this guide. It should be emphasized this guide only applies to land based HVDC systems that do not utilize ground electrodes for steady state DC ground currents as may arise due to specific operating conditions. Section 2 will provide more elaboration on this operational aspect.

The CIGRE¹ guideline [2] though dedicated to AC lines is a comprehensive reference with many sections allowing the development of simple calculation and measurement methods. The complexity of the HVDC interaction unfortunately precludes simple calculation methods and must really be approached with sophisticated computer software such as the SES² CDEGS suite of software. Nevertheless, the CIGRE Guideline is a valuable reference and many of the analytical concepts carry over to DC line application.

¹ CIGRE - Conseil international des grands réseaux électriques (International Council on Large Electric Systems)

² SES – Safe Engineering Services & Technologies Limited

1.1 Coupling Modes

Any power line, AC or DC will be coupled to a metallic pipeline by three well known mechanisms:

- Capacitive Coupling
- Inductive Coupling
- Conductive Coupling

For reasons associated with corrosion control and cathodic protection, most pipelines have an insulating coating which converts them into underground conductors insulated from earth. For the most part this guide will be focused upon underground pipelines in the presence of aerial high voltage lines. Above ground pipelines also exist but are outside the present scope of this document. Each of the above coupling modes will be discussed in more detail with regard to HVDC lines.

1.1.1 Capacitive Coupling

Capacitive coupling only occurs with aerial pipelines (or pipelines under construction) when the pipeline is in close proximity to the HV power line. Under AC conditions an induced power frequency voltage arises, but under DC conditions the field is static giving rise to static electric shocks. If the pipeline is grounded, induced circulating currents due only to the small ripple current in the DC line can flow. The electrical field under a DC line has been found to be less hazardous relative to an AC line. According to reference [3]:

“These results suggest that electrical fields below HVDC transmission lines are not sufficiently hazardous as to necessitate significant safety measures, as the environmental influence of a HVDC transmission line’s electrical field is very limited.”[3]

The same reference reports that heavy equipment, i.e. trucks, farm machinery, when parked under a HVDC line will not build up dangerous inducted voltages as might occur with an equivalent AC line. The reason for this appears to be the resistivity of the tires (about 10 Mohms) is low enough to drain the charge, keeping the voltages in the tolerable range.

1.1.2 Inductive Coupling

Inductive or magnetic coupling occurs whether the pipeline is buried or aerial. Depending upon the degree of parallelism, induced voltages can be in the kV range during fault conditions for AC lines. For HVDC lines, under fault conditions, the collapse of the current can lead to high momentary induced voltages.

Unlike AC lines, under steady state conditions, the HVDC line induced voltages tend to be negligible, with only the potential to cause telephone interference problems. Therefore under steady state conditions there are no pipeline integrity issues (neither corrosion nor coating related issues) nor shock hazards.

1.1.3 Conductive Coupling

The discharge of current through the grounding electrode at the tower can lead to a ground potential rise, GPR, in the vicinity of the faulted tower. With a current discharge, a voltage gradient exists in the soil around the tower relative to a remote earth. An insulated pipeline in the vicinity of the tower's potential gradient will experience a voltage across its insulating coating due to the difference between the pipeline (near zero voltage relative to a remote earth) and voltage rise in the adjacent soil. If high enough, the voltage stress could puncture the insulating coating possibly damaging the pipeline.

During HVDC line fault conditions, a ground current will also arise but a number of factors make this situation fundamentally different from AC faults. The current distribution factors are different for HVDC. This will be discussed in Section 2.0.

1.2 Impacts to Pipeline

The effects of any electrical disturbance upon the pipeline may be categorized as:

- Safety Problems
- Damage to Pipeline coating
- Damage to metal
- Damage to insulating flanges
- Damage to equipment connected to the pipeline

Safety issues are shock hazards to people who may come in contact with the pipeline. The danger increases as the intensity of the current increases along with its duration. For HVDC faults both the magnitude and duration of the event tend to be shorter than an AC event. Though less severe, the safety assessment requires a different interpretation of existing standards.

Coating damage in the terms of dielectric failure is to be avoided for both HVAC and HVDC fault conditions. The dynamics of the HVDC fault are different leading to different voltage stresses upon the pipe.

Damage to metal under a coating perforation can lead to high current densities for pipelines in close proximity to the faulted tower footing. Resistive coupling occurs which can also transfer the ground potential voltage rise to the pipeline where in can be transmitted tens of kilometers prior to being significantly attenuated. This issue is common to either AC or DC lines.

Insulating flanges that electrically isolate a section of the pipeline from another pipe or pump station can see large voltages across them either due to inductive or conductive coupling during fault conditions. This issue is common to either AC or DC lines.

Other metallic circuits (communication lines) and or cathodic protection systems will also be exposed to inductive and/or conductively coupled voltages. The EMI³ aspects will depend upon the equipment's susceptibility to the disturbances introduced by the fault condition.

³ EMI – electromagnetic interference

1.3 How to use this Guide

To assist in the usage of the guide, the process workflow starting from identification of pipeline/HVDC line interaction to eventual decommissioning of the pipeline (or HVDC line) is illustrated in Figure 1. A typical sequence would be:

1. To start the process accurate location (Section 9.1) of the affected utilities must be carried out by either the electrical utility or pipeline owner.
2. The affected parties then meet to discuss the project. At this stage, the preliminary screening guideline (Section 7.6) could be applied to assess the severity of the interaction. The project could end at this stage if it is agreed the interaction poses no coating integrity or safety issues. Agreement that no action is required is documented between the electrical utility and pipeline owner.
3. If the preliminary screening suggests potential problems, an assessment study needs to be carried out by a qualified consultant. More details of this process are presented in Section 8 of this guide.
4. The need for mitigation (if any) would be the main deliverable of the study. The model developed can then be used to assess the effectiveness of different mitigation options. The final report should present a recommended mitigation plan that meets the objectives at least life cycle cost.
5. After acceptance of the mitigation plan, cost allocations are finalized and an implementation schedule is agreed upon. The user's typical project process ensues along with the development of safe work procedures to be applied during construction, operation and maintenance of the pipeline.
6. After successful commissioning of the facilities, the facilities are maintained till final decommissioning of the pipeline or the HVDC line is no longer in service. Management of change processes also have to be included to ensure that when changes to the HVDC system or pipeline systems are implemented no unmitigated hazards are present.

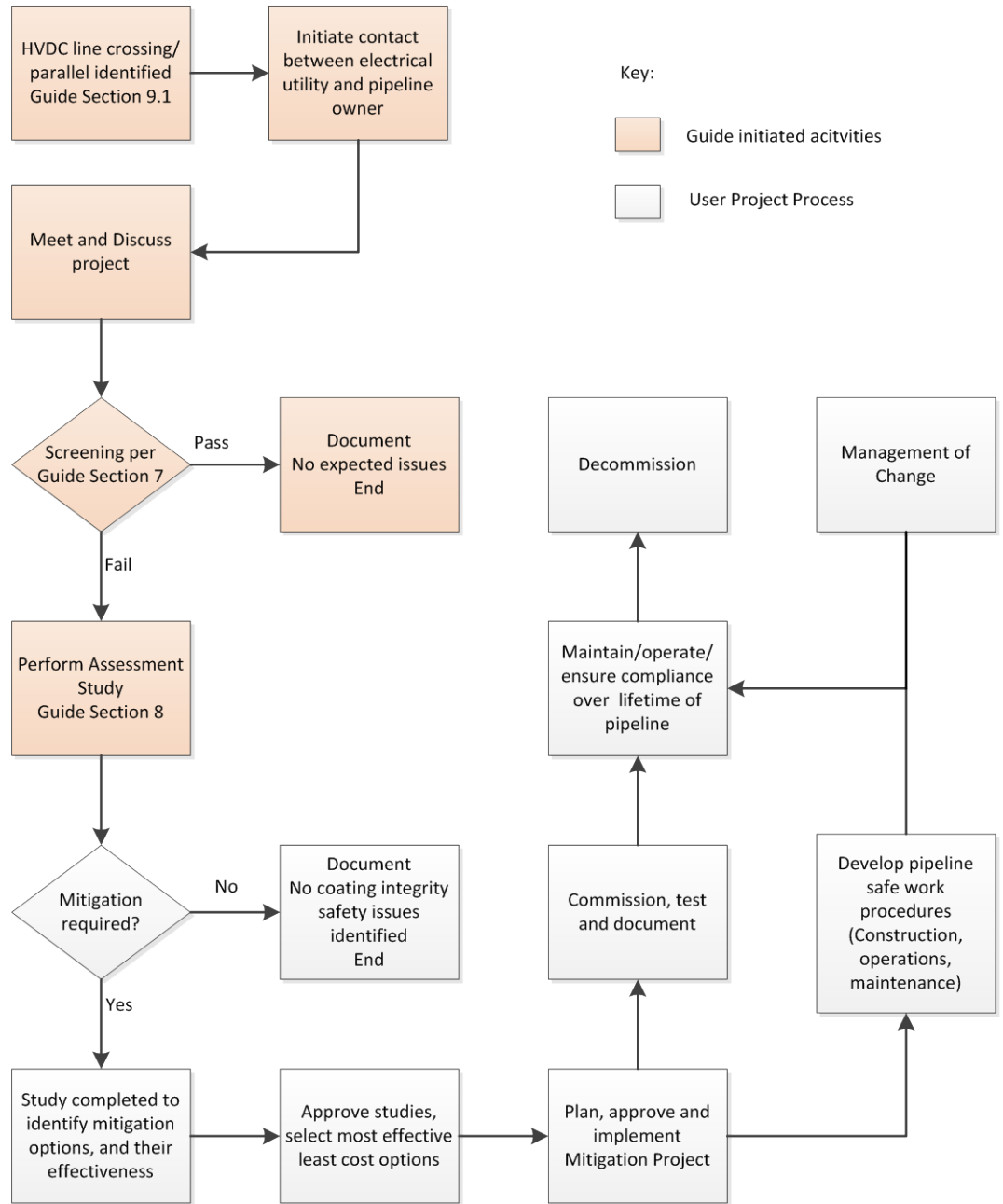


Figure 1 Pipeline/HVDC Line Interaction Project Process

2 HVDC Fault Currents

2.1 HVDC System Description

In this section, a short description of the HVDC system is presented along with a detailed description of the different line fault modes.

Older HVDC systems tended to be comprised of two terminal stations and a single interconnecting line⁴. Full wave rectifiers convert the source voltage from AC to DC for transmission and full wave invertors convert DC back to AC. These systems tended to be of bipole configuration, comprising of a positive pole and a negative pole while using ground as a neutral return for any unbalance current. If the positive pole voltage were at +500 kV, then the negative pole would be at -500 kV, and a loop current not involving ground would flow. If a ground fault occurred with the positive pole, its fault current would flow to ground prior to detection and blocking. The negative pole would continue to operate (as a monopole) using ground as a return⁵. At each station, a ground electrode (up to 1 km in earth surface diameter) was needed for collecting the ground return current during either monopole or bipole operation. With normal bipole operation an unbalance current up to 5% of rated current⁶ could flow. Ground electrode location was crucial since it was desirable to keep surface gradient currents to a minimum over most of the line to avoid corrosion issues with other infrastructures.

The proposed Alberta HVDC lines will not be utilizing ground electrodes. Instead an overhead return conductor, DMR (Dedicated Metallic Return) will be used to carry any unbalance current or return current under monopole conditions hence no stray DC current flows through ground under normal conditions. Figure 2 depicts the simplified schematic layout for the HVDC system in its stage 1 development. The EATL system has the longer line length of 500 km, whereas the WATL line is approximately 350 km. There is no connection between the EATL and WATL systems other than indirectly through the underlying AC system backbone.

In stage 1, monopole operation will occur with the DMR line typically in parallel with the negative pole. In stage 2, a second convertor will be added on each end to allow bipole operation. The DMR would only carry the steady state unbalance current under this configuration. Only the rectifier end will be grounded, leaving the inverter floating⁷. The HVDC system is capable of bidirectional control and under some circumstances the terminals can switch roles. Rated load current for both the EATL and WATL systems is 2000 Adc.

⁴ The vast majority of HVDC installations are still of this type

⁵ This mode of operation had a time limit of typically 30 minutes for land based systems

⁶ For a rated current of 2000 Adc this would amount to 100 Adc of ground injection

⁷ The inverter end is grounded via a surge capacitor for lightning protection purposes – DC currents are blocked

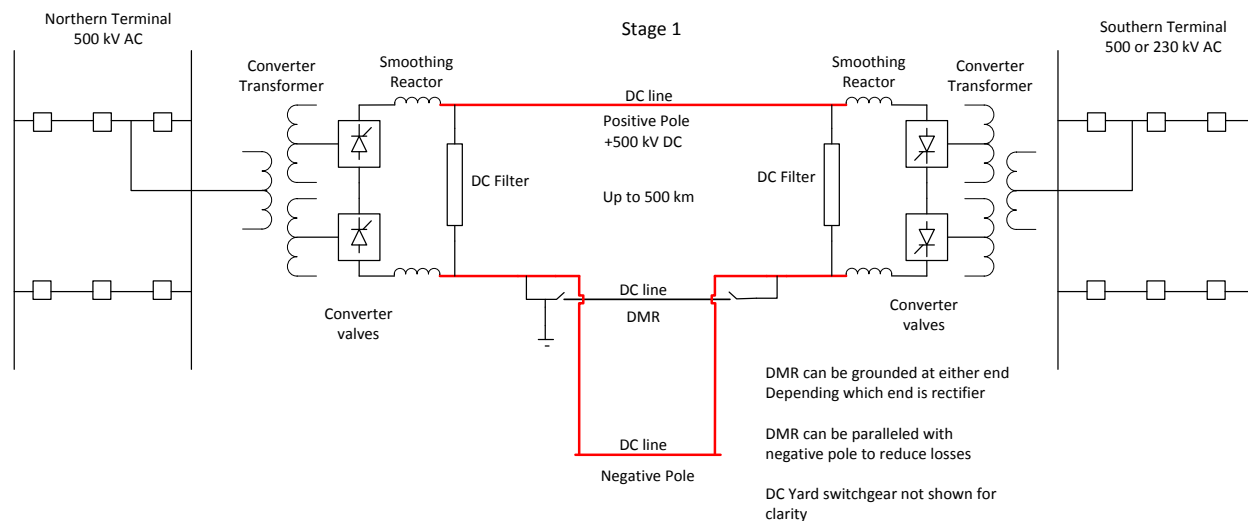


Figure 2 Monopole Circuit HVDC project

The tower design is shown in Figure 3. The standard height (without extensions) to ground to the outside pole conductors (positive and negative) is 27.4 m (90 ft.). The DMR sits inside the tower window. The pole conductors are comprised of 4 x 1590 MCM (Falcon) bundle while the DMR is a 2 conductor 1590 MCM (Falcon) bundle. There are also two shield wires on top of the structure.

The tower bears a superficial resemblance to a typical 500 kV AC line structure except for the smaller window for accommodating the DMR. The line however is being constructed for bipole operation having all the conductors available even though, initially, in Stage 1 the system will operate in monopole. Under monopole operation, the DMR is not mandatory for successful operation of the link. The Right of Way, ROW, of the line is ± 30 meters relative the tower centerline.

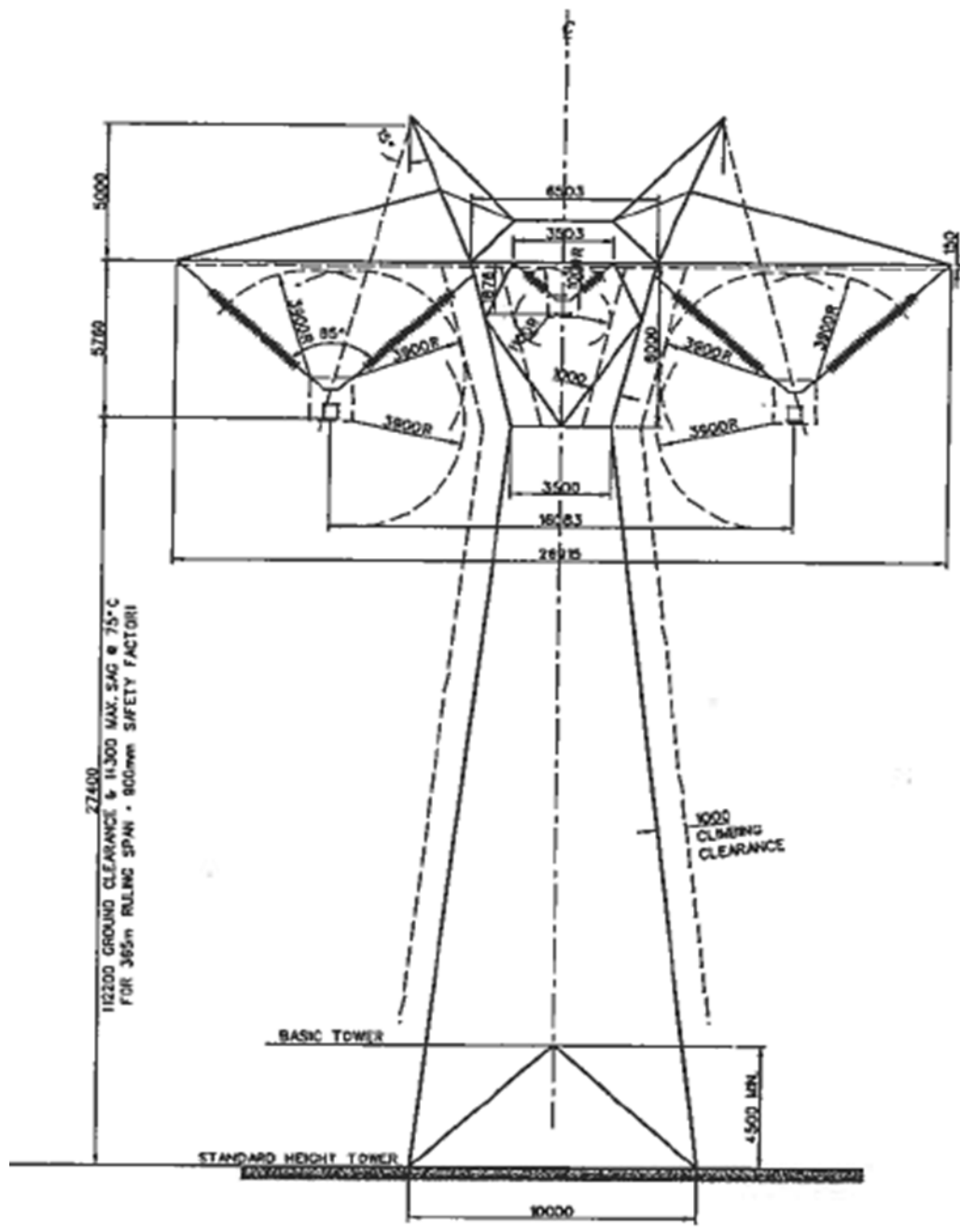


Figure 3 EATL and WATL Tower Design

2.2 Steady State Impacts

Since initial operation is monopole, the negative conductor would typically be used as the return path. Its voltage to ground will be zero at the rectifier end (where the ground reference is established) and reaches a value up to 14 kV DC to ground at the ungrounded inverter due to the ohmic drop. The DMR is used to reduce line losses by paralleling with the negative pole conductor. As noted there is only a single circuit ground hence no stray DC current flows through ground; however the DC current has a small AC ripple due to the conversion process which can be inductively coupled to nearby metallic structures. The purpose of the DC filters and Smoothing Reactor (Figure 2) is to reduce the ripple current and consequently reduce coupling to telephone communication circuits that might be paralleling parts of the HVDC line. The main current path is highlighted in red in Figure 2.

2.3 Fault Impacts

Adverse weather (lightning) will be the main determinant when considering HVDC line faults based upon AC line statistics provided in reference [4]. The pole insulation relative to the DMR is very high, nearly equivalent to a 765 kV AC line whereas the DMR has an insulation level comparable to a 138 kV AC line. The total trip out rate for the line consists of two types of lightning related flashover modes [5]:

- Backflashover (BF) - Any stroke to the tower top/shield wires will lead to a backflashover over the insulator if the potential difference across the insulator exceeds its critical flashover value. The conductor sits at its normal voltage potential relative to earth, whereas the tower top voltage (insulator base) is raised to very high voltage due to the lightning discharge.
- Shielding Failure (SF) – The shield wires are designed to intercept all lightning strokes to the line but low intensity lightning strokes can evade the shield wires and terminate on the pole conductors. The consequent voltage rise can lead to insulator flashover.

For the line design in Figure 3, both the Shielding failure (SF) rate and the Back flashover (BF) trip out rate combined are expected to be quite low (<.133 per 100 km/year)⁸. Prior to discussing the implications of either flashover event, a comparison between AC and DC current waveforms will be presented.

⁸ This works out to <3 faults every 2 years for a 500 km line. If a random distribution is assumed and the line consists of 1500 towers, the fault return period for a particular tower is > 1000 years.

2.3.1 Fault Current Comparison AC versus DC

In the DC fault case there is no fault contribution from the inverter end whereas in an AC fault, contributions can arise from both ends. In Figure 2, the DC current can only flow in one direction due to the rectifier/inverter characteristics. For comparison purposes each simulated fault is fed from only a single source, also the AC fault magnitude was set near the DC fault peak value. Results are shown in Figure 4 and Figure 5 for the back flashover event.

The initial step in fault current is similar for both cases. The first wave reflection from the source bus returns in 211 μsec for the AC fault and 240 μsec for the DC fault.

The reflection coefficient at the DC rectifier terminal is more complex due to the DC filter and some control action occurring later in the event but the two responses are initially very similar which from the pipeline perspective cannot be differentiated, the initial induced voltage spike will be similar. The initial conducted GPR will also be similar. It is only after the first 2 msec that the DC nature of the fault manifests. In the CIGRE Guideline [2], the initiating event leading to power frequency fault current is not discussed nor is the initial AC transient, the focus is more on the quasi-steadystate nature of the fault current. Due to the multi-frequency nature of the HVDC current, this initial transient will be part of the analysis but if an analogy with an AC system is made, only the tail voltage beyond the initial step change would normally be considered.

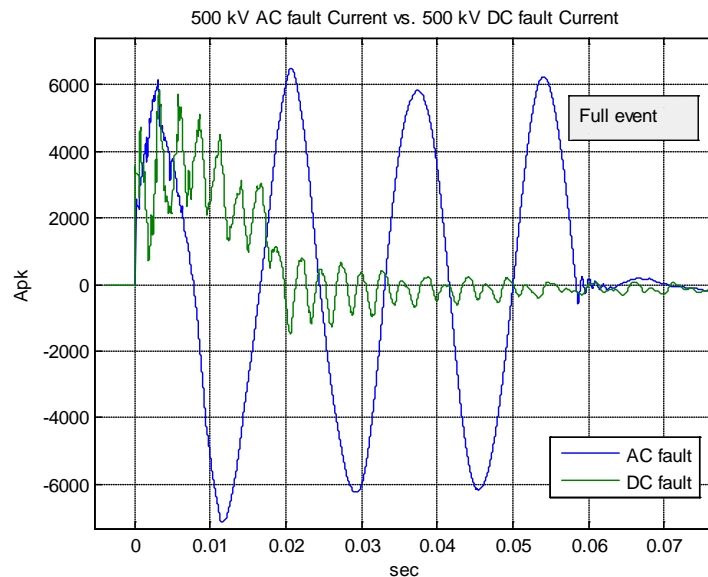


Figure 4 AC/DC Fault Current Comparison

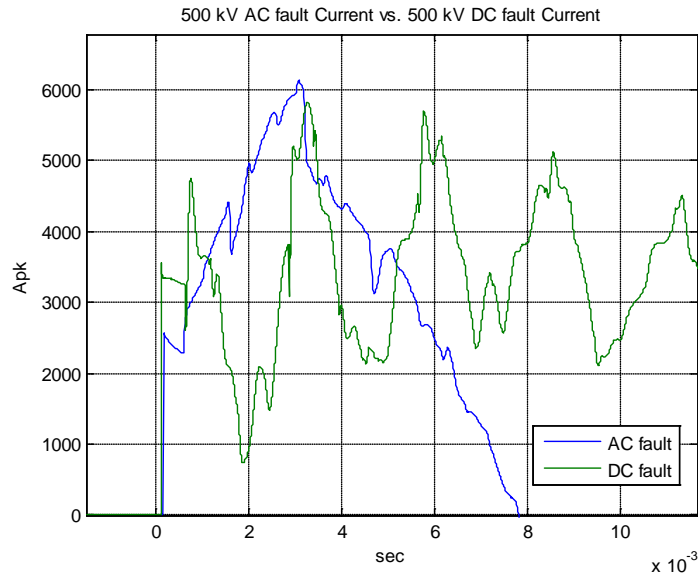


Figure 5 AC/DC Fault Current Comparison (Detail)

Unlike AC faults, the DC fault current magnitude tends to be no more than 3 times its rated load current. Both the harmonic content and duration of the DC current are different from the AC case. The peak magnitude (crest) and duration (time to the first current zero) of the DC event depends weakly on fault distance from the rectifier as shown in Figure 6 and Figure 7. The variation arises due to the difference in harmonic content as a function of distance. Faults close to the rectifier i.e. the origin in Figure 6 and Figure 7, tend to be more oscillatory as shown in Figure 4 and in Figure 8 where the rectifier positive pole currents for a shielding failure at 25, 150 and 300 km from rectifier terminal are depicted.

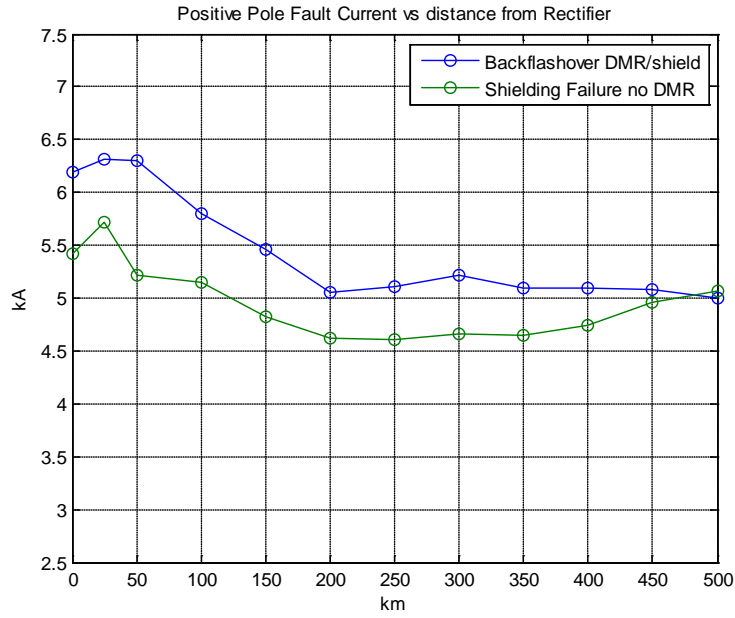


Figure 6 Peak Fault Current versus Fault Distance for BF and SF Faults

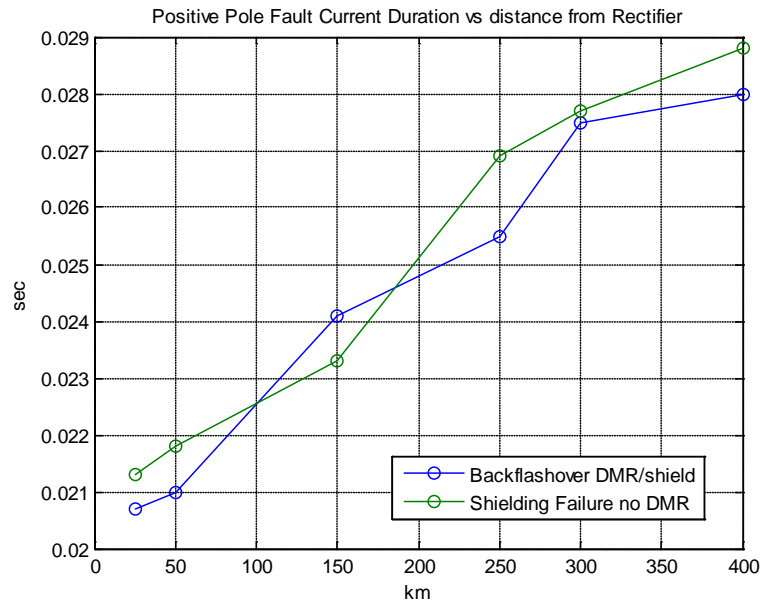


Figure 7 Fault Duration versus Fault Distance for BF and SF faults

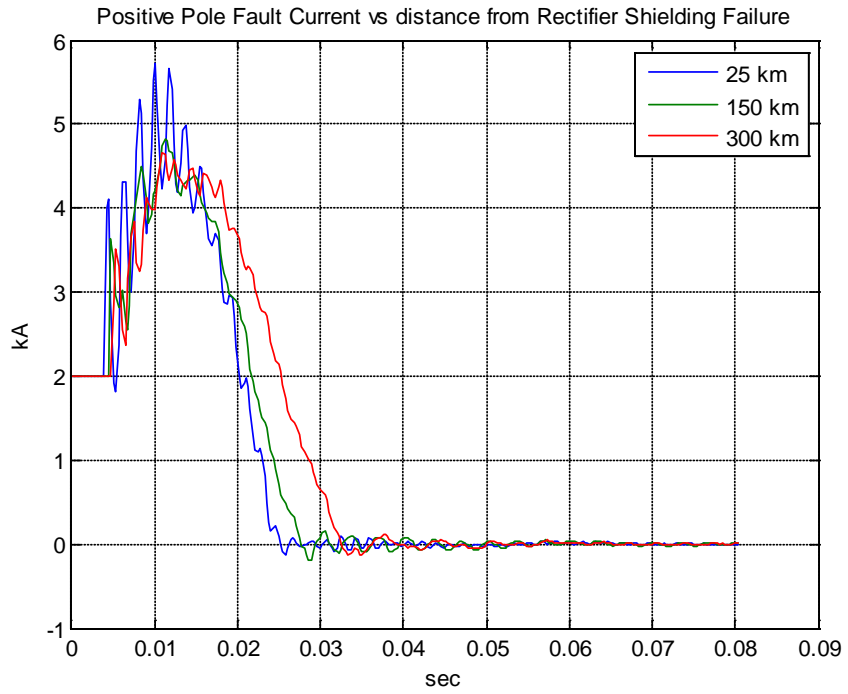


Figure 8 Positive Pole fault current for SF fault at different distances from Rectifier

2.3.2 Response to Back Flashover Faults

Any stroke of sufficient magnitude to the tower top/shield wires will lead to a back flashover of the DMR well before a potential pole conductor flashover. A sustainable DMR only flashover will introduce an additional ground point causing some DC current flow to earth for a short time till the DMR fault is detected, leading to a link shutdown and restart. The DC current injection is low due to the unfaulted negative pole conductor path. A much larger stroke would lead to both DMR and positive pole conductor back flashovers (Figure 57). The current paths are shown in Figure 9 for both monopole and bipole operation. Though the currents in the vicinity of the faulted tower are depicted, the conductor connections at the line end points are highlighted. The shield wires are continuously grounded at each tower.

In Figure 9(a), unlike an AC fault, the ground path is not necessarily the main path. In the HVDC case, a large fraction of current can return to the rectifier station via the DMR causing a decrease in the ground current. This has two important consequences:

- The ground current is reduced leading to a lower GPR
- The return current conductors act to limit the inductive coupling to the pipeline due their screening effect.

Also since the DMR and negative pole conductors are paralleled, the loop current becomes a superposition of the fault current with the negative pole current. In the bipole case Figure 9(b) the situation is similar. The negative return current commutates to the DMR. The DMR current back to the rectifier is the vectoral sum of the negative return current, and the portion of fault current not going to ground. It should be noted that the magnitude of the positive pole fault current is the same as the monopole case, but the induction to the pipeline will be different due to the screening effect of the negative pole circuit.

In Figure 4 the only source is the rectifier, upon shorting out the rectifier, there is no infeed from the inverter terminal. The location of the HVDC tower fault relative to the parallel pipeline becomes important; i.e. a tower fault point before the parallel (closer to the rectifier) will have a lower inductive coupling to the pipeline as opposed to a point at the end (or downline) of the parallel (further away from the rectifier). Of course, if the rectifier and inverter operations are interchanged, the reverse would be true. Fault points in the middle of the parallel will tend to have the maximum instantaneous coating stress voltage values.

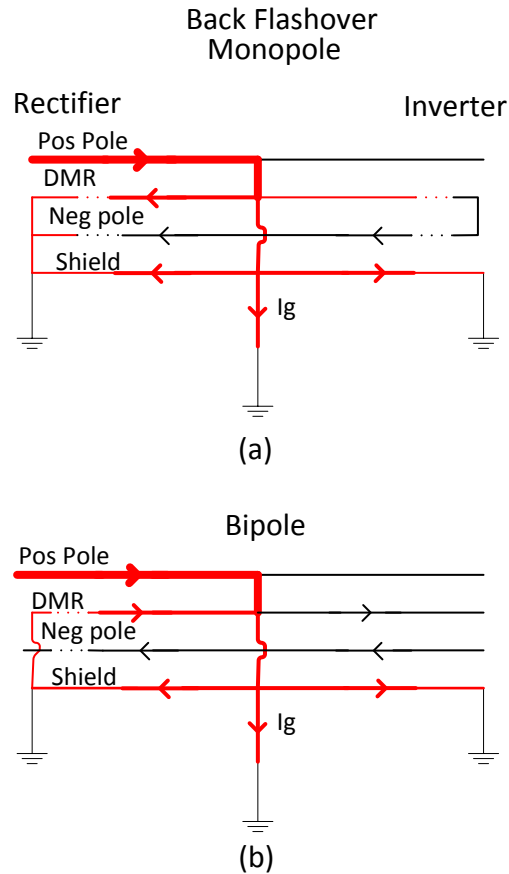


Figure 9 Back flashover current paths

2.3.3 Ground Current Distribution factors for Back Flashovers

The magnitude of an AC fault current varies depending upon its location along the transmission line. For the single source example in Figure 4, the maximum peak value will occur for a breaker terminal fault at the source end, with the minimum fault magnitude occurring at the open line end. In the more general case with two sources, the fault current profile may or may not reach a minimum somewhere along the line depending upon the relative strength of the two sources.

In this regard, the DC case is simpler since only the rectifier end supplies the fault current. For a fault involving ground irrespective of whether the fault is of an AC or DC nature, the fault current will divide with a portion going to earth and the remainder traveling along any conductors involving a ground connection (the shield wires and in addition for HVDC the DMR conductor). The earth current is responsible for the GPR at the fault point. In this regard, the DC line is significantly different from an AC line. For a DC line, the combination of DMR with the two shield wires have a much lower impedance relative to the AC line with only its double or single shield wires, therefore a larger proportion of fault current will return via the DMR in the DC line case. The fraction of fault current

returning via the DMR as a function of fault distance from the rectifier terminal is shown in Figure 10 where a uniform soil resistivity of 100 ohm-m is assumed.

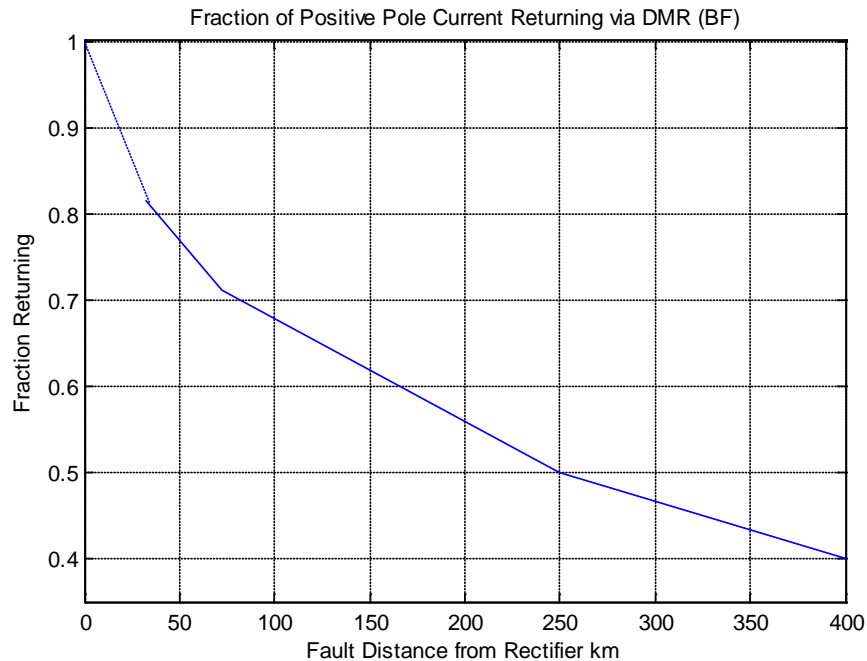


Figure 10 Fraction of fault current returning to Rectifier via DMR

In Figure 10, for a fault 75 km from the rectifier terminal 70% of the fault current will return via the DMR conductor. By contrast, for an AC fault >80% of the fault current returns via ground at a distance of several km from the source terminal, and with two sources, there is division of ground current between the two sources. For DC faults close to the rectifier, the GPR will be low, and for faults close to the inverter end, a significant fraction of current still returns via the DMR relative to the AC line case. In both the AC and DC cases, low tower footing impedance(s) will assist in minimizing the GPR at the faulted tower.

It is important that the software used in the analysis of HVDC faults be able to properly represent the ground return current. The results in Figure 10 were derived in EMTPRV⁹.

2.3.4 Shielding Failures

A shielding failure occurs when a low intensity lightning¹⁰ stroke bypasses the shield wire and terminates upon the pole conductor (Figure 57). With AC lines, shielding failure rates can be computed using EGM (Electro Geometric Model(s)) as detailed in [5]. The EGM has been refined over the years with recommended approaches given in both IEEE¹¹ and CIGRE. In reference [6] an attempt is made

⁹ EMTPRV – Electromagnetic Transients Program Restructured Version – EPRI DCG (Electric Power Research Institute’s Development and Coordination Group)

¹⁰ A stroke typically in the 3 – 20 kA range

¹¹ IEEE – Institute of Electrical and Electronic Engineers

by Manitoba Hydro to match recorded values with a mathematical model of their HVDC lines. Their measured outage values over a 2 year period are shown in Table 1.

Table 1 Nelson River Bipoles 1&2 Lightning Outages 1998-2000

Failure Count	Bin Range kA stroke current	Failure type
1	10 - 20	Shielding failure
1	20 - 30	Shielding failure
2	30 - 40	Shielding failure
1	100 - 110	Back flashover
1	130 - 140	Back flashover

To put the results in context, the Manitoba Hydro system possesses two HVDC lines running in parallel, each with a length of 900 km. The total outage rate for this data is 0.166 per 100 km/year with the shielding failure only rate at 0.111 per 100 km/year. The shielding angle is given as 35° with a single shield wire. The EATL and WATL lines will be shorter with a 15° shielding angle at the tower as well has two shield wires (see Appendix A.1). Applying the 1992 IEEE EGM [5] leads to a predicted monopole shielding failure rate of 0.019 per 100 km/year, and a bipole rate of 0.0084 per 100 km/year where it is assumed for bipole operation that negative strokes will not be attracted to the negative pole.

It has recently been recognized that the DC line voltage has an impact on the EGM model especially on higher voltage DC lines in China. The interaction is mainly between the positive pole and negative lightning strikes where it is believed +800 kV bias voltage for the lines in question weakens the effectiveness of the overhead shield wire by changing the striking distance in an unfavorable way, also cross winds might be blowing positive ions from around the negative conductor to the vicinity of the positive conductor. An EGM model specific to HVDC lines appears required. Given the Manitoba Hydro data, and the Chinese experience it appears shielding failures although rare, may be the predominant failure mode for most HVDC lines¹².

The shielding failure stroke currents are expected to lead to voltage stresses less than the DMR withstand values. Consequently the pole conductor would flashover leaving the DMR/negative pole insulation intact. The current paths are shown in Figure 11.

¹² Both the BF and SF failure rates are very small numbers, for AC lines BF rates tend to predominate but given the high insulation levels of the HVDC systems, and the very large stroke currents needed for backflashovers, the SF and BF rates appear comparable.

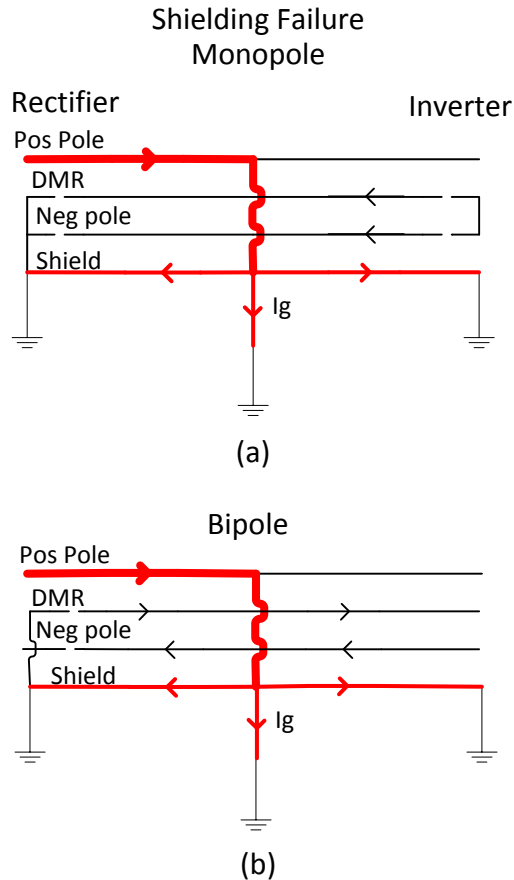


Figure 11 Current Paths - Shielding Failure

In the shielding failure mode, most of the fault current goes to earth. When considering shielding failures at a specific location, the utility must be consulted to provide the typical tower footing impedances and the DC pole fault current associated with a shielding failure at that location.

2.3.5 Ground Current Distribution Factors for Shielding Failures

As discussed in Section 2.3.4, the ground fault current at the stricken tower will equal the pole fault current less the currents being shunted to the adjacent towers via the shield wires. Inductive coupling is also affected since under monopole conditions only the currents in the shield wires will provide any screening.

2.3.6 DMR out of Service

Though the DMR is expected to be in service under monopole transmission, there may be times where it might be advantageous to have it disconnected at each end, and run the link with only the negative return conductor. In this situation the back flashover scenario becomes identical to the shielding failure scenario under fault conditions. It is more likely however that one end of the DMR would be grounded. If grounded at the inverter end, the backflashover scenario remains identical to the shielding failure scenario. If grounded at the rectifier end, the

backflashover scenario remains identical to Section 2.3.2 except in Figure 9 there is no current flow from the Inverter end. For Bipole operation the DMR is required for normal operation.

3 Inductive Coupling

The magnetic field created by the line currents will inductively couple to the pipeline creating circulating currents within the pipeline, and voltages relative to earth across the insulating layer of the pipeline.

This inductive coupling will depend upon three factors:

- Operating condition of the DC line i.e. its load or fault currents
- Distance between the line conductors and the pipeline
- Exposure length

Each will now be discussed.

3.1 DC Current

Under steadystate conditions, the DC component of current cannot be induced upon the pipeline. Only the small ripple current due to the AC/DC conversion process can be induced upon the pipeline and as discussed, this current is small and unlikely to have any adverse impact upon the pipeline.

Under fault conditions, the DC current collapses as shown in Figure 4 and under this condition an appreciable voltage can be induced on the pipeline. The induced voltage will contain multiple frequencies.

3.2 Distance to Pipeline

The induced voltage magnitude will arise due to the vector sum of magnetic field contribution of each line conductor at the pipeline location. The coupling factors will also be dependent upon the spacing between each conductor and the pipeline. An inverse relation of coupling strength to distance applies.

Under steadystate conditions only the HVDC line ripple current can be coupled to the line. The ripple current has theoretically no 60 Hz component but has a fundamental frequency of 720 Hz (12th harmonic) with harmonics at this frequency. Though the strength of the coupling will depend mainly on the separation, the frequency and earth resistivity also have an impact. If the separation distance is varied from the edge of the HVDC line ROW and coupling impedance at a particular frequency, f , is normalized to its edge ROW value:

$$k(f, x) = \frac{Z_{ip}(f, x)}{Z_{ip}(f, 30)}$$

Figure 12 arises. This ratio gives an estimate of the strength reduction of the coupling factor with distance. As earth resistivity increases, the attenuation is less however the curves maintain their relative positions.

Under line fault conditions, the natural frequencies of the HVDC line are excited which tend to be in the 300 Hz range. In Figure 12, at 1 km, the coupling strength at 300 Hz has become asymptotic at less than 5% of its initial value. Existing AC standards suggest any parallel further away than 300 meters need not be considered. Figure 12 suggests at 300 Hz, the limit would be 200 meters to have the same effect all other factors being equal.

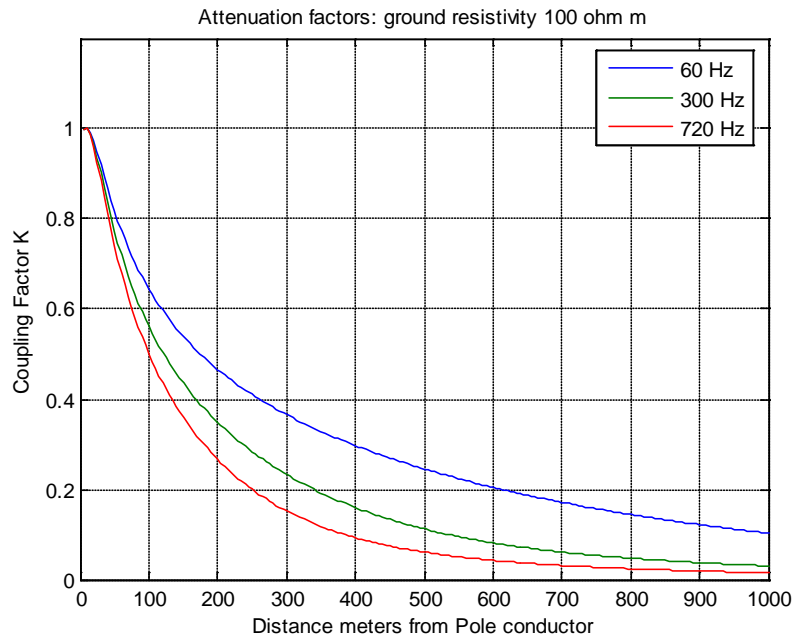


Figure 12 Decrease in magnetic coupling factor with pipeline distance

3.3 Exposure Length

For pipeline parallels, the induced voltage tends to increase linearly with exposure length up to a few kilometers depending upon pipeline coating. Beyond a few kilometers, the conductance of the coating causes the voltage to increase at a less than linear rate [2]. The higher the quality of the coating resistance, more linear the rise will be. The induced voltage due to HVDC line faults will follow a similar pattern.

4 Conductive Coupling

Conductive coupling occurs when the pipeline traverses the zone of influence of the electrical installation undergoing a ground fault condition. The GPR adjacent to the pipeline, through existing coating imperfections (or in unusual conditions through coating holidays¹³ created by extreme coating stress voltages resulting from the fault) is transferred to the pipeline and attenuates slowly with distance away from the transfer point. A simplified circuit is shown in Figure 13 illustrates the issue. In addition, Figure 13 illustrates the basic shock situation (hand to feet) if an appurtenance were present.

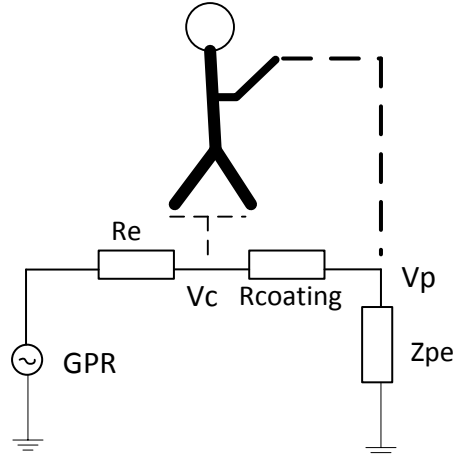


Figure 13 Simplified Circuit: GPR transfer to Pipeline showing basic shock hazard

Where R_e is the earth resistance of the pipeline in contact with the soil, $R_{coating}$ is the coating resistance of the insulating layer and Z_{pe} is the pipeline impedance. The *GPR* is the voltage rise at the tower footing. The voltage on the pipe becomes:

$$V_p = \frac{Z_{pe}}{Z_{pe} + R_{coating} + R_e} \cdot GPR$$

And the coating stress voltage, V_{cs} , (or touch voltage for electric shock¹⁴):

$$V_{cs} = V_c - V_p = \frac{R_{coating}}{Z_{pe} + R_{coating} + R_e} \cdot GPR$$

¹³ Holidays –“small faults or pinholes that permit current drainage through protective coatings on steel pipe...”
ASTM G62

¹⁴ Note in the realistic case, in the absence of the GPR, V_{cs} or the touch voltage at an appurtenance reduces to $V_{cs} = V_p$

At the transfer point, R_{coating} goes to zero and the pipe voltage is limited by R_e and Z_{pe} . In reality the soil structure is more complex and sophisticated grounding software is needed to evaluate the soil potential at the pipe. In addition, an induced voltage may also be present on the pipeline which typically adds to the stress level across the coating.

If R_e were zero, this would imply an arc due to soil ionization. This is considered unlikely since the spacing between the pipeline and tower footing would have to be very small for a power frequency discharge [2]. A lightning discharge has the ability to ionize the soil but the ionized zone has been found to only extend a few tens of cm from the tower electrode. It is further usually assumed the lightning discharge would have dissipated by the time the power frequency or DC pole current discharge commences. In this regard the 10 m spacing recommended in [1] should be more than adequate for the DC fault levels anticipated.

Ontario Hydro (now Hydro One) carried out staged faults in the early 1980s upon transmission towers in order to determine the surface voltage gradients that would occur in practice. Reference [7] discusses a sequence of measurements made upon some 765 kV and 500 kV AC towers along with comparison to SES's MALT program. The findings were the type of tower foundation greatly impacts the GPR as one moves away from the tower leg. Some of the results from [7] are reproduced in Figure 14. Pertinent information when considering the results:

- To approximate the measured result, the analytical study used a two layer soil model for the AEP tower: top layer 20 meters with 40 ohm-m resistivity, bottom layer 200 ohm-m. Similarly for the Klienburg tower, a two layer model with top layer 15 m thick with 30 ohm-m resistivity and bottom layer resistivity of 100 ohm-m. The measured footing impedances for the Ontario Hydro and AEP towers are shown in Table 2.
- In Figure 14 the distances were measured radially from the tower footings which were either bonded to ground rods or to rebar in concrete caissons.
- Though the percent drop with rebar is less with distance compared to rods, the actual GPR is less for the same distance compared to having only rods due to the lower footing resistance (Table 2). As an example if the ground current were 3 kA and the GPR at 25 meters is to be estimated for the Klienburg tower:

GPR with rebar	$(3 \text{ kA}) (1.41 \text{ ohms}) (.250) = 1.057 \text{ kV}$
GPR with rods	$(3 \text{ kA}) (2.77 \text{ ohms}) (.18) = 1.495 \text{ kV}$
- The Klienburg tower had the most uniform soil conditions but was only measured out to 10 meters. The AEP tower with poorer soil conditions was measured out to 30 meters. Extrapolation is based upon slope of AEP data.
- AEP data based upon rods.

- Of note the foot print of the lattice towers investigated is comparable to the HVDC tower (10 x10 m square) see Figure 3.

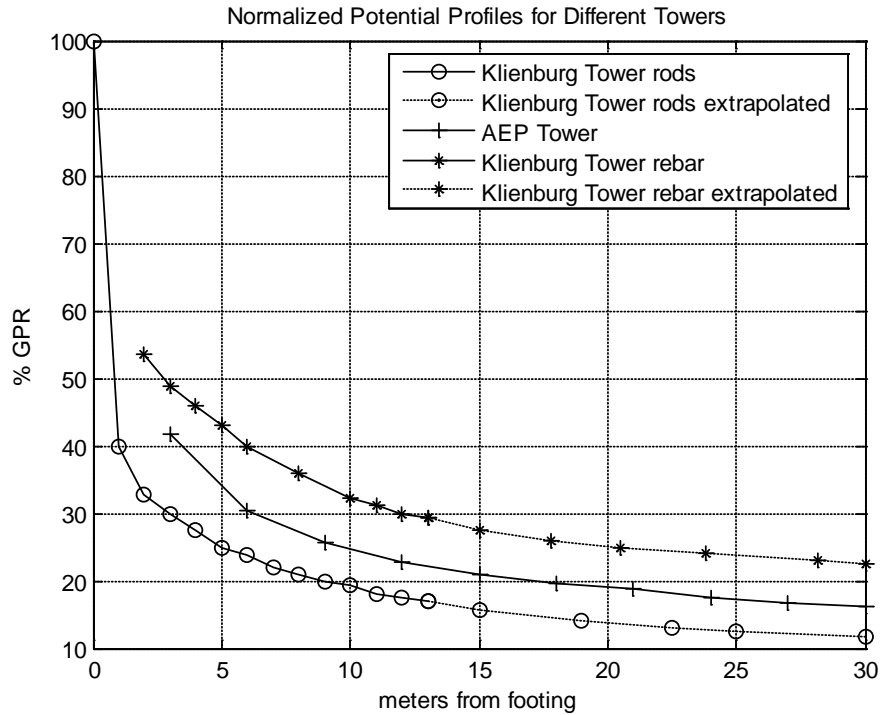


Figure 14 Normalized Potential Profiles from Reference [7] for Lattice Towers

Table 2 Ontario Hydro/AEP Lattice tower Footing Impedances

Tower	Footing Impedance ohms (measured)	Soil Resistivity Model based on measurement
Klienburg (4 rods)	2.77	30 ohm-m (15m)/100 ohm-m (bottom layer)
Klienburg (concrete caissons)	1.41	30 ohm-m (15m)/100 ohm-m (bottom layer)
AEP tower 486	3.6	40 ohm-m (20m)/200 ohm-m (bottom layer)
AEP tower 515	7.2	30 ohm-m (3.5m)/700 ohm-m (bottom layer)

For the EATL and WATL lines, actual HVDC tower foundations will consist of H piles, concrete caissons or screw anchors. The distance from the HVDC tower footing to the edge of the ROW is 25 meters for the HVDC tower. The estimated footing resistances in uniform soil for the HVDC towers are shown in Figure 15.

Calculation is based upon procedures presented in reference [8]. The H pile (mutuals) curve represents the effect of calculating each corner electrode resistance individually and then using a mutual correction term [5]. The other curves treat the 4 electrodes as a single entity. Figure 15 shows footing resistance difference between installing caissons or H piles is small provided they penetrate the same depth.

Part of the HVDC line commissioning procedure is measuring of the footing resistance at each tower with a target value of less than or equal to 10 ohms¹⁵. Early results indicate values in the 1.0 to 9.0 ohm range with median value of 5 ohms. Based upon Figure 15, it would appear the median soil resistivity lies within a range of 200 to 300 ohm-m, however given the lengths of the HVDC lines, the line commissioning measured footing resistances (seasonally adjusted) in the vicinity of a crossing or parallel should be utilized in any simulations.

Figure 14 highlights that the soil voltage gradient drops very quickly with distance from the tower footing. Since the footing impedance is mainly resistive, a similar variation with higher frequency current components is expected. This resistance is also constant for the frequency range applicable to the HVDC fault condition. As an example, if the footing resistance is 3.5 ohms and the ground fault current is 4 kA pk, then the GPR at 25 meters (edge of the ROW) would be $(0.25)(3.5)(4) = 3.5$ kV pk. The low NACE¹⁶ voltage RMS coating limit is 3 kV RMS or 4.25 kV pk (see Section 6.2). This result suggests pipelines passing as close as 25 meters to the tower footing are not at risk as far as coating stress is concerned due solely to the transferred GPR, however induced voltage effects would still have to be factored into the assessment.

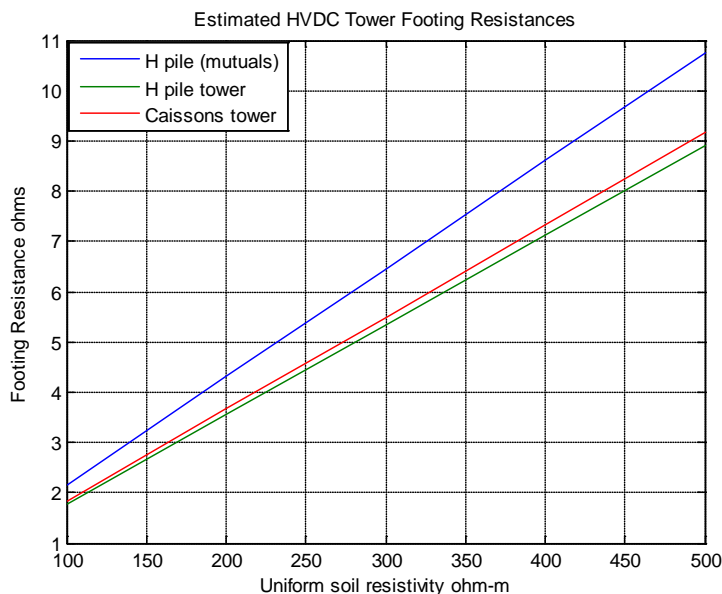


Figure 15 Estimated HVDC Tower Footing Resistance

¹⁵ If greater than 10 ohms, mitigation is applied to reduce the resistance

¹⁶ NACE – National Association of Corrosion Engineers

Compared to Figure 12, it is clear that increasing the separation between the pipeline and HVDC line has the greatest impact on conductive coupling as opposed to inductive coupling.

5 Application Example

In this section, the induced and conducted voltages for a DC tower fault will be simulated for a pipeline that parallels the HVDC line for a significant distance. In order to complete the simulation the following data is needed:

1. Power line geometry, conductor size, conductor coordinates at tower and minimum sag
2. Fault current waveform to be obtained from the utility company for a back flashover event
3. Pipeline data, diameter, steel resistivity, permeability, coating type, thickness and resistivity, burial depth
4. Pipeline path relative to power line
5. Soil resistivity data in vicinity of the nearest towers and the tower footing resistance if recorded by the utility or description of the foundation /grounding details

Suitable modeling software would also be a requirement.

The pipeline parallels the HVDC line for 2.225 km before making a 90° exit from the power line. The spacing is 30 meters from the centerline of the power line. The tower footing resistance was set at the threshold value of 10 ohms at each tower. Pipe diameter is 60 mm (NPS 2.5 OD) with PE coating having a relatively low resistivity of 1000 ohm m². Ground resistivity is set at 100 ohm-m. A back flashover fault involving the DMR is simulated. The pipeline/HVDC line configuration is shown in Figure 16.

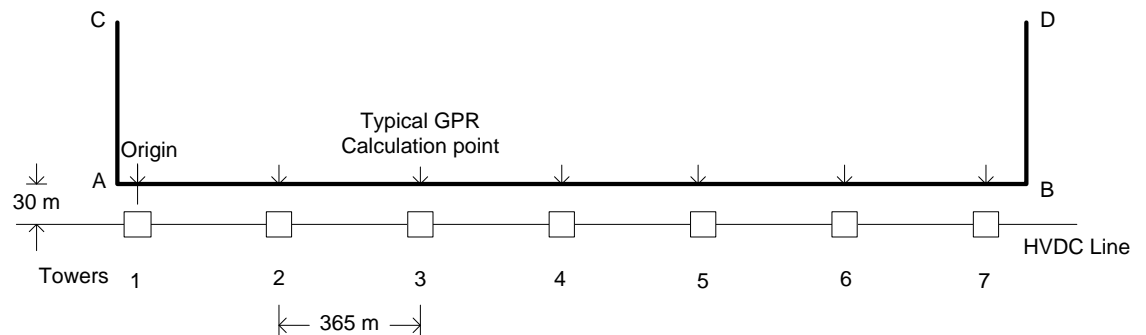


Figure 16 Pipeline/HVDC line geometry

Parametric studies of pipeline coating thickness, pipeline diameter, and coating resistivities suggest smaller diameter pipelines with highly resistive coatings present the least electrical loading to the power line, which lead to the highest induced voltages. In Figure 16, tower 1 is closest to the rectifier terminal.

The worst case overvoltages occur when the tower fault occurs at the mid parallel point (tower 3 or 4) or at tower 7.

In Figure 17, a comparison of the EMTPRV output and the output from SES's Multi Fields program is displayed (induction only).

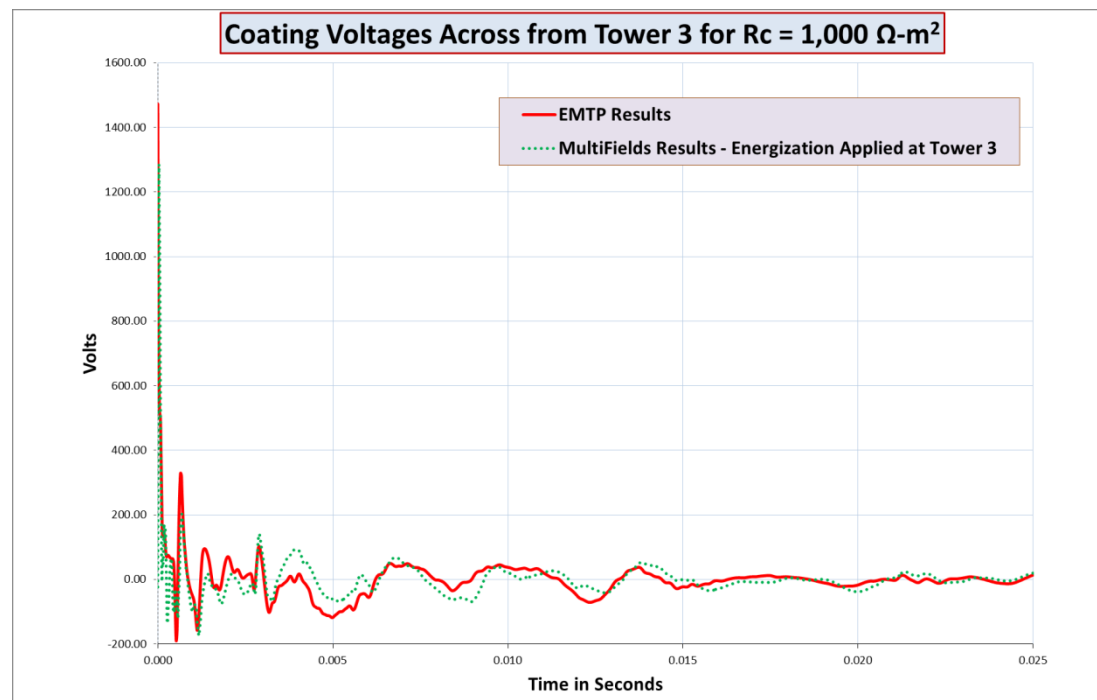


Figure 17 SES CDEGS output compared to EMTPRV output

The two results are very similar but there are some differences. Of note:

1. The initial spike is due to the step change in current at the beginning of the fault. As discussed, this initial transient would be common to either an AC or DC fault. In terms of magnitude it is the dominant feature.
2. Beyond the initial spike, a lower but albeit relatively high frequency component due to wave reflections on the line manifest.
3. The low frequency ripple which makes up the bulk of the wave form reflects the natural frequency of the line transient.
4. Beyond the initial spike, the voltage doesn't exceed 330 Vpk
5. The entire event lasts only 20 msec.

6. The waveforms represent the induced voltage without a conducted component since EMTP type programs have to approximate the conducted component empirically using data such as depicted in Figure 14. Also EMTP type programs cannot represent the frequency dependence for mixed systems of overhead and underground conductors and must be tuned to the dominant frequency present. This becomes a problem if two dominant frequencies are present. In Figure 17, the EMTP program is tuned to 300 Hz which would cause any lower frequency components to be amplified leading to a more conservative result. The SES CDEGS software doesn't suffer from these restrictions and can also calculate any conducted voltage component¹⁷.

The impact of soil layer modeling is displayed in Figure 18 as set up in SES's software. In this example, the upper layer has thickness 0.4 m with resistivity of 75 ohm-m; bottom infinite layer has resistivity of 18 ohm-m.

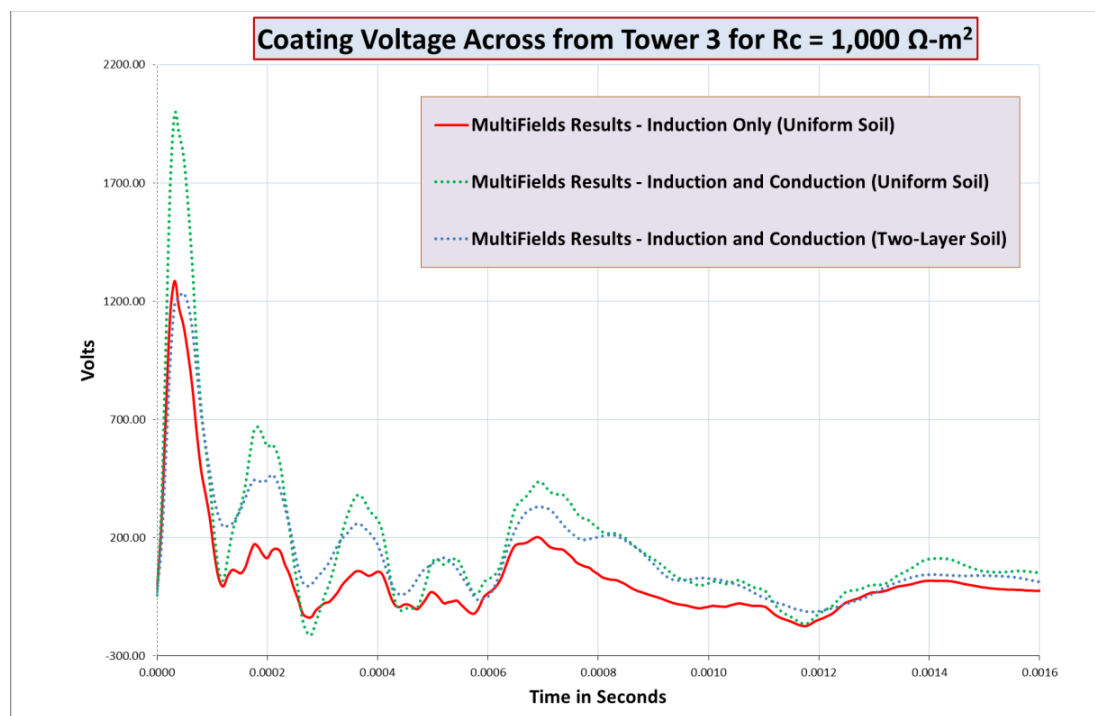


Figure 18 SES CDEGS output for example problem

In Figure 18, the worst result occurs when both induction and conduction are considered for uniform soil. For a two layer soil, the results are less severe. Note the time scale is expanded compared to Figure 17.

¹⁷ Both programs are needed to handle the conduction/induction problem, SES CDEGS (or an equivalent program) for the induced/conducted voltages appearing on the pipeline and an EMTP like program for calculating the fault current for injection into the SES CDEGS program.

6 Result Interpretation

The simulated results from the last section must be interpreted in the context of pipeline impacts discussed in Section 1.2. The first two aspects: safety and damage to the pipeline coating will be considered in detail.

6.1 Safety

6.1.1 IEEE Standard 80

IEEE Standard 80 [9] deals mainly with safety within energized substations but by necessity presents a criterion for evaluating personnel safety in the presence of electric shocks. The criterion was developed by Charles Dalziel over a period of 25 years of empirical research on both humans and animals.

The human shock hazard associated with a person touching a pipeline appurtenance (being exposed to the induced/conducted pipeline voltage, V_{cs} in Figure 13) can be estimated by using Dalziel's energy relationship for impulse shocks [10]:

$$E_{body} = \int_0^{\infty} \frac{V_{cs}^2}{R_b} dt < E_{fr}$$

Where R_b is the resistance of the human body and the minimum energy to cause heart fibrillation is given by E_{fr} . Within the IEEE standard, the internal body resistance is set at 1000 ohms. Frequency effects are not discussed but a reduction due to frequency per IEC 60479 would reduce this value to 775 ohms for frequencies less than 2 kHz.

What modern research has shown is that there is a vulnerable period during the heart cycle when disruption can lead to ventricular fibrillation (**Figure 17** in [11]). Timing of the impulse or oscillatory discharge becomes critical since the disruptive current while appearing similar in magnitude can have a shorter duration if it coincides with the heart's vulnerable period.

To simplify the shock hazard evaluation, the energy approach is approximated by equating the hazard with the RMS value of the shock current. This allows equations for step and touch potential to be derived per IEEE Standard 80 which provides two equations for tolerable body current (low risk of ventricular fibrillation ($\leq 0.5\%$)):

$$I_b = \frac{0.116}{\sqrt{t_s}}$$

Dalziel for 50 kg Body Weight ($0.03 < t_s < 3.0$ seconds)

$$I_b = \frac{0.157}{\sqrt{t_s}}$$

Dalziel for 70 kg Body Weight (0.03<t_s<3.0 seconds)

For event durations greater than 30 msec the above equations should apply. The second formula for larger body weight would apply to the average adult male. Both these equations are based upon energy concepts and will apply to current impulses.

6.1.2 IEC 60479 Parts 1&2

The IEC standard 60479 parts 1&2 focuses entirely on the effects of electric currents upon humans and animals. Besides referring to Dalziel’s work, work from other contributors is highlighted. An impedance model of the human body is provided for estimating the shock hazards for both AC and DC currents. The total body resistance includes both the effects of skin impedance (which has a capacitive component) and internal resistance. The internal body resistance is 775 ohms (hand to hand) at 60 Hz [11]. The total body resistance depends upon both contact voltage and frequency. The high frequency (<2 kHz) approximation approaches 600 ohms (**Figure 12** in [11]).

One of the main results in the IEC Standard 60479 Part 1 is **Figure 20** in [11] “Conventional time/current zones of effects of a.c. currents (15 Hz to 100 Hz) on persons for a current path corresponding to left hand to feet”, part of which is reproduced in Figure 19 in this guide.

Different regions are delineated with curves and definitions given in **Table 11** in [11]. In **Figure 20** in [11] the minimum shock duration is 10 msec which corresponds to 1 cycle at 100 Hz (shown as the horizontal boundary line in Figure 19 in this guide). The *c1* curve defines the boundary between regions AC-3 and AC-4. The region AC-3 to the left of *c1* is defined as:

“Strong involuntary muscular contractions. Difficulty in breathing.
Reversible disturbances in heart function. Immobilization may occur.
Effects increasing with current magnitude. Usually no organic damage to be expected.”

For curve *c1* and to the left no fibrillation should occur.

Region AC-4 is divided into 3 regions. The region AC-4.1 is defined between curves *c1* and *c2*. This region is described as having a probability of ventricular fibrillation increasing to 5%. The region between *c2* and *c3* has the probability of ventricular fibrillation rising to 50%. From an absolute safety perspective, the shock currents should not be allowed to increase beyond the *c1* boundary. Arguably there may be some instances where the regions between *c1* and *c2* can be tolerated and in even rarer cases the region between *c2* and *c3*.

It is also noted that for durations less than 200 msec, ventricular fibrillation can be initiated in the vulnerable region of the heart cycle if the same magnitudes are exceeded. For short duration events an additional element of probability now arises.

For unidirectional impulses, **Figure 20** in [12] applies. The *c1* and *c2* curves are continuous from **Figure 20** in [11] having the same meaning.

The two **Figure 20** curves in [11, 12] are combined and shown in Figure 19 in this guide, the IEEE 80 fibrillation thresholds have been added for reference. Note at 60 msec, the IEEE 50 kg curve¹⁸ becomes more stringent than the *c1* curve.

The following procedure is recommended to estimate the shock hazard potential of body currents due to HVDC fault events:

1. The body resistance, Z_T , is set at 600 ohms for the body path hand to hand or hand to foot, or 450 ohms for the path hand to feet if the highest frequency components are less than 2 kHz. This is a conservative approximation since shock currents are maximized¹⁹.
2. The event duration is defined as the shortest time interval of the event waveform that contains 95% of the energy over the total duration of the event waveform. Alternatively, the waveform can be enclosed in an exponentially decaying envelope. According to IEC 60479-2 [12] when the decay value of the envelope has reached 5% magnitude, the duration of the event waveform is defined. The former definition is less arbitrary and can deal with more complex wave shapes.
3. The RMS value of the event waveform can be calculated for the decay duration defined in point (2) above, and after application of the heart-current factor, F , compared to the *c1* curve Figure 19.
4. Any high initial current (within the first 4 msec) needs to be considered prior to the biphasic oscillations per IEC 60479-2[12]. The approach is to calculate the specific fibrillation charge, F_q or the specific fibrillation energy, F_e which are defined with the following limit conditions:

$$I_{crms} = \sqrt{\int_0^T \frac{1}{T} i_b^2(t) dt} \text{ Where } T=.004 \text{ sec}$$

$$F_q = I_{crms} T < .002 \text{ Coulombs (A sec) or 2 mC}$$

$$F_e = I_{crms}^2 T < .001 \text{ A}^2 \text{ sec}$$

¹⁸ Care is required since IEEE 80 assumes $R_b = 1000$ ohms for internal impedance which is greater than the IEC value. With this R_b value assumed, the difference in severity between the two standards is much smaller when consistently using only the IEEE methodology.

¹⁹ This approach effectively calculates the maximum hand to feet body current if $Z_T=450$ ohms, since shoe impedance plus the contact impedance of the soil layer is ignored see also Appendix L [2].

Where it is assumed the body path is hand to feet otherwise the heart-current factor, F needs to be applied to I_{crms} .

Annex A.2 contains more detailed information upon the background and application of the above procedure.

Within this guide, usage of Figure 19 is based upon a hand to feet discharge path, for other discharge paths such as hand to hand, the heart-current factor, F , discussed in Section 5.9 in IEC 60479-1[11] needs to be applied. The heart-current factor, F is used to equate the same fibrillation probability for the reference current I_{ref} with the current I_h for the path in question:

$$I_h = \frac{I_{ref}}{F}$$

Where I_{ref} is the body current for the path left hand to feet given in Figure 19

I_h is the body current for the path in question (Table 12 in IEC 60479-1)

F is the heart-current factor (Table 12 in IEC 60479-1)

As an example, $F=0.04$ for left foot to right foot path. If the hand to feet current was $I_{ref}= 90$ mA, I_h would be 2250 mA. A foot to foot path requires a current of 2250 mA to have the same fibrillation effect as a 90 mA hand to feet current.

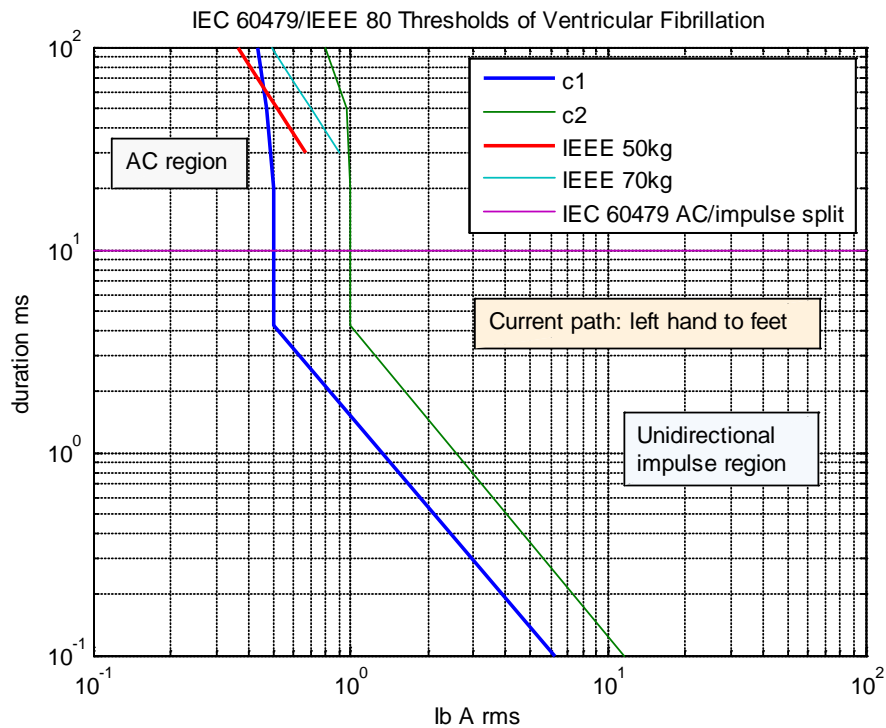


Figure 19 IEC 60479/IEEE 80 Ventricular Fibrillation Thresholds

6.1.3 Application Example

During the evaluation of a pipeline parallel issue, the following body current waveform shown in Figure 20 is obtained for a back flashover on the tower. Following IEEE Standard 80, the loading effect of the body resistance is ignored in the circuit. The IEEE 80 standard prefers to work with touch and step voltages but in the context of the transient waveforms expected with HVDC faults, it is more preferable to work directly with currents which allow comparison to both IEEE and IEC standards. The shock current becomes the coating stress voltage in RMS, V_{cs} , divided by the body resistance R_b set at 450 ohms. The hand to feet discharge path is assumed at the hypothetical appurtenance.

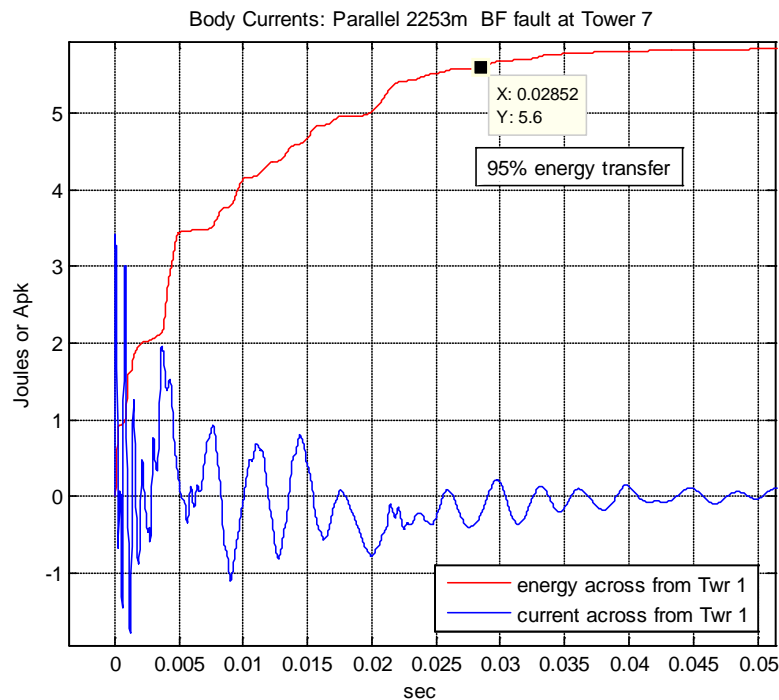


Figure 20 Induced Body Current at Tower 1 with BF at Tower 7

The first step is to determine the duration of the event using an exponential envelope as shown in Figure 21 or determine the 95% energy transfer point as shown in Figure 20. According to Figure 21 the duration for this event is 33.6 msec (the envelope current has declined to 5% of its initial value) or 28.5 msec based upon energy. Note the absolute value of the current is plotted to obtain the envelope²⁰. The total event RMS current is calculated based upon either of the time intervals. Since the energy transfer gives the shorter window it is chosen.

Table 3 presents the event summary calculations.

²⁰ In this example the simple exponential decay envelope works well

Table 3 Event Summary Shock Current across from Tower 1

Event Waveform Duration (msec)	28.5
Total Event A RMS	0.665
Path	Hand to feet
Heart current factor	1.0
Specific Fibrillation Charge, F_q (4 msec) mC	5.1
Specific Fibrillation Charge limit (4 msec) mC	2.0

In Table 3 the event is unsafe in regard to IEC standards in terms of total event RMS current and also fails during the initial oscillatory impulse region since the specific fibrillation charge, $F_q > 2$ mC. See Annex A.2 for a more detailed discussion on the general analysis of shock currents.

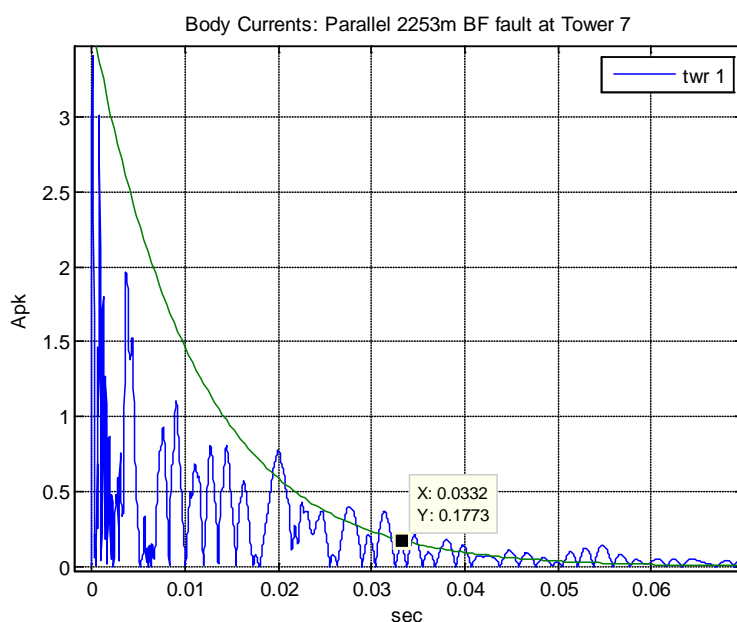


Figure 21 Exponential Envelope applied to absolute value of Body Current

As another example, Figure 22 illustrates the body current profile for a shallow mid span crossing of 9.4 degrees. Like the parallel scenario, this fault involves a back flashover at tower 2. The crossing point is between towers 1 and 2 with the pipeline zero reference across from Tower 1. This curve was obtained by estimating the average event duration, generating the RMS value of current from the coating stress voltage data.

At the start and end of the crossing the pipeline runs perpendicular to the power line. The maximum induced voltages/body currents occur at these points as shown in Figure 23; however, these are not the points having the highest initial current spike as shown in Figure 24 which occurs directly across from Towers 1 and 2 (note the conducted voltage is being ignored at Tower 1) in this example. The

fault point was Tower 2. In Figure 24, the red exponential envelope refers to the Tower 2 waveform, whereas the cyan exponential envelope refers to the Tower 1 waveform. The body resistance assumed in this example was 600 ohms implying a hand to hand current path²¹.

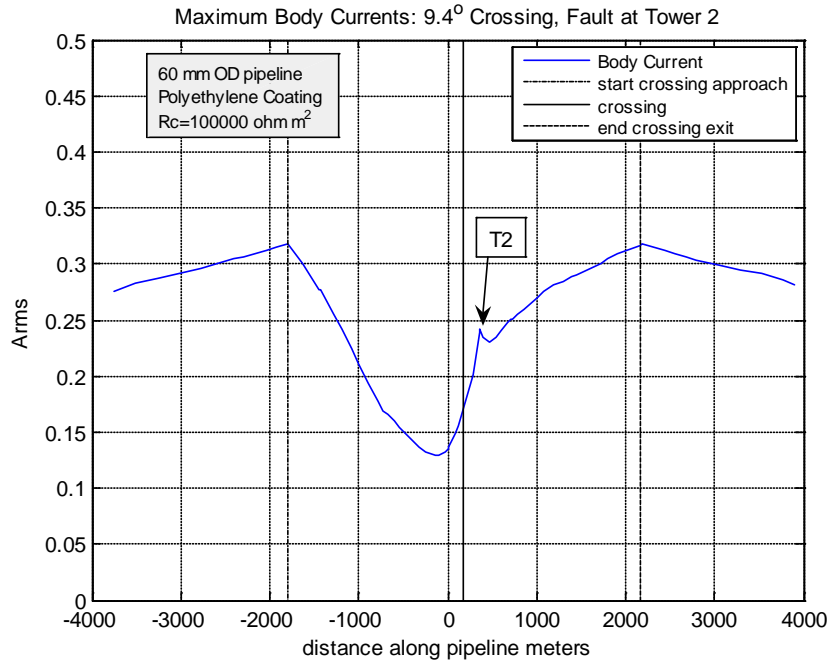


Figure 22 Estimated Induced Body Current Profile along Pipeline (hand to hand path)

²¹ To scale the current for the hand to feet (adjusting for reduced body impedance Z_T) path the RMS current is multiplied by 1.333, of course in a specific case the touch voltage appropriate for hand to hand contact should be calculated. The same holds for the touch voltage appropriate for hand to feet contact.

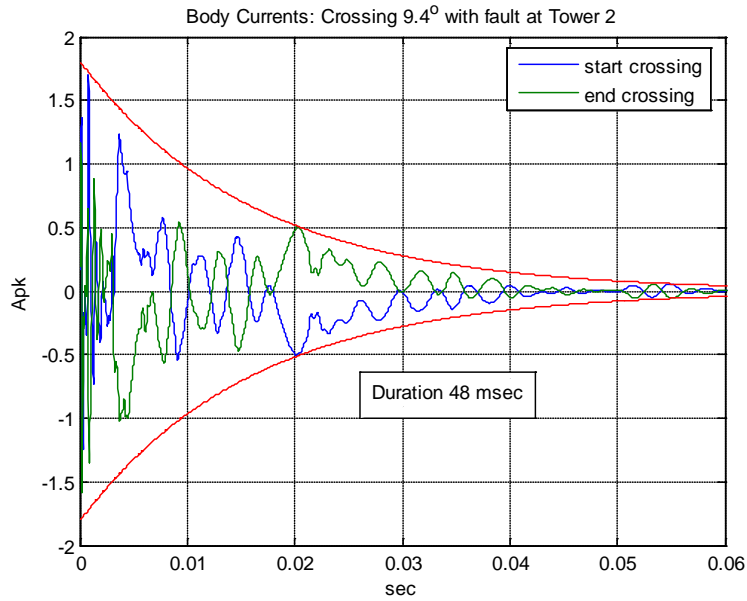


Figure 23 Induced Body Current (hand to hand path) with largest RMS value

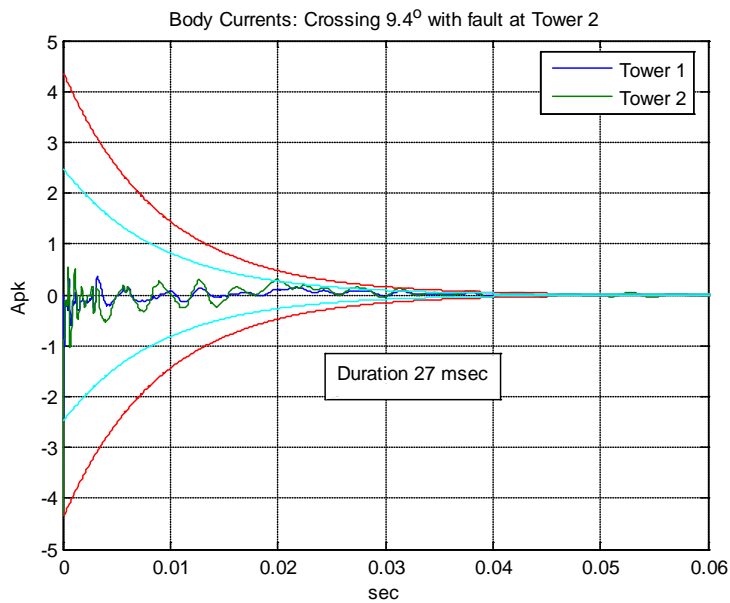


Figure 24 Induced Body Current (hand to hand) with highest initial value

In Figure 23 and Figure 24 the event durations are 48 and 27 msec respectively. The calculated RMS current values and specific fibrillation charge (for Tower 1 & 2 cases) is summarized in Table 4 where the heart-current factor, F , is 0.4 for the hand to hand path.

Table 4 Body Currents for Crossing Results Hand to Hand path (Fault at Tower2)

Pipeline Location	Duration Msec	I_T Complete event, Arms	Fibrillation Current Arms $F I_T$	I_{crms} Arms (at 4 msec)	Specific Fibrillation Charge mC (at 4 msec) $F I_{crms} (0.004)$	Specific Fibrillation Charge limit mC
Path		Hand to Hand		Hand to Hand		
Heart current factor			0.4		0.4	
Start crossing	48	0.291	0.116	.693	1.12	2
Across from Tower 1*	27	0.164	0.066	.243	0.523	2
Across from Tower 2	27	0.291	0.116	.166	0.357	2
End crossing	48	0.290	0.116	.643	1.39	2

*Conducted voltage ignored

The cI current limit at 50 msec is 0.475 Arms, and at 27 msec is 0.485 Arms. After application of the heart-current factor all events are to the left of the cI curve. The specific fibrillation charge is less than 2 mC; hence safety hazards are not created.

If the current path were hand to feet with the lower body resistance of 450 ohms, the result would be quite different as shown in Table 5. While the total event current RMS value is less than the IEC limit, safety problems occur in the first 4 msec of the event at the start and end of the crossing.

Table 5 Body Currents for Crossing Results Hand to Feet path (Fault at Tower 2)

Pipeline Location	Duration Msec	I_T Complete event, Arms	Fibrillation Current Arms $F I_T$	I_{crms} Arms (at 4 msec)	Specific Fibrillation Charge mC (at 4 msec) $F I_{crms} (0.004)$	Specific Fibrillation Charge limit mC
Path		Hand to feet		Hand to feet		
Heart current factor			1.0		1.0	
Start crossing	48	0.387	0.387	.934	3.73	2
Across from Tower 1*	27	0.219	0.219	.324	1.30	2
Across from Tower 2	27	0.387	0.387	.220	0.88	2
End crossing	48	0.387	0.387	.857	3.43	2

6.2 Coating Stress

When voltage is applied to a dielectric material, the electric field applies a force on the bound electrons in the outer orbital of the atoms. At the breakdown electric field stress, a few electrons are lifted to the conduction band and quickly accelerated. Collisions with other atoms can release more electrons leading to an avalanche effect culminating in breakdown of the dielectric. Electrical breakdown is a complex phenomenon depending upon the electric field strength, geometry of the sample (thick or thin film), temperature and homogeneity (freedom from defects). When such materials are used in electrical devices, proof tests are needed to verify quality of the device. Both power frequency voltage withstand tests and impulse tests (both below the failure level) are required.

Impulse breakdown characteristic due to lightning induced transients lead to higher crest voltages being required. In general as the voltage duration is reduced, a higher voltage is needed to cause breakdown. This suggests a minimum energy requirement for breakdown to occur. The impulse ratio is the ratio between impulse voltage (V_{pk}) needed for breakdown over the AC voltage RMS breakdown value. This ratio can vary from 1.6 for air up to 2.5 for polyethylene.

6.2.1 Holiday Test on Pipelines

According to ASTM G62 [13] the continuous test voltage that may be applied to the pipe for holiday detection is (where T_d must be in mils):

$$V_{test} = 1250\sqrt{T_d} \text{ Vdc} \quad T_d > 41 \text{ mils (1.04 mm)} \quad (1)$$

Below this thickness, equation below applies:

$$V_{test} = 525\sqrt{T_d} \text{ Vdc} \quad T_d < 41 \text{ mils (1.04 mm)} \quad (2)$$

For a coating thickness of 30 mils (760 microns), the test voltage would be 2.87 kV DC, whereas for extruded polyethylene coatings (1.08 mm or 42.5 mils) the voltage withstand would be 8.15 kV DC.

Under DC voltage stress, the voltage grading for a composite coating will be based upon shunt resistance across each coating layer. With extruded polyethylene tending to have the highest apparent volume resistivity and thickness, nearly all the voltage drop is across this layer (>90% for high performance composite coatings).

The primary purpose of the DC test voltage in the ASTM standard is to detect voids, metal particles protruding through the coating, pinholes and thin spots. Clearly the level of detection voltage will determine the defect level of interest. A low level will only detect gross defects such as metal protrusions whereas a high test level will detect thin spots and large voids. The quality of the factory coating which was applied in a controlled environment should have withstands at least approaching the ideal AC test voltages, whereas field coating of welded joint sections will be lower.

6.2.2 NACE Standards

According to [14] the NACE AC fault limits (in No. 21021-2007) may be too conservative. For FBE and polyethylene coated pipes a NACE AC limit of 3 to 5 kVrms applies respectively for short duration faults. The authors, using 410 microns (16 mils) as an example and equation (1) suggests a continuous test voltage of 5 kV DC. While this correlates with the NACE upper limit of 5.0 kVrms AC at least numerically, a thicker coating would have a much better value. An apparent contradiction in withstand time under fault versus an indeterminate time under test conditions arises.

The authors then compare equation (1) along with the Australian limit of 5 kV for a 410 micron (16 mils) thickness. The Australian limit appears to be using ASTM formula (1) for setting the DC test level but without the discontinuity at 1.04 mm (41 mils). The NACE equation is applicable to non-thin film (FBE) coatings:

$$V_t = 1250\sqrt{T_d} \quad \text{Vdc} \quad \text{appears in NACE SP0274 – 2004}$$

The above equation has an applicability range from 0.51 to 1.9 mm (20 to 750 mils) for non FBE coated pipes, i.e. would apply to extruded polyethylene and should apply to multilayered coated pipe with FBE as the first layer since the PE layer takes most of the dielectric stress. For FBE coating only pipes the formula below applies:

$$V_t = 525\sqrt{T_d} \quad \text{Vdc} \quad \text{is similar to requirement of NACE SP0490 – 2007}$$

The above equation has an applicable range of 250 to 760 microns (10 to 30 mils). And the typical FBE coating thicknesses are in the 250 to 500 micron (10 to 20 mils) range.

The theoretical AC field test withstands for the ideal coatings²² are quite high when compared with the NACE AC fault limits. The holiday test voltages are DC and also far below the theoretical DC withstand capability based upon an ideal coating. Given that the purpose of holiday testing is to search out gross coating defects (pin holes, voids, metallic protrusions), it is really the withstand level of air as manifested in these defects that is being tested. Once the holiday test has been successfully passed, the pipe coating is now considered adequate for its primary purpose which is to limit cathodic protection current leakage. This suggests, in practice once the intrinsic strength of the dielectric material is accounted for, the AC withstand levels are higher than the NACE fault limits. This becomes clearer when the crest value of the NACE AC fault limits is compared to the ASTM/NACE DC test standards. Figure 25 summarizes the results. Note all curves are in units of kV DC or kV pk and therefore on the same comparative base.

The air withstand strength as defined by the Paschen Curve [15] is also presented. The ideal field test voltages for different pipe coatings along with a sensitivity calculation of the ideal test voltage if the outer 100 microns (4 mils) of the PE

²² If treated as an electrical product with minimal insulation defects.

layer were damaged are also included. Note the Paschen curve closely follows the Australian limit.

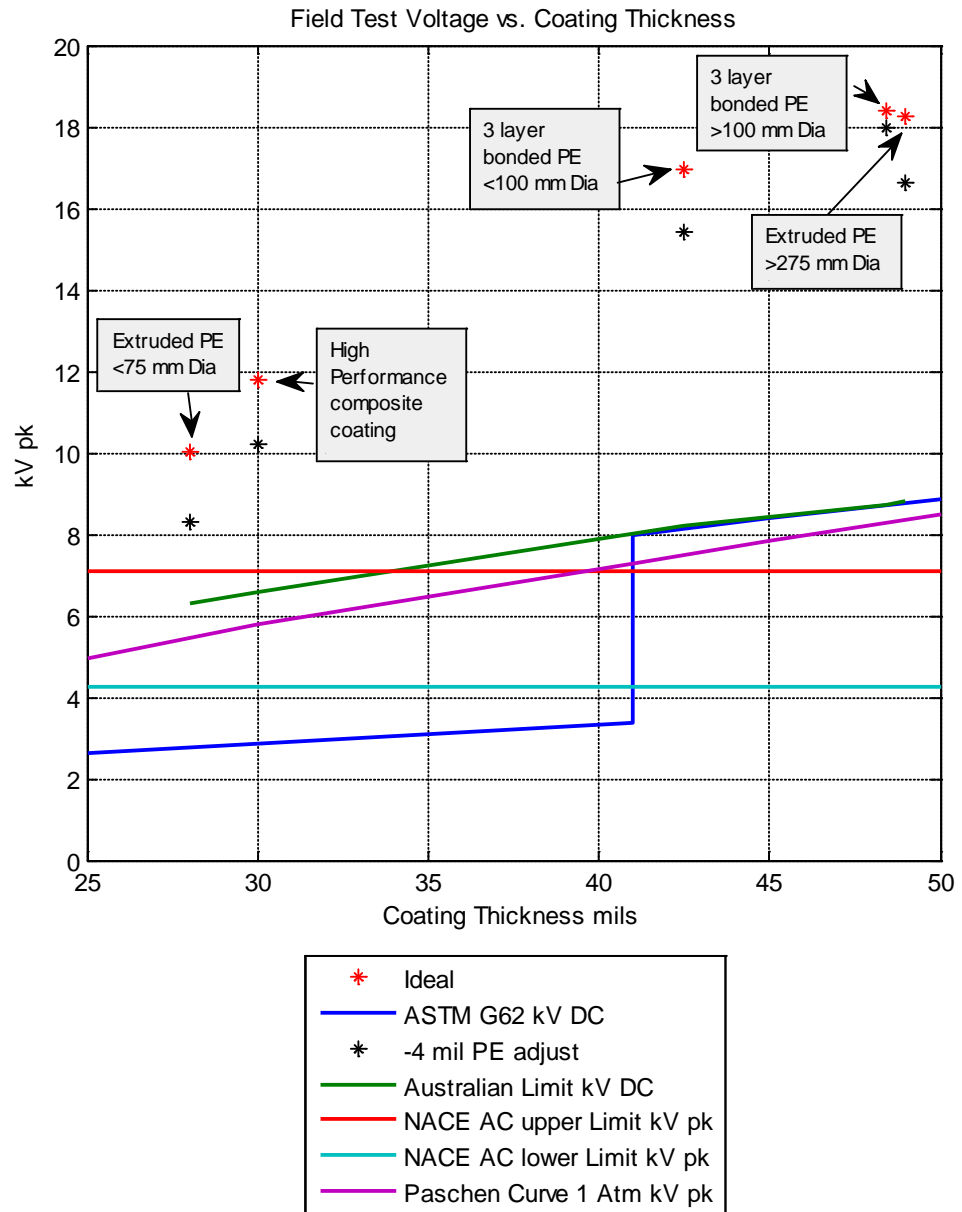


Figure 25 Comparison of NACE AC withstand limits with DC test voltages

The Australian limit exceeds the Paschen curve since any test voltage should exceed the breakdown strength of air for the coating thickness considered. Conversely, it is not clear why the lower ASTM curve (< 1 mm or 41 mils) is less than the breakdown strength of air. The upper and lower NACE AC fault limit curves appear to approximate the test voltages depending upon coating thickness.

In summary, it appears the NACE AC fault upper limit along with a safe impulse level of 12.5 kV pk (impulse ratio based upon polyethylene) appears to represent the low withstand boundary. This low level should provide a large coating safety level for voltages exceeding this limit.

Modern multilayer coatings should follow the upper NACE limit since most of the voltage drop occurs across the outer polyethylene layer. Depending upon the coating thickness and type either the NACE upper or lower limit will apply. Table 6 should be considered a conservative assessment criterion for application to the transient pipeline coating stress voltages arising during HVDC fault conditions.

Table 6 Transient Withstand Criterion for HVDC Coating Stress Evaluation

Coating Thickness Microns (mils)	Coating type	AC Withstand Power frequency kV pk	Impulse Withstand kV pk
500 to 19,000 (20 – 750)	Polyethylene, Composites where outer layer is Polyethylene	<7.07	<12.5
250 to 760 (10 -30)	FBE(Fusion bonded Epoxy)	<4.24	<7.5

When the above criterion is applied to the coating voltages shown in Figure 17 and Figure 18, the withstand margin is large (peak transient voltage below the AC power frequency withstands in Table 6).

6.3 Damage to Metal

As is discussed in Section 4.0 the portion of fault current entering earth is low relative to an AC line, this leads to a lower GPR profile and a lower risk of a flashover through the soil. In that regard as long as a minimum distance of 10 m is maintained between all tower footings (tower ground) and pipelines [1], the probability of damage(metal) to the pipe due to DC power line faults is considered extremely unlikely.

Should a study determine perforation of the coating could occur, mitigation similar to what is used for mitigating AC issues can be applied.

6.4 Damage to Insulating Flanges

Voltages across insulating flanges under DC fault conditions are expected to be relatively lower than its AC counterpart. However, if software simulations suggest that high voltages will arise during fault events; the same mitigation used for AC problems can be applied.

6.5 Damage to Electrical Equipment connected to the Pipeline

The DC induced transients will be generally less severe but if required, the same mitigation in terms of surge protection on LV circuits can be applied.

6.6 Mitigation Methods

Should a study determine that any of the safety or integrity issues discussed in Section 6.1 through Section 6.5 are of concern, mitigation shall be specified for the subject pipeline(s). The same mitigation used for AC interference issues can be applied to mitigate HVDC issues. Mitigation methods such as ground rods, ground wells, mitigation wire, etc. can be utilized.

Mitigation systems are typically connected to cathodically protected structures through DC decouplers. DC decouplers are applicable for mitigating both lightning and HVAC issues on pipelines. Since HVDC fault waveforms fall between lightning waveforms and HVAC fault waveforms in terms of frequency response and amplitude, DC decouplers are applicable for mitigating HVDC fault issues.

7 Screening Guidelines

Buried pipelines behave like underground conductors in the presence of an HVDC line disturbance (fault). Buried pipelines have a certain voltage withstand limit, and in addition safety aspects arise at above-grade appurtenances. The interaction is geometry dependent, and this screening guideline differentiates between those crossing/parallel geometries requiring study from those that might be dismissed as posing no risk to the pipeline or personnel working in proximity to above-grade pipeline appurtenances.

Since the HVDC fault transient is composed of different frequencies, the magnitude of the induced voltage will display frequency dependence. In this section, these interdependencies are presented with the intent of answering how different pipe diameters, parallel lengths, crossing angles, coating qualities (thickness and resistivity) impact the induced voltage. It should be recalled that the conducted voltage tends to be a short range phenomena with GPR voltages dropping to low values at more than 50 meters from the tower footing with typical soil conditions about the fault point, whereas the induced voltage can extend over several km depending upon the relative paths of the HVDC line and pipeline. In this sense, any pipeline passing within 30 meters from a tower footing should be studied, but for induced voltages the situation is more complex, the effect of several parameters upon the induced voltage needs to be reviewed. It should be noted that any voltage constraints due to safety issues need to be more exact and stringent than those applied to coating stress evaluations.

It is impossible to cover all possible geometries and the guidelines presented are to be used with care. If in doubt, a study should be carried out. For example a dry area where tower footing resistance exceeds 10 ohms or resistivities exceed 100 ohm-m by a large margin, a study should be considered.

7.1 Parameter Sensitivities

7.1.1 Impact of Pipe Diameter

For underground pipelines the coating conductance and capacitance per unit length of pipe depend upon the surface area of the pipe which is directly proportional to the pipe diameter. The capacitance as a function of coating thickness and pipe diameter is shown in Figure 26. For pipe diameters greater than NPS 12 a FBE layer is assumed with increased permittivity relative to polyethylene (which is assumed for pipe diameters NPS 12 diameter and below). There is more than an order of magnitude difference between the smallest diameter pipe considered and the largest. If the volume resistivities for common coating materials are used, high coating resistances arise. Coating resistivities in practice appear much lower. For a given resistivity per m^2 the variation in coating resistance per meter for different pipe diameters is shown in Figure 27.

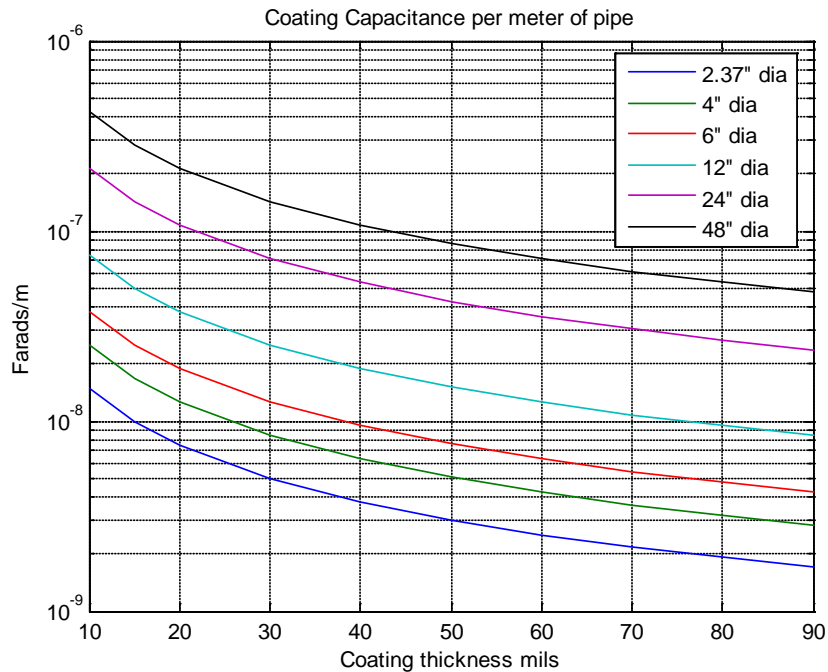


Figure 26 Coating Capacitance Variation with thickness and pipe diameter

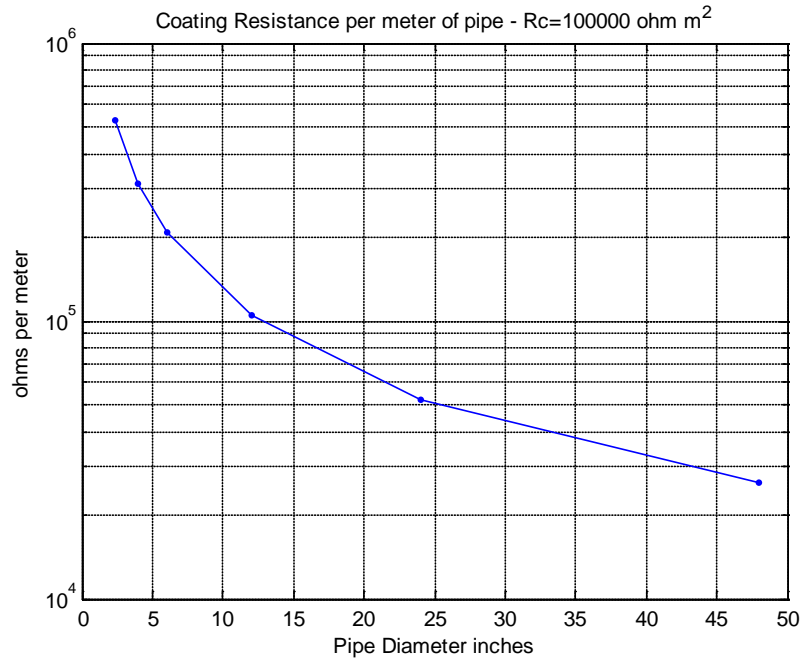


Figure 27 Variation in Coating Resistance with pipe diameter

During induction, the pipeline represents an electrical load to the power line, and as this load increases (larger capacitance and decreased coating resistance) the induced voltages decrease. This occurs as the pipe diameter increases, also the pipe coating reactance decreases with frequency, causing the higher frequency induced components to be more attenuated. An example of this is shown in Figure 28 where a NPS 24 OD pipe is compared to a NPS 2.5 OD pipe. For the larger diameter pipes, the lower natural frequencies of the HVDC line tend to be the dominant frequencies with the implication that larger diameter pipes will be insensitive to impulsive transient, leaving only the sensitivities to the lower natural frequency HVDC line transient (i.e. the tail of the waveform). This tends to explain why the initial transient is not considered in AC inductive coordination studies. In Figure 28, the coating resistivity is the same for both pipe diameters.

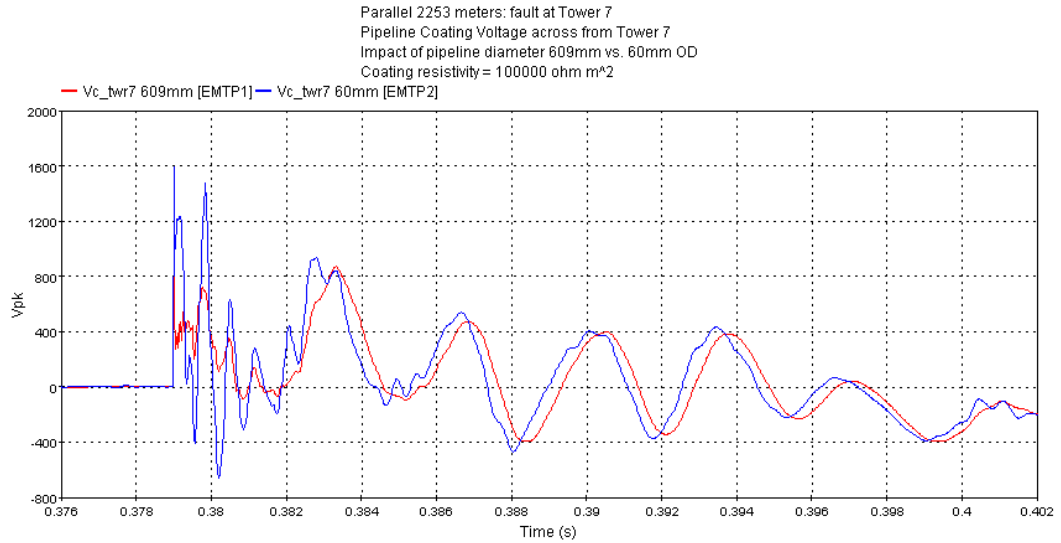


Figure 28 Impact of pipe diameter upon coating voltage (BF)

7.1.2 Impact of Coating Resistance

Lower coating resistances will have a greater impact on the damping of the induced voltage as shown in Figure 29 where the coating resistance is varied from 1000 to 100000 ohm m² for a NPS 2.5 OD pipe. The effect is most pronounced on the high frequency components especially the initial voltage spike.

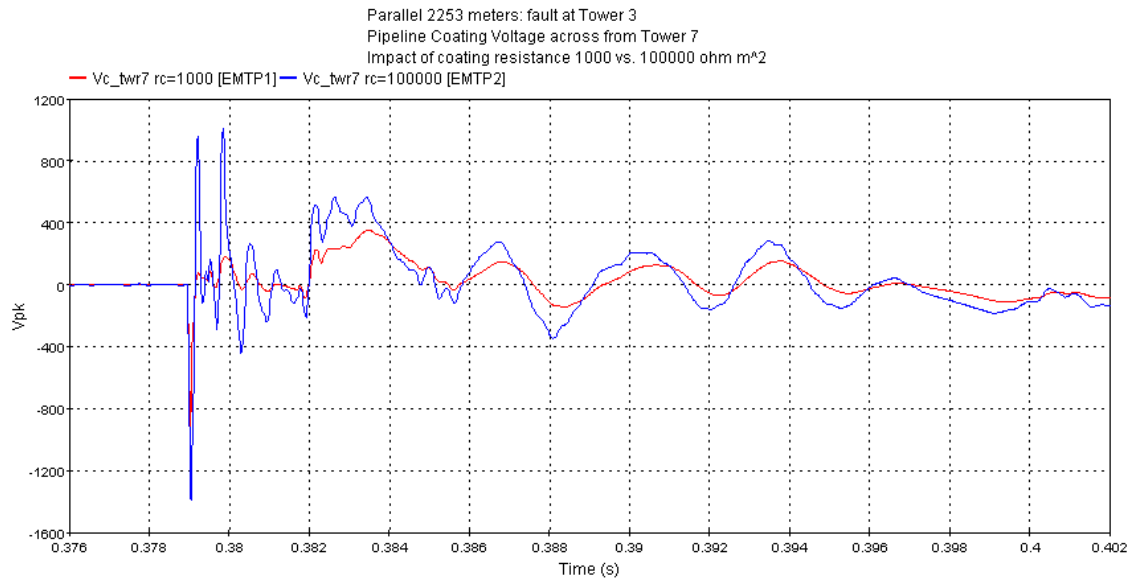


Figure 29 Impact of coating resistance - pipe diameter constant (BP)

7.1.3 Impact of Tower Footing Impedance

This was discussed in Section 4.0. In general a lower footing resistance due to lower ground resistivity or deeper tower foundations will lead to a lower GPR at the edge of the HVDC line ROW.

7.2 Maximum Parallels for Back Flashover Events

What would be the maximum parallel distance before reaching the coating withstand limit? The answer will depend upon several variables, but the intent in this section to provide a rough estimate that can be used to screen the severity of some actual parallels. As noted in Section 3.3, the induced voltage will increase with distance. Given the parameter sensitivities, a smaller diameter pipeline with a high coating resistance should provide the worst case. The pipeline spacing in this example is set at 30 m from the tower center line.

The problem is complicated when it comes to considering which voltage is dominant, i.e. the peak voltage in the event or the tail voltage. Figure 30 displays the peak impulse voltage as a function of distance and compares it to the limits in Table 6. Figure 31 displays the tail voltage as a function of distance and compares it to the AC limit in Table 6. Of note, the impulse voltage tends to be constant with increasing distance. Multiple points are shown representing the coating voltages across from each tower in the simulation. The slight rise in Figure 30 is due to the increasing magnitude of the tail voltage. There is a considerable margin with the lower impulse limit and the lower NACE AC power frequency limit.

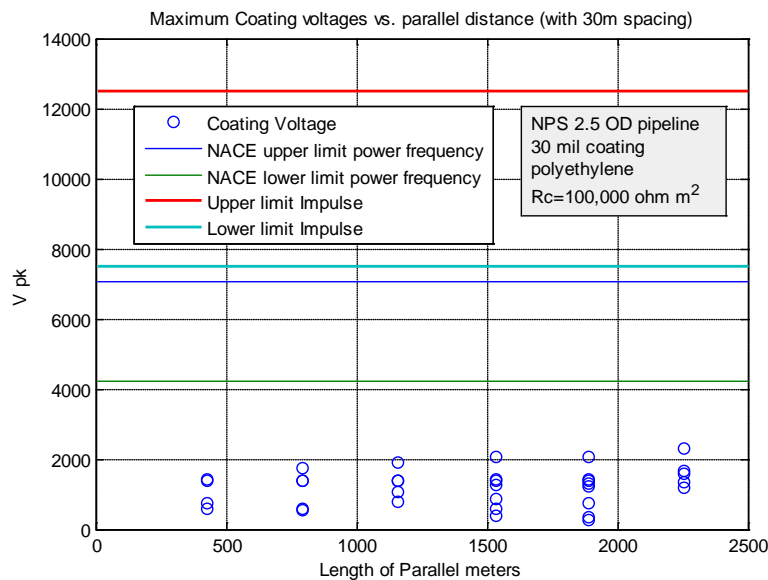


Figure 30 Peak Voltage Summary for Back Flashover Events

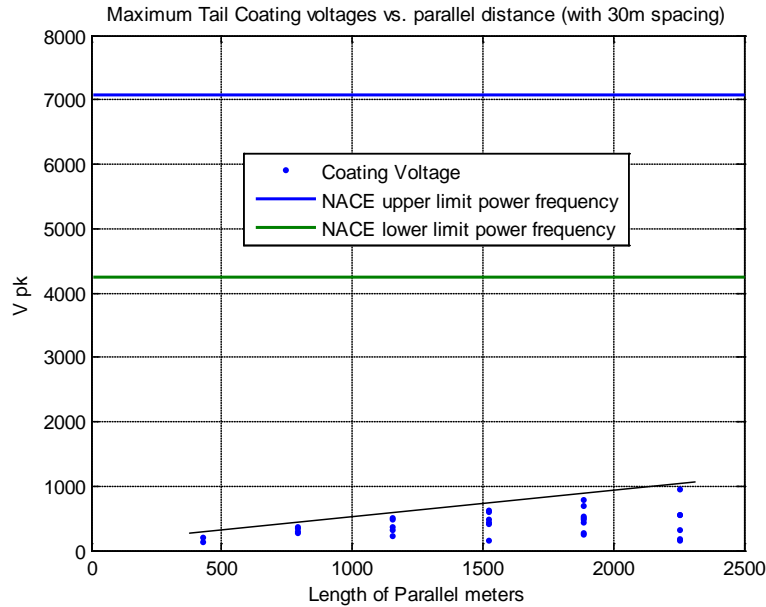


Figure 31 Tail Voltage Summary for Back Flashover Events

In Figure 31 the tail voltage tends to rise linearly with distance. Assuming linearity is maintained, the lower NACE AC fault limit would be reached in 10 km²³. With larger pipe diameters, based upon Figure 28, the limit would be similar. For lower coating resistivities longer parallels are needed to reach the NACE limits. Similarly, a longer parallel with a larger spacing between the pipeline and HVDC line is needed to reach the NACE limits. For pipes running within the HVDC line ROW (<30m) all distances would be shorter.

Note that the above aspect of the screening guideline is not assessing any personnel safety risks associated with the lengths involved by assuming that in this example there is no access to the pipeline. If above-grade appurtenances exist two situations arise:

1. Line fault is remote and downline from the parallel
2. Line fault occurs along the parallel

The down line fault will result in induced pipe voltages with no local GPR, whereas the fault along the parallel will have a large induced component along with a GPR component. The remote line fault will also have a lower frequency content compared to the fault along the parallel. The worst body currents (hand to feet) for the different parallel lengths (at 30 meter spacing) are summarized in Table 7. This is based upon induced voltage only; any appurtenance within 100 meters of the faulted tower will also have a conducted component that will add to the F_q or I_b values. Event duration is based upon the 95% energy transfer²⁴.

²³ For the polyethylene coating assumed the upper NACE AC limit would be reached in 17 km

²⁴ Duration varies with each event; short parallel SF faults have durations less than 20 msec.

Table 7 Shock Hazards (induced voltage) for BF events at different parallel lengths

Parallel Distance km	Remote fault Specific fibrillation charge F_q , mC	Remote fault I_b , Arms	Fault end of Parallel Specific fibrillation charge F_q , mC	Fault end of Parallel I_b , Arms
0.437	0.987	0.147	1.82	0.275
0.802	1.77	0.249	2.81	0.372
1.532	2.7	0.415	4.82	0.635
2.262	2.77	0.514	5.74	0.773

For remote downline BF events, the critical parallel distance based upon F_q is 1 km. For a fault at the end of the parallel based upon F_q , the critical distance is about 0.5 km. This data is in line with Figure 30, the peak initial voltage where F_q is based tends to be independent of the parallel length. Based upon the total event RMS current, I_b , the linear increase with parallel distance is in line with Figure 31. For this particular example of small pipe OD and high coating resistance, the F_q criterion leads to a more severe limit than overall event RMS current.

7.3 Minimum Crossing Angles for Back Flashover Events

An oblique crossing can be approximated by short parallel segments per reference [2] (this is the approach EMTPRV and similar circuit based programs have to use). End effects (those points at the start and end of the crossing) can impact the results and to some extent reflect the real world since crossings seldom extend indefinitely. For the test case, the intersection point is somewhere in the tower span and the pipeline is not closer than 30 meters to a particular tower centerline as shown in Figure 32. In the test case set up, the angle is varied by rolling the pipeline on a circle with a 30 m radius centered upon Tower 1.

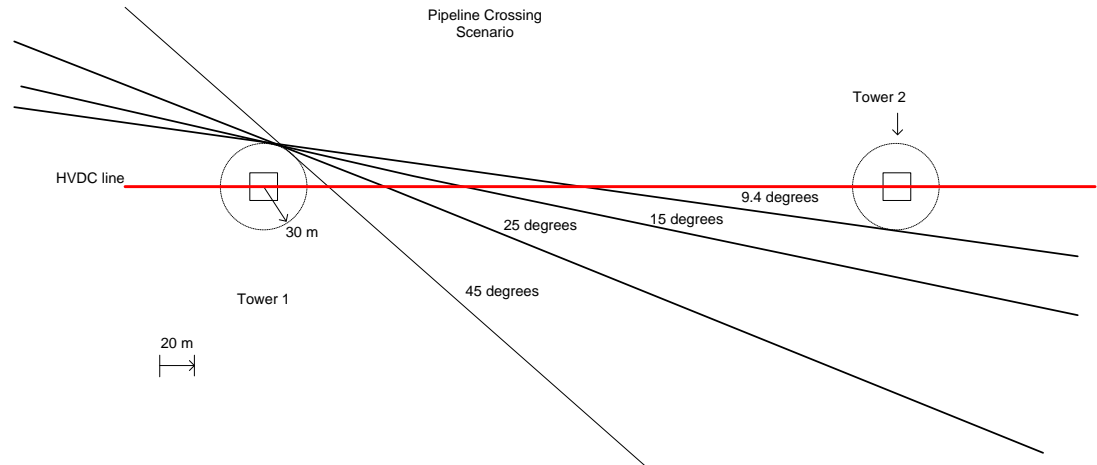


Figure 32 Crossing Geometry

Figure 33 displays the transient peak voltages that arise for faults that occur at Tower 2 and Tower 1 for the different crossing angles. The shallowest angle possible (9.4 degrees) begins to approach a parallel condition. A NPS 2.5 OD pipe with PE coating is assumed. The peak voltages are similar to the parallel case for this angle. As the angle increases, the coupling reduces.

In Figure 34, the tail components reflecting the natural frequency of the HVDC line are displayed. At the start and end of the crossing (where the pipeline is perpendicular to the HVDC line) the voltage peaks appear as slope discontinuities. If the crossing continued for a much longer distance, it would eventually smoothly peak and decline as shown for the 25° case. The length of this crossing is 4 km. By way of comparison, a 4 km parallel (Figure 31) would have an induced tail voltage of 1760 Vpk. The result suggests that crossings are unlikely to have coating stress problems except across from Tower 1 where conduction effects could be large. As the pipe diameter increases, the transient peaks in Figure 33 would decline, becoming insignificant for NPS 24 OD pipelines and above.

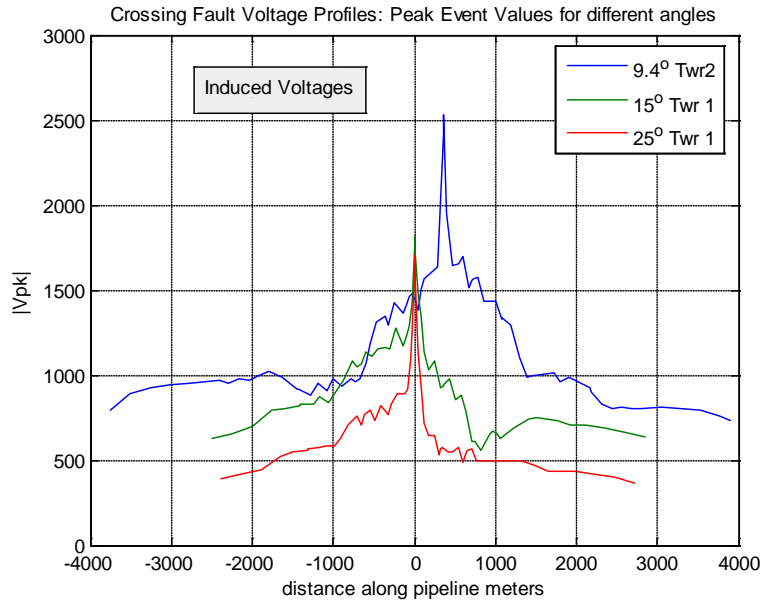


Figure 33 Peak induced Voltages NPS 2.5 OD pipeline with different crossing angles

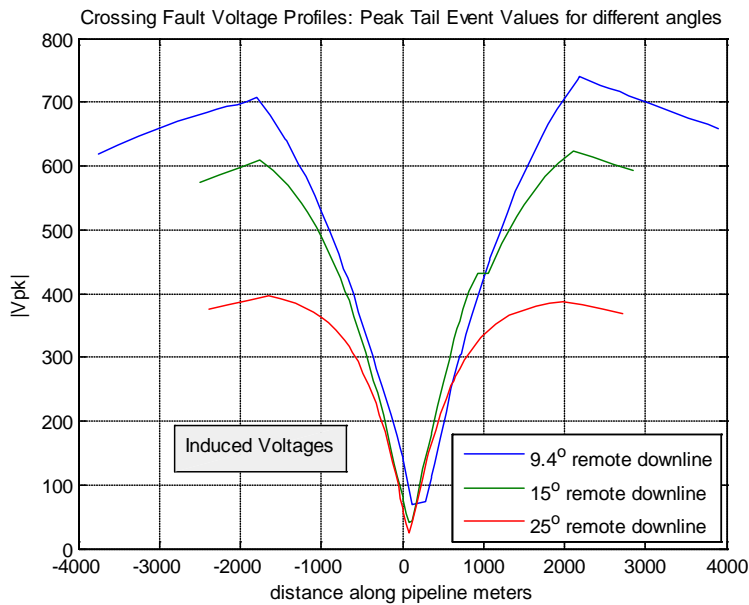


Figure 34 Peak tail voltages NPS 2.5 OD pipeline with different crossing angles

The shock hazard for the 25° crossing case is depicted in Figure 35. The specific fibrillation charge, F_q is calculated along the pipeline for the hand to feet touch voltage scenario. Except for pipeline location across from the faulted tower, $F_q < 2$ mC and the event is safe per IEC. Remote downline faults will cause $F_q > 2.0$ mC. Given the proximity to 2 mC, the 15° crossing case will exceed the limit value.

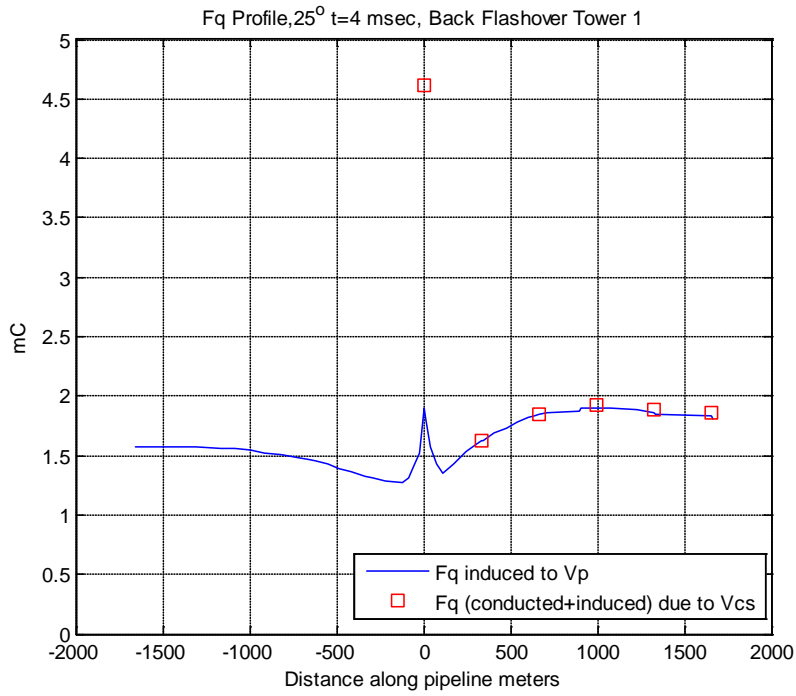


Figure 35 F_q (4 msec duration, hand to feet) profile along pipeline, 25° crossing for BF fault

7.4 Maximum Parallel for Shielding Failure Events

A shielding failure should lead to a larger ground current relative to the back flashover event. The ground current for back flashover failure is shown in Figure 36, and for the shielding failure is depicted in Figure 37.

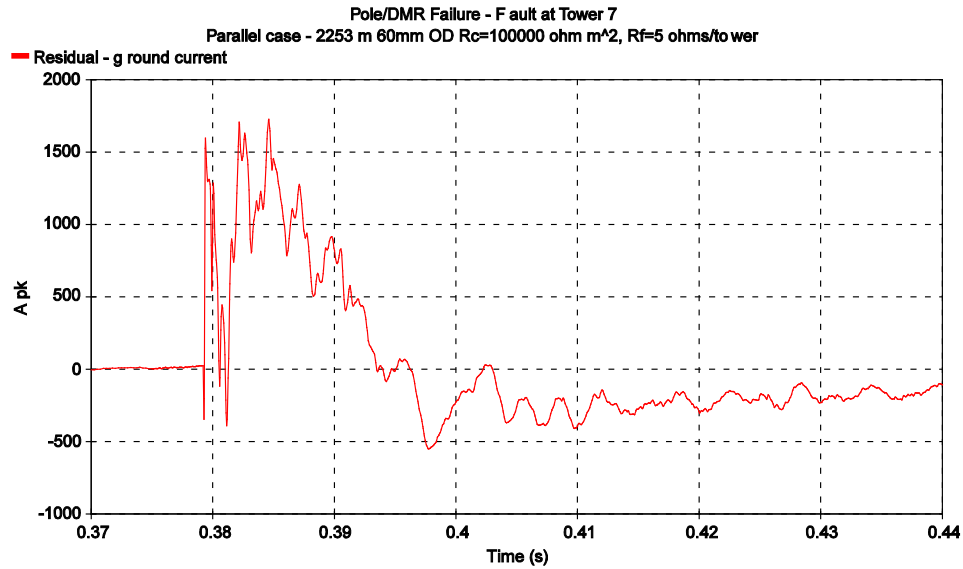


Figure 36 Ground Current at Rectifier - Back Flashover Event

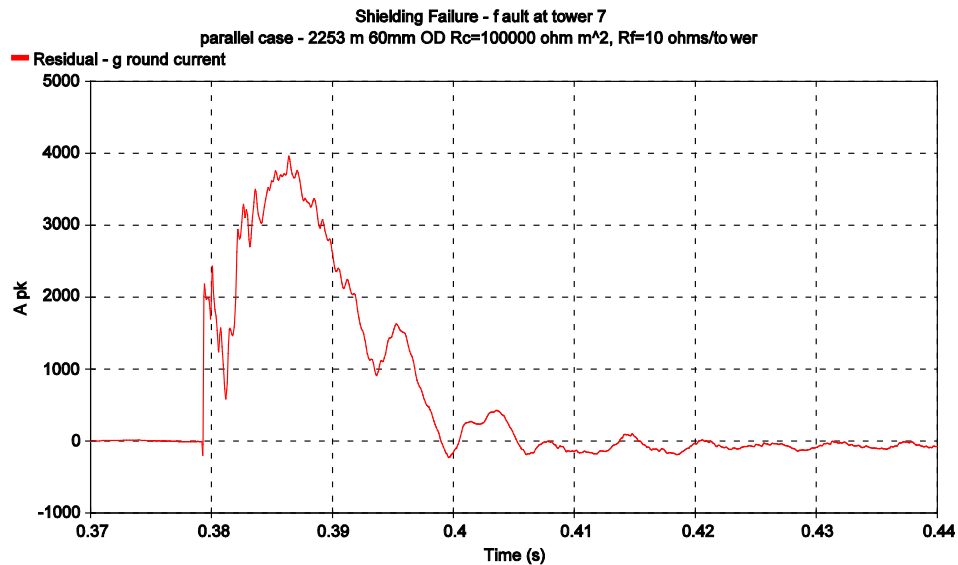


Figure 37 Ground Current at Rectifier - Shielding Failure

Of note the shielding failure current has less harmonic distortion, appearing more like a half cycle of 45 Hz AC fault current. Figure 37 should be compared to

Figure 5. The tower GPR waveform will have the same shape as the ground currents, assuming typical footing impedance of 5 ohms the different tower ground currents for the fault at Tower 7 are depicted in Figure 38.

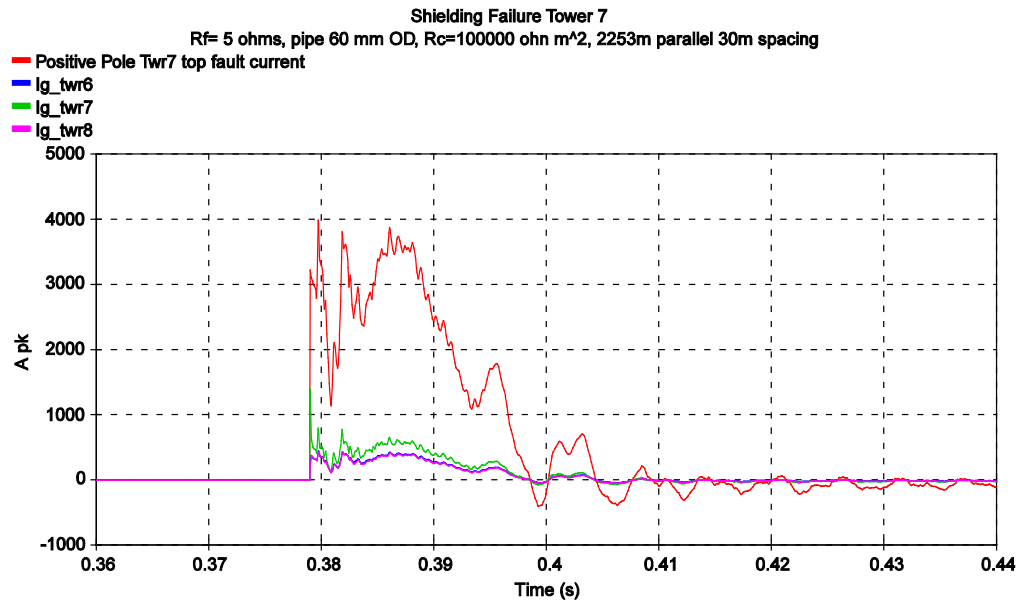


Figure 38 Tower Ground Currents - Shielding Failure

The low frequency component is discharged at multiple towers. Ignoring the initial current transient, shows only 17% if the fault current is discharged at the faulted tower with decreasing percentages at adjacent towers.

The worst case coating stress occurs when the fault is at the end of the parallel as shown in Figure 39. The lower NACE AC limit is also depicted.

The coating voltage across from Tower 1 is approximately the induced voltage. It depicts the geometric voltage rise as a function of parallel distance. Ignoring the transient voltages, there is a low frequency envelope that peaks at 940 Vpk.

The coating voltage across from tower 7 is an empirical estimate that assumes 25% of the GPR appears at the pipeline coating per the concrete caisson data provided by Figure 14. The coating stress, V_{cs} , becomes the difference between the conducted voltage, V_c and the induced voltage, V_p on the pipe as discussed in Section 4. The envelope voltage of V_{cs} is 1652 V pk which is less than the low NACE AC limit. The coating stress voltage across from the faulted tower as a function of parallel distance, x in km, where the faulted tower is at the end of the parallel, is given by:

$$V_{cs} = 0.451x + .636 \quad \text{kV pk}$$

The low NACE AC limit is reached at $x= 8$ km. The high NACE AC limit is more applicable to the extruded PE NPC 2.5 OD pipe assumed and would be reached at 14 km.

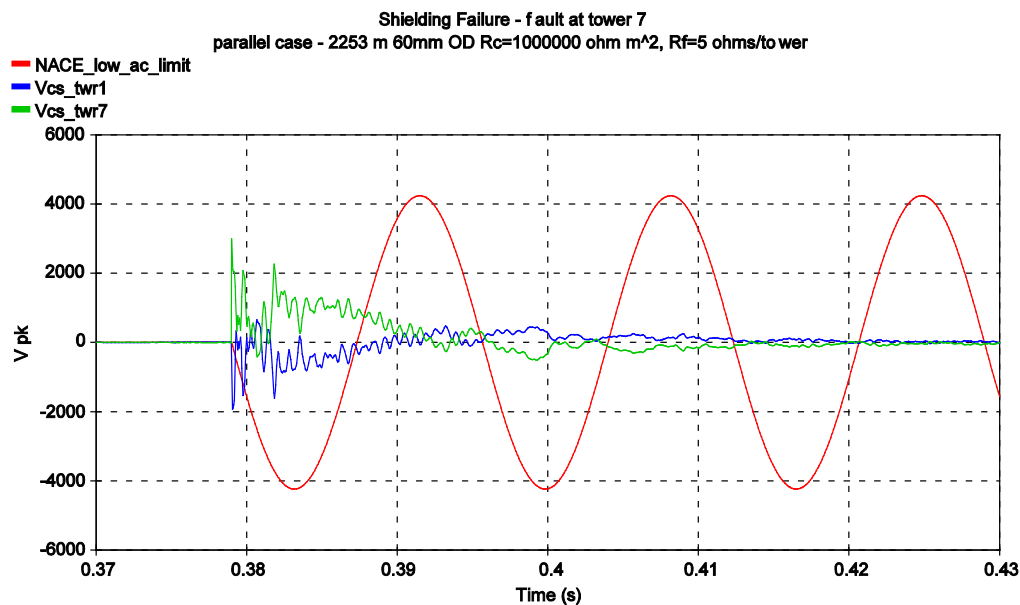


Figure 39 Coating Stress transient relative to low NACE AC limit

This result though expected to be conservative cannot be generalized since soil conditions vary from tower to tower and a more accurate calculation using SES CDEGS software is needed to verify the result for a particular location.

In general, for coating integrity with the lower frequency voltage envelope at any point along the pipeline, the inequality below applies:

$$|V_{cs}| = (|V_c| + |V_p|) < 4.25 \text{ or } 7.5 \text{ kV pk depending upon the type of coating}$$

Where V_c and V_p are maximum simultaneous values of the conducted and induced voltage envelope (ignoring the voltage transients) appearing on the pipe.

Figure 40 depicts the voltage profile along the pipeline with Tower 1 across from the pipeline at the origin and Tower 7 at a distance of 2.253 km from the origin. The curve “ $V_p > 2$ msec” is the maxima of the waveform beyond the first 2 msec from the start of the event. This voltage tends to overestimate the voltage envelope of the tail by including the 2nd transient oscillation shown in Figure 38 and in Figure 39.

The coating stress voltage tends to drop to the induced value 3 spans away from the faulted tower. Given a footing resistance of 5 ohms, a pole fault current of 4 kA pk, and assuming 20% of the pole current goes to ground at the faulted tower along with the 25% adjustment at the edge of the ROW, leads to a V_c value of 0.8 kV pk. This requires that $V_p < 3.45$ kV pk to stay within the lower NACE AC limit.

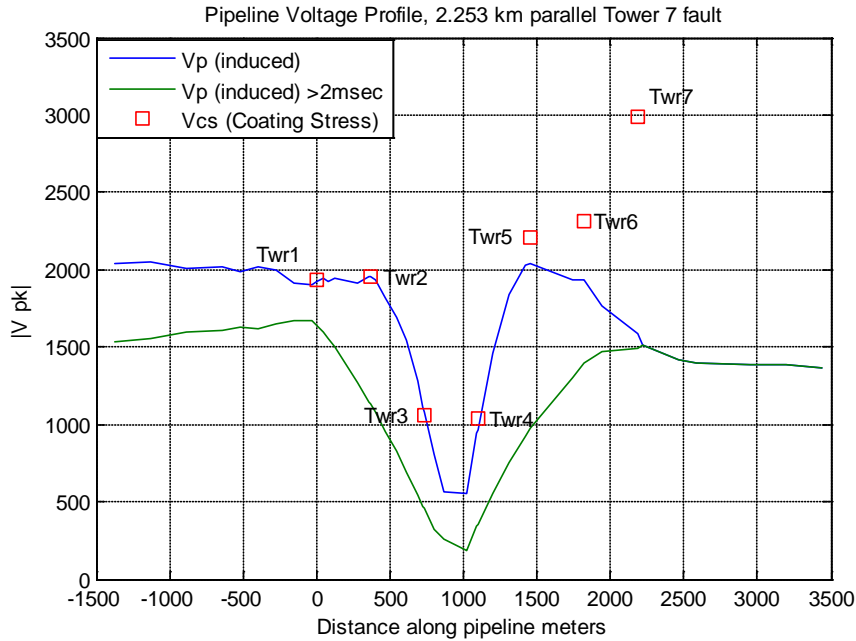


Figure 40 Pipeline voltage profile, Shielding Failure at Tower 7, 2253m parallel

In Figure 39 the initial impulse is less than the associated AC impulse limit (Table 6) of 7.5 kV pk, and beyond 1.5 cycles of the NACE AC withstand curve, the event is nearly over.

The worst initial transient voltage occurs on the pipeline directly across from Tower 3 if Tower 3 is the fault point as shown in Figure 41. The voltage peaks at 4.1 kV pk but is less than the low impulse withstand of 7.5 kV pk. For this location there is little induced voltage in the waveform i.e. $V_{cs} \sim V_c$.

At 3 or more tower spans away from the fault point $V_{cs} \sim V_p$.

The spatial decay of voltage beyond the parallel (beyond the induction zone) depends upon the initial voltage at either the start or end of the parallel and pipeline's characteristic attenuation length which depends also upon frequency. Due to dispersion, the high frequency components will decay more rapidly with distance. The decay equation is:

$$V_p(x) = V_A e^{-x/\gamma}$$

Where γ is the characteristic attenuation length and V_A is the starting voltage at start/end of the parallel (for this equation $x=0$ at either the start or end of the parallel).

Table 7 provides the attenuation length at different frequencies and coating resistances for NPS 2.5 pipe in this example. The initial high frequency transient decays quickly with distance dropping to 37% of its initial value at its

characteristic attenuation length. Since a very high coating resistance is assumed for this example the attenuation is small with distance. For larger pipe diameters the value of γ declines i.e. for NPS 24 with coating resistance of 50000 ohm m² and a frequency of 1300 Hz, $\gamma=3.9$ km.

Table 8 Attenuation Length, γ , in km for NPS 2.5 pipe

Frequency Hz	Coating Resistance Ohm m ²			Comment
	50000	10000	2000	
1300	7.42	3.81	1.27	Initial transient range
300	14.0	5.14	1.95	HVDC line natural frequency
50	20.8	8.27	3.6	Envelope

The worst shock hazard (hand to feet) tends to occur either at the start or end of the parallel as shown in Figure 42 where the measurement interval was standardized to 33 msec. For a ground fault at Tower 7, the shock current in RMS evaluated from the waveform is 0.845 Arms for a pipe location across from Tower 1, and 1.447 Arms across from the faulted Tower 7. Problems exist across from adjacent Tower 8 (not shown) due to symmetry with Tower 6. The IEC limit for this duration is 0.475 Arms suggesting the induced voltage exposure (since $V_{cs} \sim V_p$) for the 2.253 km parallel exceeds the safety limit across from Tower 1. The shock hazard across from the Towers 7, 6 and 8 exceed the safety limit but this result cannot be generalized since a specific hazard evaluation should entail using the SES CDEGS software. A rough estimate of the decay distance to reach the 0.5 A rms limit is 5.5 km based upon $\gamma=10$ km. What can be generalized is that the induced voltages for any remote downline fault from the parallel will lead to induced voltages of similar magnitude.

Table 9 shows the impact of parallel distance (at the 30 m spacing) with the maximum F_q and I_b values recorded based upon the induced voltage. A hand to feet current path is assumed. The critical parallel length for the parallel end fault is roughly 1 span of the HVDC line. The result is similar to the BF case when dealing with the F_q index. The critical length based upon event current, I_b , is 1 km in this example. The decay of F_q beyond the parallel will be similar to the exponential decay of V_p and can be approximated as follows:

Distance from start or end of parallel to decay to 2 mC:

$$3.5 L \text{ For } L < 2.5 \text{ km or } L + 6.25 \text{ if } L > 2.5 \text{ km}$$

Where L is the length of the parallel

Since Table 9 is based upon induced voltage only; any appurtenance within 100 meters of the faulted tower will also have a conducted component that will add to the F_q or I_b values.

Table 9 Shock Hazards (induced voltage) for SF events at different parallel lengths

Parallel Distance km	Remote fault Specific fibrillation charge F_q , mC	Remote fault I_b , Arms	Fault end of Parallel Specific fibrillation charge F_q , mC	Fault end of Parallel I_b , Arms
0.437	1.33	0.184	2.06	0.253
0.802	2.4	0.350	3.18	0.415
1.532	4.0	0.610	5.50	0.800
2.262	4.2	0.900	7.00	0.950

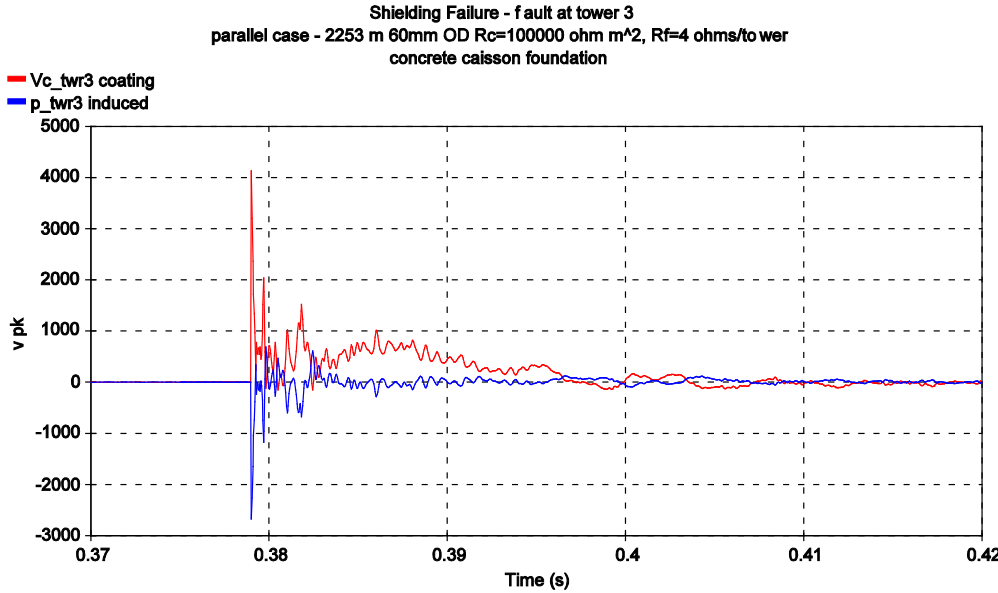


Figure 41 Impulse stress for a fault mid parallel

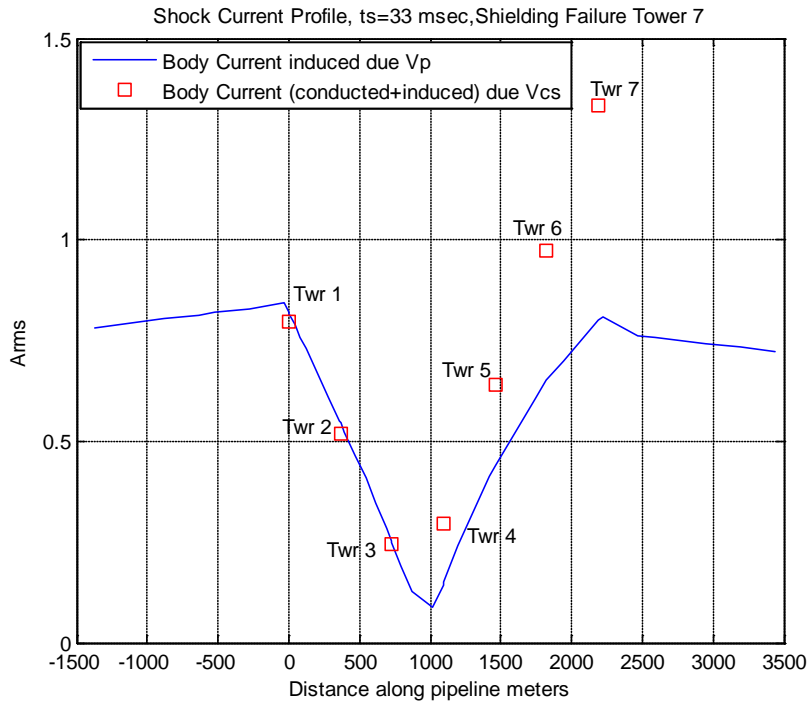


Figure 42 Shock Current profile (Total Event, hand to feet), t = 33 msec, Shielding Failure at Tower 7

7.5 Minimum Crossing Angles for Shielding Failure Events

In Figure 32 four different crossing angles are displayed. The GPR effects will be the most pronounced opposite the tower closest to the pipeline. The pipeline voltage profile for the 25° crossing case is shown in Figure 43 for a SF fault at Tower 1 (30 m spacing from the pipeline). A NPS 2.5 OD pipe with a PE coating is assumed with the same characteristics as was used in the back flashover case.

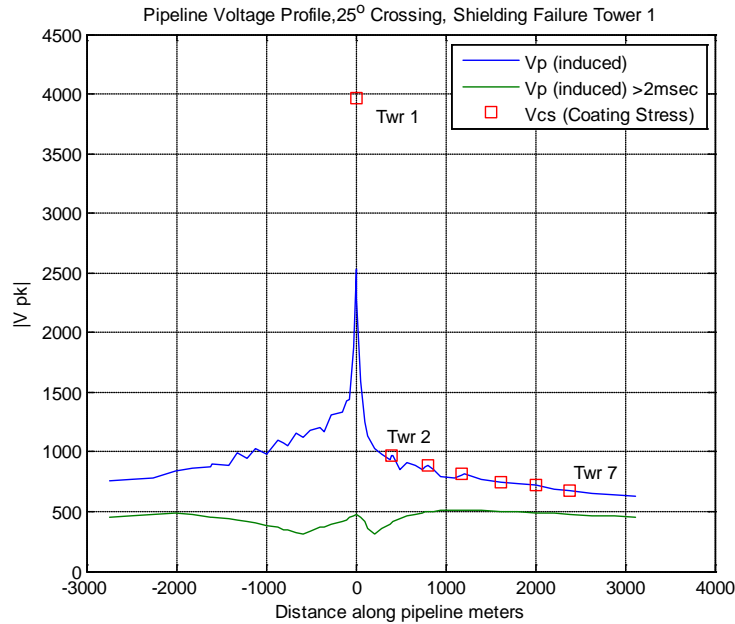


Figure 43 Voltage Profile along pipeline, fault at Tower 1 (origin), 25° crossing

The maximum instantaneous coating stress voltage V_{cs} occurs across from Tower 1 with a value of 4.0 kV pk similar to the parallel case but less than the low impulse withstand limit of 7.5 kV pk per Table 6. The coating stress voltages, V_{cs} , at the adjacent towers consist of only the induced voltage V_p . The induced tail voltage reaches its maximum value of 504 V pk near the start and end points of the crossing (at 1 km). The only location capable of supporting high instantaneous coating stress voltage is across from Tower 1. At other locations, instantaneous stresses are less than 1300 V pk and the envelope voltage is ≤ 504 V pk.

The coating stress waveform voltages at Towers 1 and 2 are shown in Figure 44. Ignoring the voltage transients, the envelope voltage has a peak value of 926 V pk for Tower 1 and 371 Vpk for Tower 2.

The inequality introduced in the last section is repeated below:

$$V_{cs} = (|V_c| + |V_p|) < 4.25 \text{ or } 7.5 \text{ kV pk depending upon the type of coating}$$

The V_c term only arises across from the faulted tower closest to the pipeline. At all other pipeline points (across from adjacent towers) V_c is effectively zero. The induced voltage can also peak, but due to the lower induction with a crossing, the above inequality is unlikely to be violated at other tower structures for this angle.

Figure 45 depicts ground current at towers 1 and 2. The footing resistance was 4 ohms in this crossing case.

Figure 46 depicts the voltage profile for a fault at Tower 2. The pipeline location across from Tower 1 displays both V_c and V_p components but both values are much reduced relative to Figure 43. Unlike the parallel case there is no hard limit

when induction ceases, it decays at a rate determined by the crossing angle. In this example the peak occurs at roughly 1 km from the crossing point. Of course end effects are more likely to create a hard limit.

The estimated total event shock currents are shown in Figure 47 for the Tower 1 fault. A violation of the safe limit only occurs across from Tower 1 based upon total event current. The measurement interval is 25.5 msec giving an IEC limit of 0.50 Arms. The safe shock limit is exceeded on the pipeline across from Tower 1 due to the conducted voltage. At all other locations the current is due to the induced voltage. Of note, the maximum induced currents arise remote from the crossing point, in this case at 1 km and decay only slowly with distance. For a fault at Tower 2, the maximum currents at 1 km exceed 0.50 Arms, mainly due to additional fault current coupling beyond the crossover point. An evaluation of the specific fibrillation charge, F_q , over the initial 4 msec interval is shown in Figure 47, $F_q > 2$ mC across from Tower 1 but also at the start and end of the crossing hence exceeding the IEC safe limit [12].

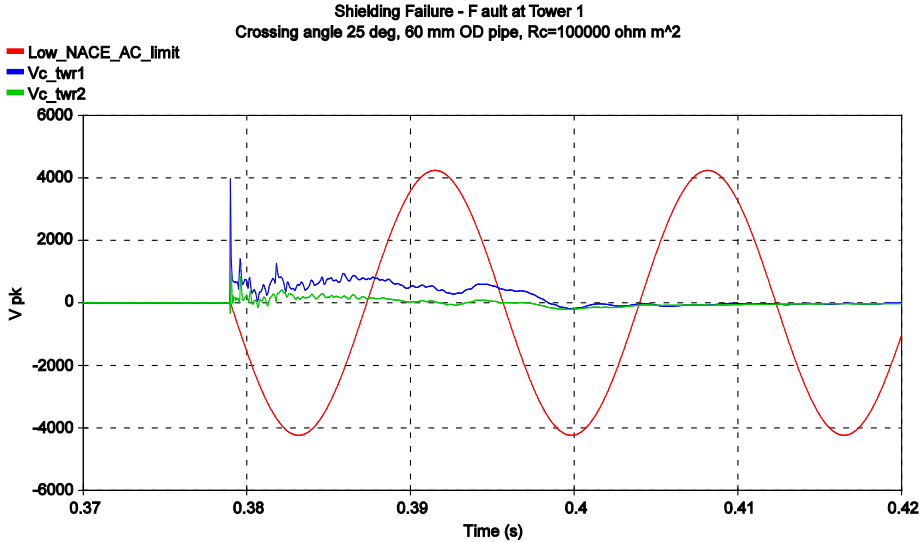


Figure 44 Coating Voltage Stress across from Towers 1&2

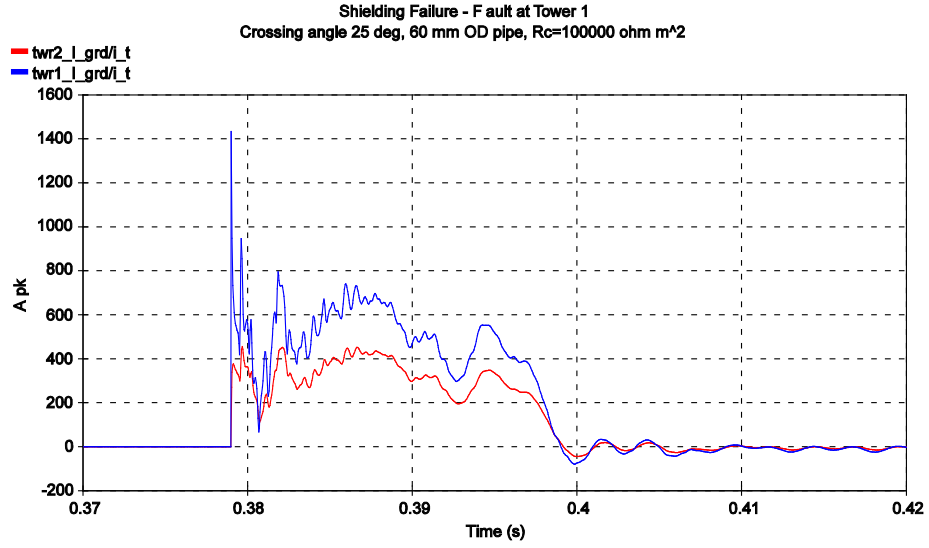


Figure 45 Tower Ground Currents Towers 1&2

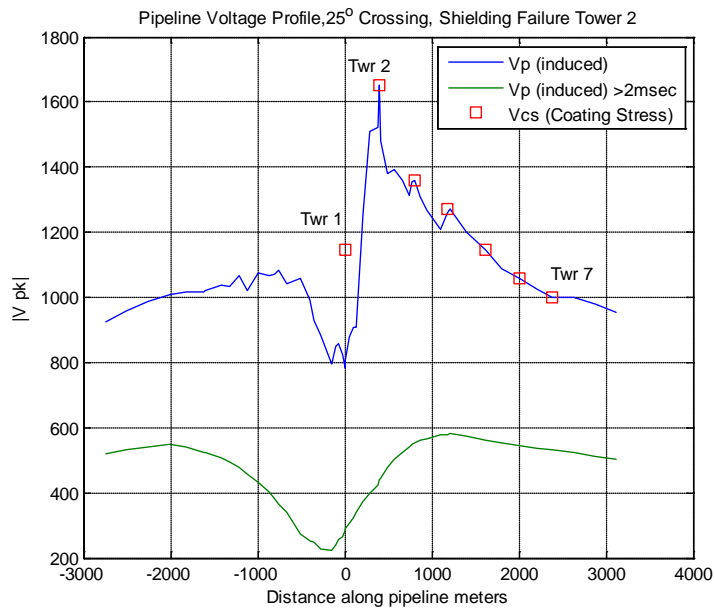


Figure 46 Voltage Profile along pipeline, fault at Tower 2, 25° crossing

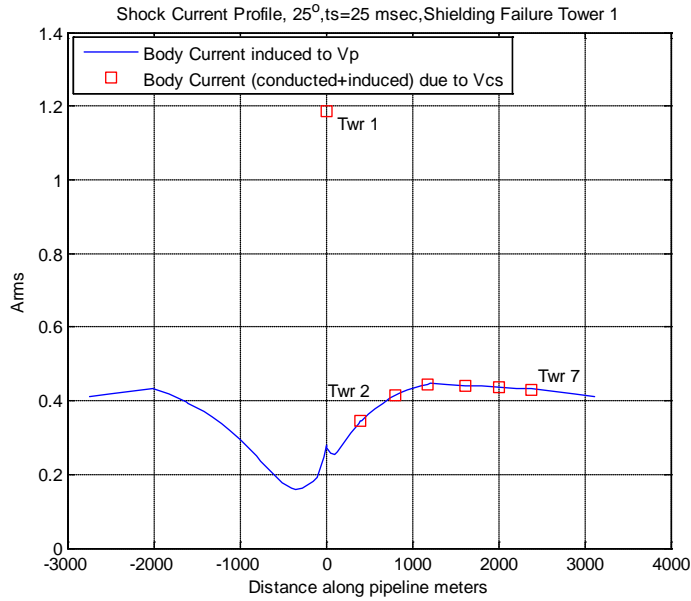


Figure 47 Total Event Shock Current (hand to feet) at different pipeline points, fault at Tower 1, 25° crossing

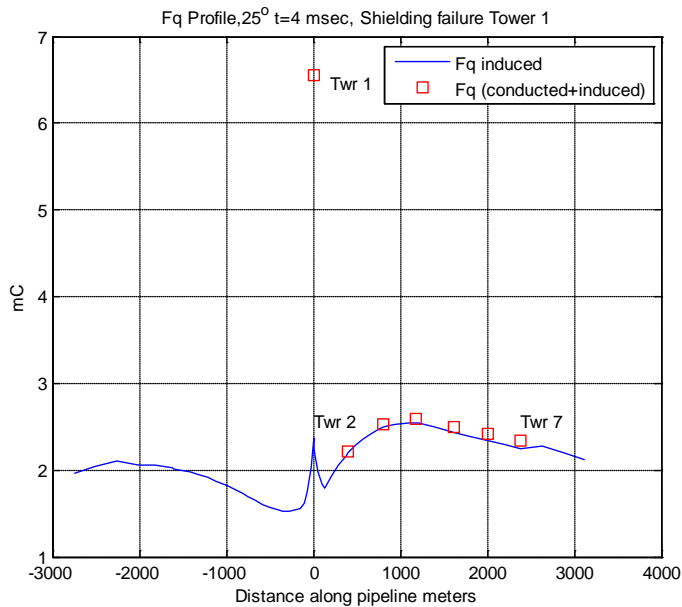


Figure 48 Specific fibrillating Charge, F_q , (hand to feet) at different pipeline points, fault at Tower 1, 25° crossing

The results for a shallower angle crossing of 15° are shown in Figure 49 for a fault at Tower 1. In this case, the perpendicular distance from the pipeline to Tower 2 is 68 meters. The peak transient coating voltage V_{cs} across from Tower 1 has increased due to an increase in the inductive component, V_p . This value is still much less than the lower impulse withstand limit. The tail voltage envelope

follows the induced voltage profile (>2 msec) away from Tower 1. Though not shown, the tail envelope for V_{cs} across from Tower 1 is 1500 Vpk. The result suggests for most practical crossing cases greater than 15° , the coating voltage stresses shouldn't be an issue.

In Figure 50 the estimated shock hazard is presented for the 15° crossing with the duration set at 27 msec. The IEC limit is 0.482 Arms. Across from Towers 1 to 5 a violation arises. Note the end effects (where pipeline orientation becomes perpendicular to power line) of the crossing limits the total event current rise but the current still exceeds the IEC limit. Spatial attenuation of V_p beyond the coupled distance will be same as for the parallel. For faults down line from the crossing where GPR effects are minimal the maximum specific fibrillating charge and body current due to V_p increase as shown in Table 10. Extrapolation places the minimum crossing angle at 30° .

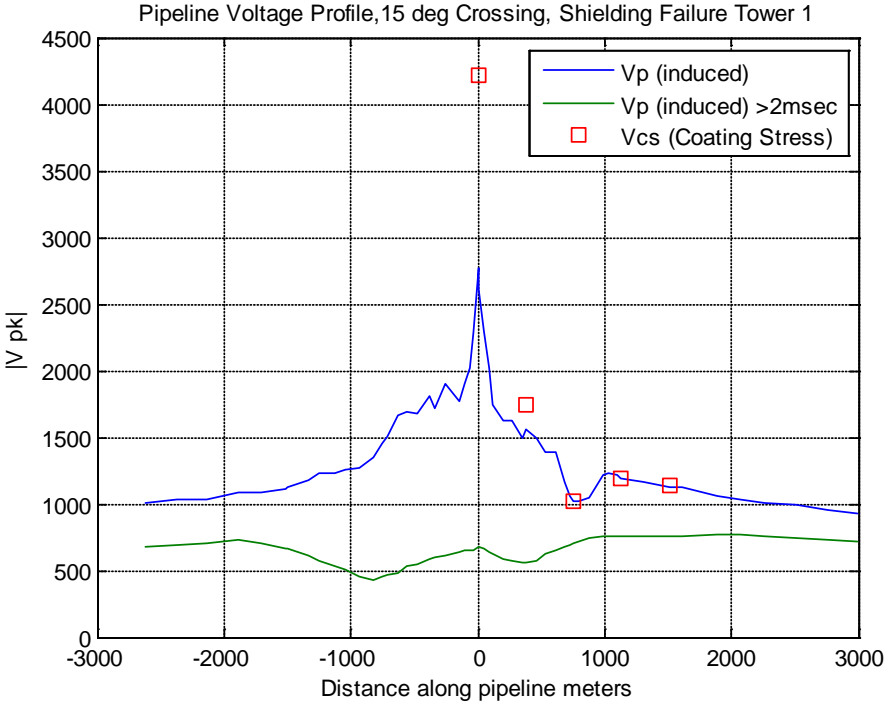


Figure 49 Voltage Profile along pipeline, fault at Tower 1, 15° crossing

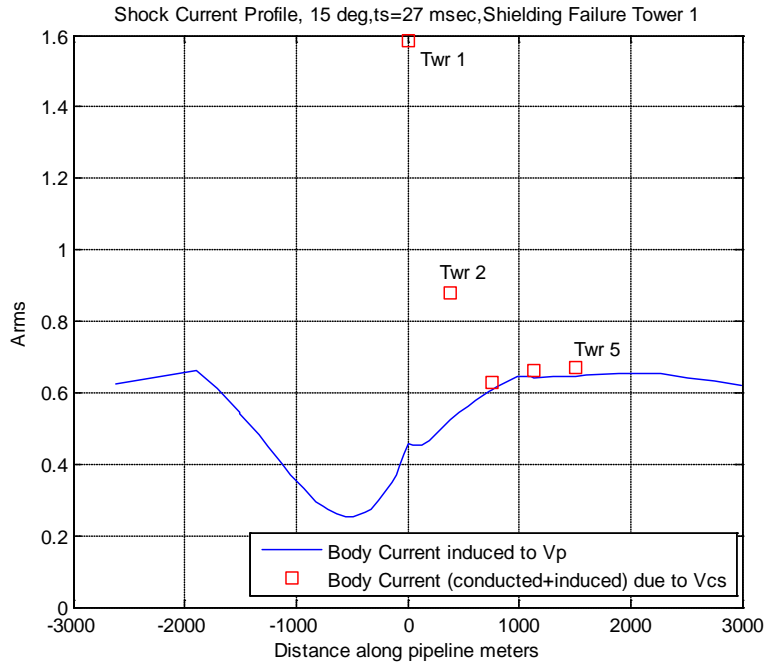


Figure 50 Total Event Shock Current (hand to feet) at different pipeline points, SF fault Tower1, 15° crossing

Table 10 Shock Hazards (induced voltage) for SF events at different crossing angles

Crossing Angle, degrees	Remote fault Specific fibrillation charge F_q , mC	Remote fault I_b , Arms	Fault at Tower 7 Specific fibrillation charge F_q , mC	Fault at Tower 7 I_b , Arms
15	4.76	1.17	6.20	1.21
25	3.19	0.79	4.36	0.81

7.6 Preliminary Guidelines

The following preliminary guidelines are presented to assist the user for pre-screening pipeline/HVDC line geometries, separating those presenting little risk from those requiring a detailed study (analysis) to determine the risk caused by the HVDC line under fault conditions. Since shielding failures lead to higher GPR conditions, this fault type forms the basis of this guide. There are two aspects that must be considered:

- Coating integrity
- Safety hazards

Each will be considered separately with safety hazards generally leading to more severe limits.

7.6.1 Coating Integrity

Soil resistivities and layering can have an impact on conductive effects and when in doubt a SES CDEGS (or an equivalent software package) study should be completed. From a screening perspective minimum 30 m spacing between the faulted tower and the pipeline is suggested when there is no significant inductive component. More experience with actual situations could lead to an even less restrictive spacing. The initial transient voltage due to the step change in fault current appears to be an issue only with smaller diameter pipes (NPS 2.5 OD and smaller). Even for these pipes, there appears to be sufficient impulse margins to suggest coating stress voltages are below the pipeline withstand (allowable) limit. This leaves only the tail (envelope) voltage for consideration and only the crest value of this envelope voltage is considered in this preliminary guideline.

In general:

1. If the pipeline intersects the HVDC power line ROW at an angle greater than 15° , and the pipeline at its closest approach is more than 30 meters from the nearest tower center²⁵, coating stress voltages should always be within allowable limits and no study is required. More experience with actual situations will refine this limit which is likely still too conservative.
2. If pipelines(s) parallel the HVDC line for less than 8.0 km with spacing's of more than 30 meters from the tower center line, coating stress voltage issues are unlikely.
3. Pipeline parallels and/or laterals and extensions to the pipeline that are never closer than 300 meters from the HVDC power line's ROW do not have to be considered for study. More experience with actual situations is expected to reduce the 300 m limit which is based upon AC mitigation standards [1].

The conclusions are summarized in

Table 11 and illustrated in Figure 51 and Figure 52 .

²⁵ For the tower design in Figure 3 this would be 25 meters from the tower leg (footing).

Table 11 Conditions leading to Coating Integrity Studies

Pipeline Spacing to closest towers	Less than 30 meters	Greater than 30 meters
Parallel with HVDC line (Figure 51)	any parallel length	Parallel > 8 km (at 30 meter spacing, allowable length increases with wider spacing)
Crossing the HVDC line (Figure 52)	any angle	Angle < 15°

Assumptions:

1. 100 ohm-m soil resistivity (uniform), see Sections, 3.2 and 4 for further information on impact of soil resistivity
2. Shielding failure mode (DMR not involved), see Sections 2.3 and 7.4 for more information on fault impact
3. Tower footing resistance of 5 ohms, see Section 7.1.3
4. NPS 2.5 OD pipe, coating resistance of 100,000 ohm m². See Sections 7.1.1 and 7.1.2 for discussions regarding impact of pipe diameter and coating resistance.

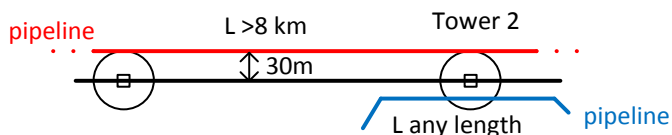


Figure 51 Parallel conditions leading to coating integrity studies

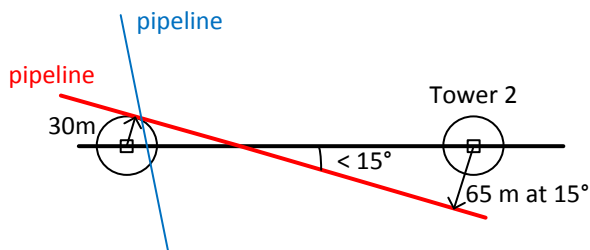


Figure 52 Crossing conditions leading to coating integrity studies

7.6.2 Safety Criteria

For a safety concern to arise there must be a point of human access (typically an appurtenance) on the pipeline. The current path hand to feet is assumed. Shock hazards can arise from:

- Conducted voltage only
- Conducted and induced voltage
- Induced voltage only

A **conducted voltage only scenario** arises when the above ground appurtenance is within zone of influence of the ground fault and there is very little induced voltage. The pipe would be at a near zero potential, and the shock would arise from the GPR at the pipe location. In Figure 14, the decay in GPR for the tower leg caisson case is relatively shallow. Using 450 ohms for body resistance and the total event IEC limit of 0.5 Arms the safe touch voltage would have to be less than 225 Vrms which corresponds to 8% of the GPR of the assumed study case. According to the study case this might exist after roughly 80 meters and for virtually all scenarios by 100 meters from the tower footing. While these results are considered reasonable, it will depend upon local soil conditions and only a SES CDEGS (or equivalent software package) study can produce more accurate results.

Conversely, an **induced voltage** can appear on the pipeline at locations relatively remote from the HVDC line. Remote faults downstream (further away from the rectifier terminal) from the parallel can lead to high induced voltages if the parallel is long enough at the minimum spacing with the HVDC line. The parallel would have to exceed 0.5 km (at 30 meter spacing) to create a safety hazard per IEC criteria. Induced voltages decay slowly with distance in the absence of continued induction. The attenuation length depends heavily upon the pipeline's electrical characteristics however the high magnitude, high frequency components in the initial transient would decay more quickly with distance.

It is much more difficult to generalize the result for crossing angles due to end effects. For induced voltage only scenarios no study is required for crossings with angles greater than 30°. With crossings, the induction decreases with distance away from crossing point. In the absence of end effects the induced voltage will peak and then decline. It is recommended that all appurtenances within L_m of the crossing point²⁶ be checked. L_m is based upon:

$$L_m = \frac{3}{\sin(\theta)} \text{ km}$$

Where θ is the crossing angle which should not be less than 9.4°

When **both conductive and inductive effects** are present a safety hazard assessment will likely be required.

²⁶ This assumes a high coating resistance (>50000 ohm m²) applies and issues have arisen due to the initial high frequency transient currents. More typical coating resistances would be in the 10000 ohm m² range, in which case a value of (2/3) L_m can be used.

Table 12 summarizes the guidelines where a radial limit of 100 meters is taken as the conducted voltage safety limit for the faulted tower. Spacing for parallel refers to the distance between the HVDC line's tower leg (footing) and pipeline. For a crossing, spacing refers to the closest approach distance between the pipeline and the HVDC line. An access point is an above-grade appurtenance. Figure 53 and Figure 54 illustrate the contents of Table 12.

Table 12 Conditions Leading to Safety Studies

Appurtenance Spacing from closest tower leg	Less than 100 meters	Greater than or equal to 100 meters
Parallel with HVDC Line (Figure 53)	any parallel length	Parallel greater than $L=0.5$ km (at 30 meter spacing to tower center line). A longer parallel length is needed if spacing increases, appurtenances within $3.5L$ if $L < 2.5$ km or $L+6.25$ for $L > 2.5$ km from the edge of the parallel
Crossing the HVDC Line (Figure 54)	any crossing angle	Crossing angle less than $\theta=30^\circ$ and appurtenances within $3/\sin(\theta)$ km along pipeline, either side of crossing point

Assumptions:

1. 100 ohm-m soil resistivity (uniform), see Sections, 3.2 and 4 for further information on impact of soil resistivity
2. Shielding failure mode (DMR not involved), see Sections 2.3 and 7.4 for more information on fault impact
3. Tower footing resistance of 4 ohms, see Section 7.1.3
4. NPS 2.5 OD pipe, coating resistance of 100,000 ohm m². See Sections 7.1.1 and 7.1.2 for discussions regarding impact of pipe diameter and coating resistance.
5. Hand to feet discharge path with $R_f=0$ (Section A.2), Section 4, Section 6.1
6. Attenuation length, $\gamma=6$ km Section 7.4
7. Maintaining specific fibrillation charge, $F_q < 2$ mC Section 6.1.2

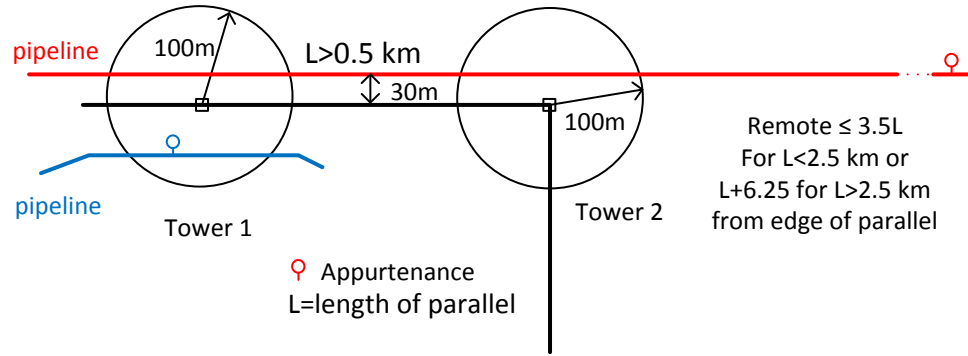


Figure 53 Parallel conditions leading to Safety Studies

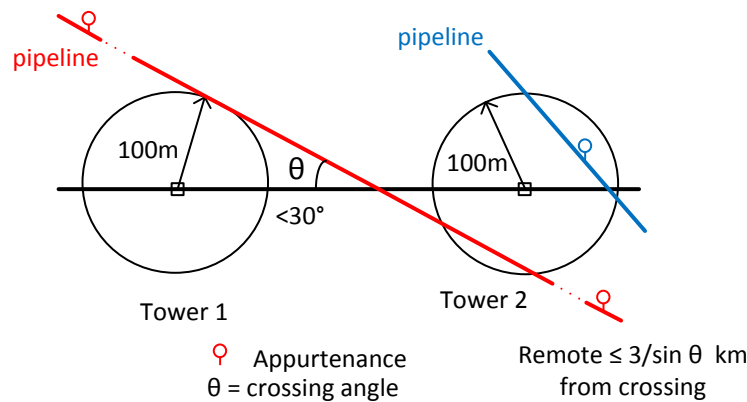


Figure 54 Crossing conditions leading to Safety Studies

7.6.3 Non-Metallic Pipelines with Tracer wires

Non-metallic pipelines falling within the safety screening guidelines do not require study however tracer wires buried with these pipelines represent a conductive path subject to induction issues that could potentially represent a safety issue. Rather than perform detailed studies it is recommended mitigation be applied directly to the tracer wires falling within the screening guideline.

If the non-metallic pipe has been installed with a tracer wire, one of two methods may be used to ensure safety from induced voltages on the tracer wire.

- If the tracer wire is terminated above grade, ensure it is terminated in a dead front style test post or enclosure.
- If the tracer wire is terminated below grade, ensure it is connected to an appropriately sized sacrificial anode to provide proper grounding of the tracer wire and to protect it against corrosion.

7.6.4 Examples HVDC/Pipeline Geometries

Some possible HVDC line/pipeline geometries with screening interpretations are presented in Figure 55. The first review may only look at coating integrity as the appurtenance locations may not be known. A second review, once appurtenance locations are known examines safety aspects.

Review of coating integrity:

In Figure 55(a), the approach angles are steep with a short parallel prior to crossing HVDC line with a closest approach of 60 meters to the tower, no study is needed. Figure 55(b) is similar except the tower to pipeline spacing is now 25 meters; a study should be undertaken due to conductive effects with outcome dependent upon the soil model in proximity to the tower.

Figure 55(c), presents a long parallel at 80 meter spacing which is tolerable, but the pipeline then crosses the HVDC line at a shallow angle, then remains underneath the line for 60 meters before veering south. It then comes close to the tower (35 m). Given the more complex geometry upon crossing, it isn't clear if a problem exists or not. A study is warranted.

Figure 55(d) represents a non-standard case that has not been studied. The wellhead sits in the GPR gradient about the tower. It is not coated, and an insulating flange electrically isolates it from the pipeline with a good coating. There is induction on the pipeline and GPR component at the insulating flange. In this scenario, the well head will disturb the GPR profile about the tower. Some mitigation is likely required across the insulating flange and a study is required.

Review of safety (shock hazard assessments):

In Figure 55(a) induction is not an issue but the 60 m spacing could be a problem if an appurtenance exists. Figure 55(b) would have similar issues

In Figure 55(c) there is both conduction and inductive effects near possibly both towers adjacent to the crossing point, and the last tower spacing to the pipeline. Figure 55(d) would pose similar concerns. There could be hand to hand, along with hand to feet safety issues with the insulating flange.

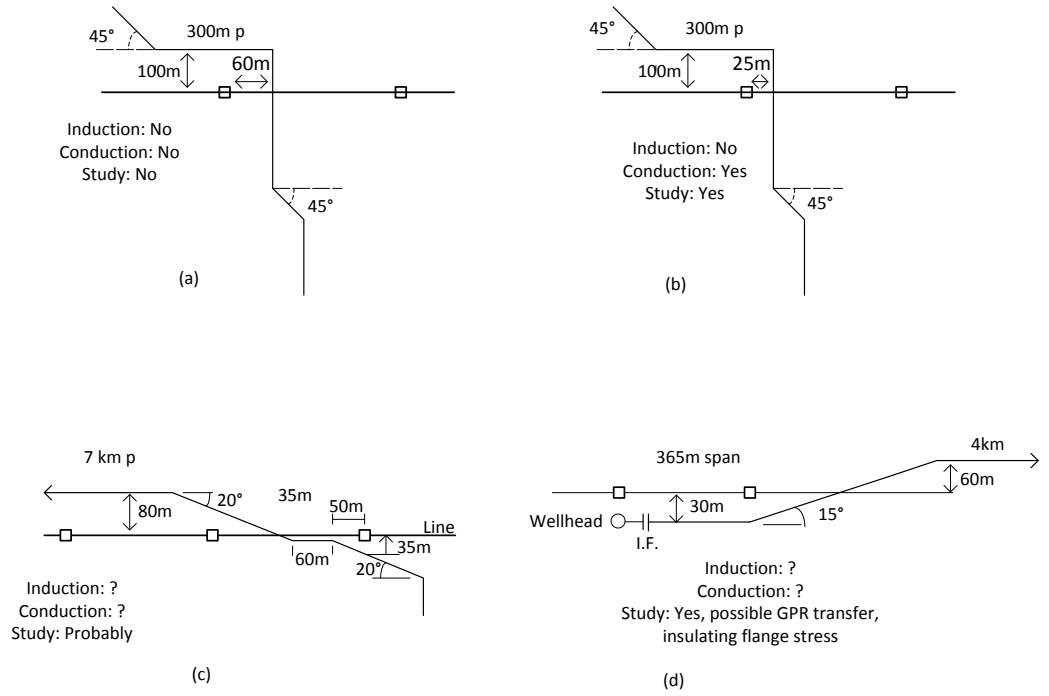


Figure 55 Possible pipeline/HVDC line geometries for considering coating integrity

8 Study Workflow

The suggested workflow for a pipeline/HVDC interaction study, assuming interaction scenario doesn't pass preliminary assessment (Section 7.6) is illustrated in Figure 56.

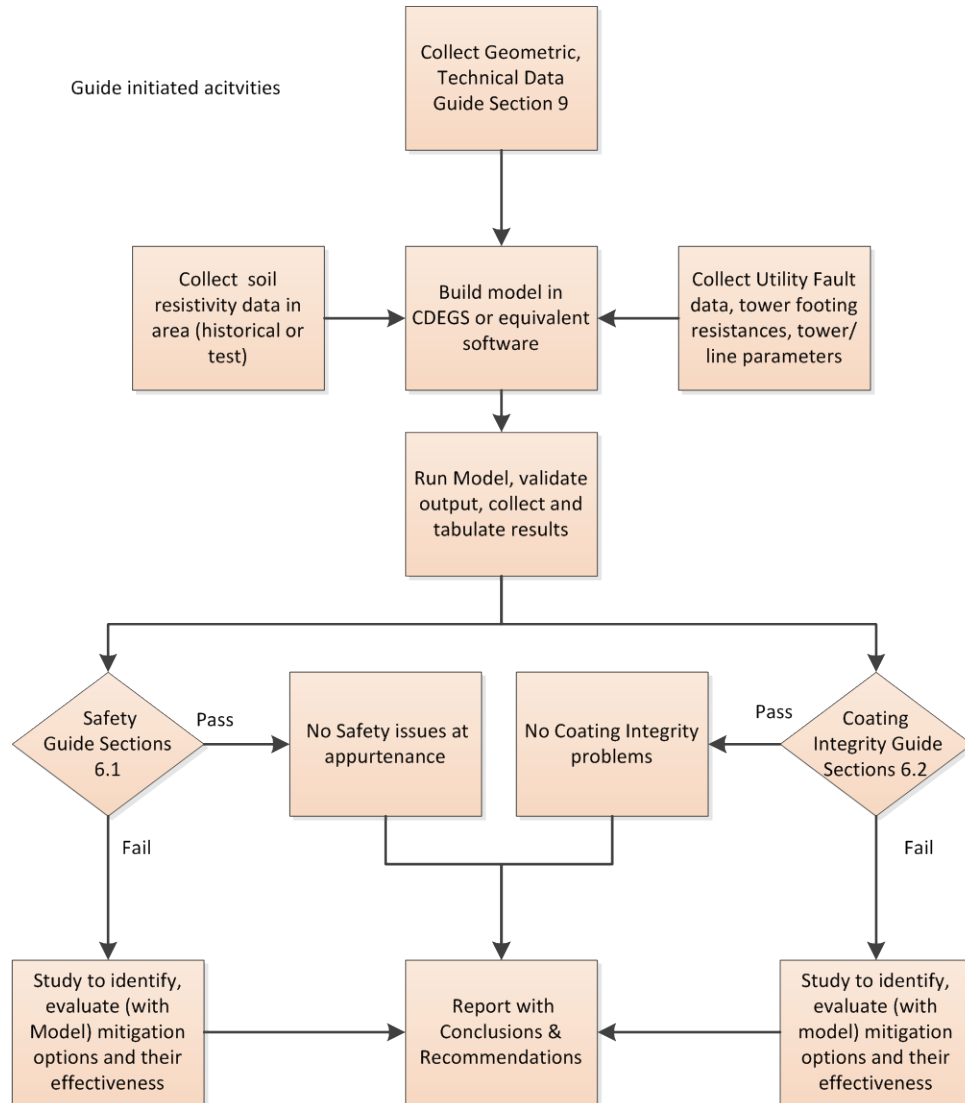


Figure 56 Study Workflow

Notes:

1. If there are no safety issues, coating integrity problems are unlikely
2. There must be an appurtenance for a safety issue to arise (Section 7.6.2)
3. Utility Fault type being considered should be clearly identified (Section 2.3).
4. Assumptions on coating quality (type, degradation with age etc.) should be clearly identified (Section 6.2).

9 Information Interchange

For a successful study and possible mitigation outcome key data have to be interchanged between the electrical utility, the pipeline owner and any consultant retained by either party for the work. The following is suggested in reference [1]'s Appendix and is modified slightly for HVDC line application and represents the minimum requirement.

9.1 Maps

A general location map of the area is required to establish the location accurately, plan and profile drawings showing construction details, including relative location of proposed facilities with respect to existing plant.

9.2 Technical Data Pipeline

1. Diameter of pipe
2. Wall thickness
3. Type of steel (or other metal i.e. aluminum if applicable)
4. Coating system (establish NACE fault withstand limits), thickness, type resistivity
5. Product transported
6. Pressure
7. Cathodic protection system
8. Location and type of appurtenances
9. Grounding facilities
10. Existing mitigation if any

9.3 HVDC line

1. Voltage is 500 kV dc monopole; ± 500 kV dc bipole
2. Load current 2000A dc present and immediate future (the line is capable of higher currents but no foreseeable plan to increase link loading)
3. Fault current magnitude and duration (will be similar to Figures 6 -8)
4. Structure dimensions and conductor assignment
5. Conductor data, pole and DMR, maximum sag
6. Shield wire data
7. Ground facilities, footing impedance if available for structures in vicinity
8. Corrosion control data
9. Fault recovery practices

9.4 Common Data

1. Soil resistivity profiles
2. Soil type
3. Future expansion
4. Mutual testing requirements

10 Safety during Installation of Pipelines

The safety measures suggested in [1] can also be followed during installation of pipe under or near a DC line. While the magnetic and electric fields associated with the HVDC line have less environmental influence than an AC line it is prudent to follow the same safety procedures. These safety procedures should include:

1. Any pipe section should be earthed via a low resistance electrode in the immediate vicinity of the workplace. New safety grounds should be made prior to breaking any point.
2. Insulating gloves should be used to avoid contact with metal
3. The HVDC tower should never be used for grounding the pipeline. The earth electrodes should be far enough away from the towers to preclude any coupling of the tower fault ground current to the installation area.

If the pipeline owner has safe work practices in place for AC lines, the same practices can apply to HVDC lines.

11 References

- [1] CAN/CSA -22.3 No. 6 – M91 (2013) “Principles and Practices of Electrical Coordination between Pipelines and Electric Supply lines”
- [2] CIGRE 95 “Guide on the Influence of High Voltage AC Power Systems on Metallic Pipelines” Working Group 36.02, 1995
- [3] “Environmental Characteristics of HVDC Overhead Transmission lines” L.A. Koshcheev, HVDC Transmission Institute, St. Petersburg, for Third International Workshop on Grid interconnection in North Eastern Asia
- [4] 2011 Annual Report “Forced Outage Performance of Transmission Equipment” Canadian Electricity Association - CEA
- [5] “Insulation Coordination of Power Systems” – A.R. Hileman, Marcel Dekker Press 1999
- [6] “Monte Carlo Simulation of Lightning strikes to the Nelson River HVDC Transmission lines” S.J. Shelmy, D.R. Swatek of Manitoba Hydro. Presented to IPST (International Conference on Power System Transients) 2001
- [7] “Step and Touch Potentials at Faulted Transmission Towers” E.A. Cherney, K.G. Ringler, N. Kolcio, G.K. Bell, IEEE Transactions on Power Apparatus and Systems, Vol. PAS -100No. 7, July 1981
- [8] “Lightning Surge Response of Ground Electrodes” William Chisholm, Wasyl Janischewsky, IEEE Transactions on Power Delivery, Vol. 4, No. 2 April 1989
- [9] IEEE 80-2000 “IEEE Guide for Safety in AC Substation Grounding”
- [10] “A Study of the Hazards of Impulse Currents” Charles F. Dalziel, AIEE October 1953
- [11] IEC 60479-1 2005-07 “Effects of current on human beings and livestock – Part 1: General Aspects”
- [12] IEC 60479-2 2005-07 “Effects of current on human beings and livestock – Part 2: Special Aspects”
- [13] ASTM G62 Standard Test Methods for Holiday Detection in Pipeline Coatings
- [14] “Pipeline AC Mitigation Misconceptions” R.A. Gummow, S.M. Segal, W. Fieltch – Coreng Consulting Service Company Ltd. A subsidiary of Corrosion Service Company Limited – Presented to NACE Northern Area Conference Feb 15 -18, 2010, Calgary AB
- [15] “Standard Handbook for Electrical Engineers – 10 Edition” Donald Fink, John Carroll – McGraw Hill 1969 Section 4 -301

Appendix A Supplementary

A.1 HVDC Tower Shielding Angle

The shielding angle for the HVDC tower is illustrated in Figure 57 along with the different arc paths for an impinging lightning stroke depicting successful shielding (potential back flashover event still possible) and shielding failure (Section 2.3).

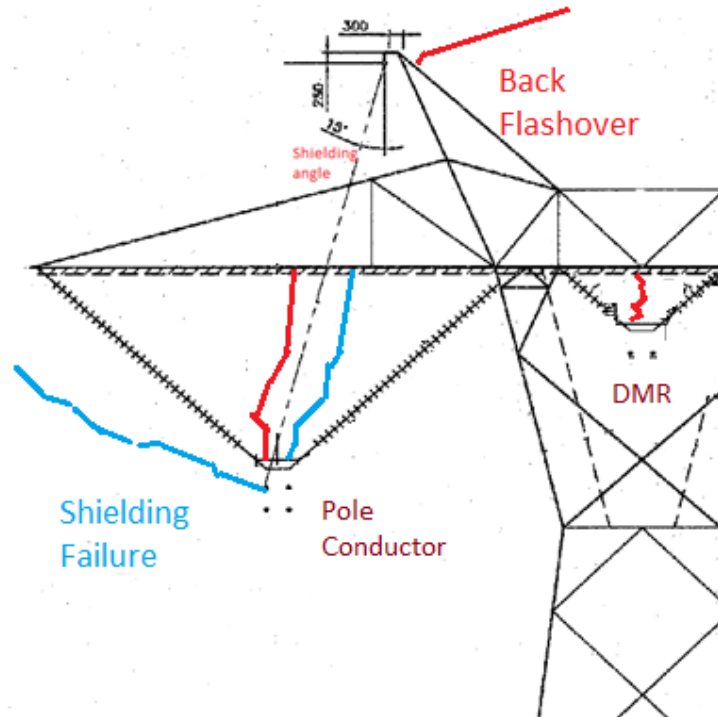


Figure 57 Shielding Angle HVDC Tower showing arc paths

Several electro-geometric theories have been developed by transmission line designers to estimate the minimum shielding angle needed to reduce the shielding failure rate to an acceptable level (including theoretically zero). Older more generally accepted theories are empirically based and tend to give reasonable results with AC lines.

To obtain perfect shielding (zero failures) the shielding angle for a particular line design will approach a certain minimum value depending upon the particular theory²⁷ adopted. The presence of trees along the ROW, being on top of hill or on its side, all affect the perfect shielding angle needed. In very exposed areas, a low angle of 10° may be suggested but both mechanical limitations and or line cost may become a limiting factor. Reference [5] may be consulted for more information on shielding design.

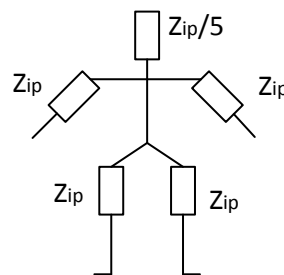
²⁷ Suggested by either IEEE or CIGRE

A.2 Background information Body Current Hazard Interpretation

A shock hazard evaluation consists of two components:

1. Determination of the appropriate body impedance, Z_T , based upon the body path and calculation of the body current with the appropriate touch voltage occurring at the extremities of body path.
2. Evaluation of the ventricular fibrillation hazard based upon the body path and application of Figure 19.

According to **Figure 12** [11] the variation in body impedance for applied voltage of 1000 V as a function of frequency varies little from 775 ohm at 50 Hz to 600 ohm at 2 kHz. The impedance of the skin layer is bypassed at 50 Hz due to voltage magnitude and the small decrease with frequency is likely due to capacitive effects. This value of Z_T applies to both the hand to hand, and the hand to foot paths and is predominantly the internal body impedance. The body impedance model that best fits this data is shown in **Figure 3** [11] and is reproduced in Figure 58.



Z_{ip} internal impedance of one extremity
(arm or leg)

Figure 58 Simplified diagram for internal impedances of the human body [11]

Of note in Figure 58, the hand to feet path impedance becomes 75% of Z_T or 450 ohms.

The most common body impedance paths explored are the hand to feet or hand to hand scenarios. To calculate the current in the impedance path selected, the appropriate voltage between the extremities must be selected, i.e. either the touch voltage for pipe to local ground (hand to feet) or pipe via an insulating flange to ground (hand to hand). With the resulting proper current for the path established, the 2nd evaluation component discussed above may be determined.

The ventricular fibrillation curves shown in Figure 19 apply only to the body path left hand to feet. For different pathways, **Section 5.9** [11] defines the heart-current factor, F to convert the calculated path current to its equivalent value based upon the left hand to feet curves. The equation is:

$$I_h = \frac{I_{ref}}{F}$$

Where I_{ref} is the body current for the path left hand to feet given in Figure 19

I_h is the body current for the path in question (**Table 12** in IEC 60479-1)

F is the heart-current factor (**Table 12** in IEC 60479-1)

Table 13 summarises some of the heart-current factor data from **Table 12**[11].

Table 13 Heart-Current factor F for different current paths (IEC 60479-1)

Current Path	Heart-current factor, F
Left hand to left foot, right foot or both feet	1.0
Both hands to both feet	1.0
Right hand to left foot, right foot or to both feet	0.8
Left hand to right hand	0.4
Chest to left hand	1.5
Left foot to right foot	0.04

As an example, $F=0.04$ for left foot to right foot path. If the hand to feet current was $I_{ref}=90$ mA, I_h would be 2250 mA. A foot to foot path requires a current of 2250 mA to have the same fibrillation effect as a 90 mA hand to feet current.

To clarify the overall evaluation process a few examples will be provided.

Example 1

A hypothetical body current for a nearby HVDC tower ground fault in proximity to a pipeline appurtenance is depicted in Figure 59 .

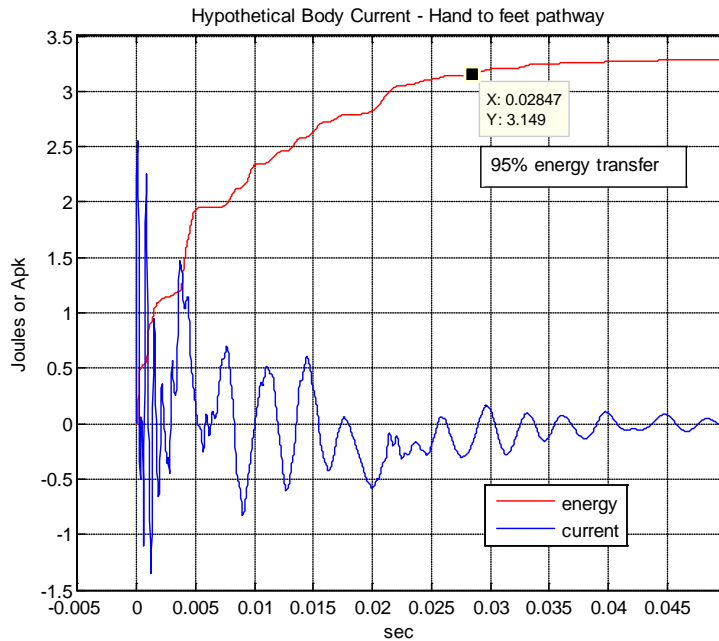


Figure 59 Hypothetical Body Current with $Z_T = 450$ ohms (hand to feet path)

In this example there is an impulsive peak followed by an oscillatory tail. The event's total duration is in the order of 40 msec. This waveform doesn't fall neatly into the IEC 60479 standard since it is the composite of two waveforms that are contiguous in time. It should be noted that some waveforms may not possess the shape depicted in Figure 59. There may be less of an impulsive peak and the overall response might appear more like a $\frac{1}{2}$ cycle low frequency sinusoid, a result expected for larger diameter pipelines.

Prior to considering the event analysis some additional definitions are required from IEC 60479 -2 for an impulse:

Shock duration of a capacitor discharge

t_i

Time interval from the beginning of the discharge to the time when the discharge current has fallen to 5% of its peak value (see **Figures 17 and 18**) [12]

Shock duration for complex asymptotic waveform

t_i

Shortest duration of that part of the impulse that contains 95% of the energy over the total duration of the impulse [12]

To be meaningful the whole signal must be treated when discussing energy transfer or charge transfer. The above definitions tend to apply to unidirectional (single polarity) signals and should be equivalent under the correct conditions. Implicit in the calculation is the assumption the person has established good contact with the appurtenance prior to initiation of the event. Establishing contact during the event would require a transient impedance model, **Figure 1**[11] that would account for skin breakdown (reduction of the contact resistance due to changes in contact area and breakdown voltage thresholds). Such a model is outside the scope of this guide.

Figure 19 illustrated the combined **Figure 20** [11,12] ventricular fibrillation curves for the time durations of significance for HVDC faults for the hand to feet discharge path. These fibrillation curves apply to men, women and children and are irrespective of age, weight and general health, and therefore conservative. There should be a considerable safety margin for a qualified adult worker outfitted with personal protective gear (i.e. safety boots, gloves, fire retardant overalls etc.).

It is important to emphasize the following note from IEC 60479-2 section 11.4.1 regarding the ventricular fibrillation curves:

“the specific fibrillating charge F_q or the specific fibrillating energy F_e determines the initiation of ventricular fibrillation of unidirectional impulses for shock durations shorter than 10 ms.”[12]

This is in contrast to event durations exceeding 10 msec where only RMS current magnitude and duration appear significant²⁸. It should be noted, however that for event durations less than 10 msec, the curve in Figure 19 is still calibrated in RMS current.

The total RMS current is calculated using:

$$I_{rms} = \sqrt{\int_0^{t_i} \frac{1}{t_i} i_b^2(t) dt} = \sqrt{\int_0^{t_i} \frac{1}{t_i} \frac{V_b^2(t)}{(Z_T + R_f)^2} dt}$$

The presence of foot resistance, R_f implies Z_T refers to the hand to foot or feet pathway. R_f is due to shoe and contact resistance at the soil interface and will be ignored in this simplified example but some grounding software will calculate and incorporate this value. The value of R_f can be significant and can be estimated using the following formula from [9]:

²⁸ Charge transfer for AC signals is meaningless but energy still holds but is difficult to apply and as such is not discussed in part 1 of IEC 60479 which deals with events > 10 msec. See Example 2 in section 11.4.2 of IEC 60479-2 which shows how a unidirectional impulse >10 msec in duration is dealt with.

$$R_f = \frac{\rho}{4b}$$

Where ρ is the earth resistivity in ohm-m and b is the radius of a metallic disk in contact with the earth surface. The typical value of b is set at 0.08 meters. If $\rho=100$ ohm meter, R_f for a single foot would be 312 ohms. For the hand to feet path, the feet resistance at the soil layer would be $\frac{1}{2}$ of this value or 156 ohms. If this resistance is included in the hand to feet path the sum becomes $450 + 156 = 606$ ohms (back to the 600 ohm value). The above formula assumes the top layer of soil is reasonably thick. If a thin layer of gravel is present, a de-rating due to a lower resistivity underlying layer is required. Under moist conditions ρ can be quite low in the 10 ohm-m range and the R_f correction is slight.

For the hand to hand current pathway R_f is deleted and the appropriate value of Z_T must be used. Any loading effect due to the body resistance upon the voltage waveform is also ignored.

If the absolute value of Figure 59 were plotted, and an exponential envelope is fitted, the duration of the event, t_i , could be estimated when the magnitude of the envelope falls to 5% of its initial value as shown in Figure 60.

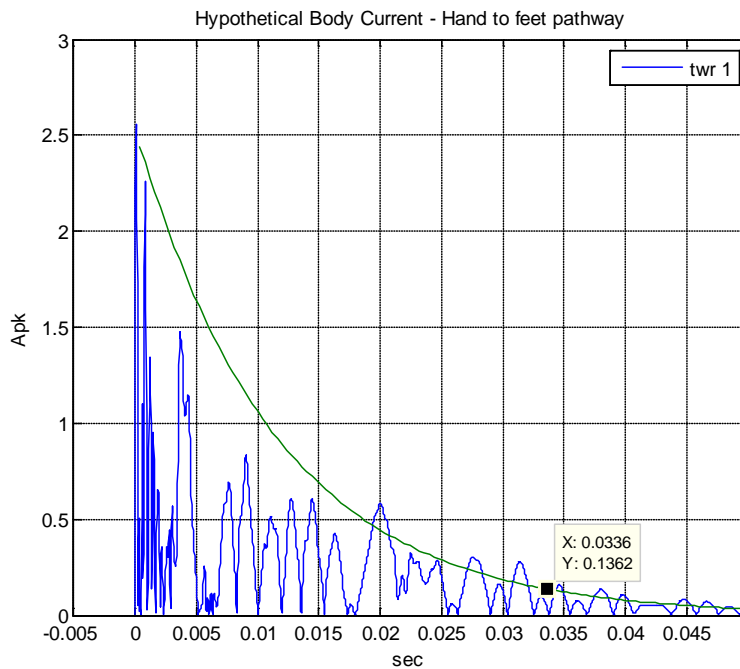


Figure 60 Exponential Envelope Construction

For most practical cases this event duration will exceed 20 msec and the IEC characteristic above 10 msec would apply to the waveform. There is some arbitrariness in selecting the decay envelope and the 95% energy transfer approach is more accurate. In this case, based upon energy, the duration would be 28.5 msec, where the event waveform deviates significantly from Figure 59 and

application of a single exponential decay curve is not meaningful i.e. those waveforms with little or no impulsive initial peak, the energy transfer approach is recommended.

The RMS value of current for the entire event is 0.457 Arms (based upon 33.6 msec duration) and while still marginally acceptable is close to the *c1* curve for events lasting longer than 10 msec.

The problem that arises is the initial severity of the impulse can be missed since it is averaged over the much longer total event interval. From the heart perspective if fibrillation occurs in the initial 10 msec time frame²⁹, the remainder of the event represents only additional energy being absorbed. In Figure 19, for durations less than or equal to 4 msec an energy transfer relationship exists³⁰. For duration of 4 msec the following safety criterion (specific fibrillating charge, F_q , or specific fibrillating energy, F_e per IEC 60479-2) should hold:

$$F_q = I_{crms} T < 0.002 \text{ A sec} \quad (2 \text{ mC}) \quad \text{Where } T = .004 \text{ sec}$$

$$F_e = I_{crms}^2 T < 0.001 \text{ A}^2 \text{ sec}$$

Where I_{crms} is RMS amperes calculated in the first 0.004 sec of the event:

$$I_{crms} = \sqrt{\int_0^T \frac{1}{T} i_b^2(t) dt}$$

Since the heart current factor, $F=1$ for this example:

$$F_q = I_{crms} T = (.9496)(.004) = 0.0038 \text{ A sec}$$

$$F_e = I_{crms}^2 T = (.9496)^2(.004) = 0.0036 \text{ A}^2 \text{ sec}$$

Since the F_q and F_e limits are exceeded a safety issue has arisen, note I_{crms} is close to the *c2* curve in Figure 19.

In summary for the event shown in Figure 59 analysis has shown it to be marginal when using the entire event waveform (very close to the *c1* curve). A detailed analysis of the initial impulse shows it to exceed the *c1* curve in the less than 10 msec region.

²⁹ Initial conditions are zero (no prior disturbance to heart function) and may also coincide with the vulnerable portion of the heart cycle

³⁰ Between 4 and 10 msec only a single RMS current value exists (0.5 Arms) a value of specific fibrillation charge transfer, F_q , of between 2 and 5 mC defines the *c1* curve depending upon duration. If the time limit were 10 msec in the integral, then the limit condition becomes <5 mC. For durations less than 4 msec, the appropriate F_q and F_e values must be derived from the *c1* curve. For other current paths, the heart-current factor must be applied.

Example 2

As a final example, the waveform in Figure 61 is more difficult to approximate with a simple exponential decay envelope. The energy transfer approach is illustrated. Figure 61 also depicts the associated energy transfer with a body resistance of 600 ohms. This could represent a hand to hand safety consideration.

In Figure 61, the 95% energy transfer limit sets the duration of the event at 21.6 msec. Based upon this duration the RMS event current is 0.504 Arms which slightly exceeds the IEC *cI* limit if a hand to feet current path existed but since a hand to hand pathway is assumed, the heart-current factor of 0.4 is applied:

$$FI_{rms} = I_{ref} = (0.4)(0.504) = 0.202 \text{ Arms}$$

So according to IEC, this hand to hand current is equivalent to the ventricular fibrillation risk associated with 0.202 Arms hand to feet current. In the first 4 msec the F_q value is:

$$FI_{crms}T = (0.4)(.7768)(0.004) = 0.00124 \text{ A sec}$$

After applying the heart-current factor, F , the specific fibrillation charge, F_q becomes 0.00124 C or 1.24 mC < 2 mC limit referred to Figure 19 curve.

In summary the event in Figure 61 would be considered safe for the hand to hand current pathway.

Assuming the pipe voltage to ground³¹ were the same as the touch voltage for the hand to hand case, the scenario for the hand to feet would be much worse. After correcting for the lower Z_T value of 450 ohms, the current would be increased by a factor of 1.333 and the heart-current factor of 1.0 would apply. The event would be unsafe on both total event RMS current and in the initial 4 msec interval. The F_q trajectory for this event is shown in Figure 62 where event duration is varied from 0 to 10 msec from the start of the event. Cross over of the IEC *cI* curve occurs at 2.75 msec. Note the 2 mC checkpoint at 4 msec for the IEC *cI* curve represents a local minimum.

³¹ At an appurtenance where the GPR is zero, with only an induced voltage on the pipe, the touch voltage pipe to ground would be the same as the touch voltage hand to hand across an insulating flange assuming the pipe section beyond the flange is at zero potential.

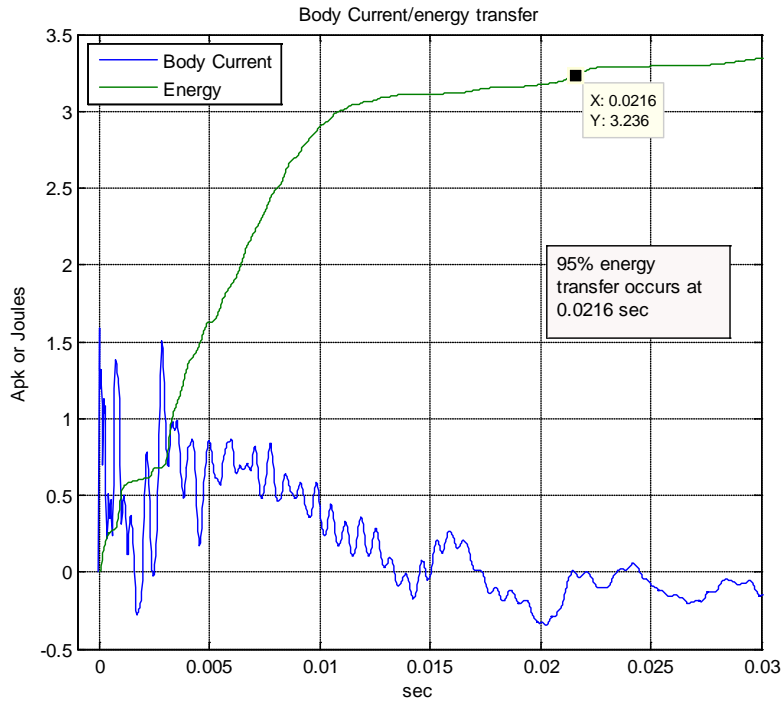


Figure 61 Body Current (hand to hand) with transferred energy

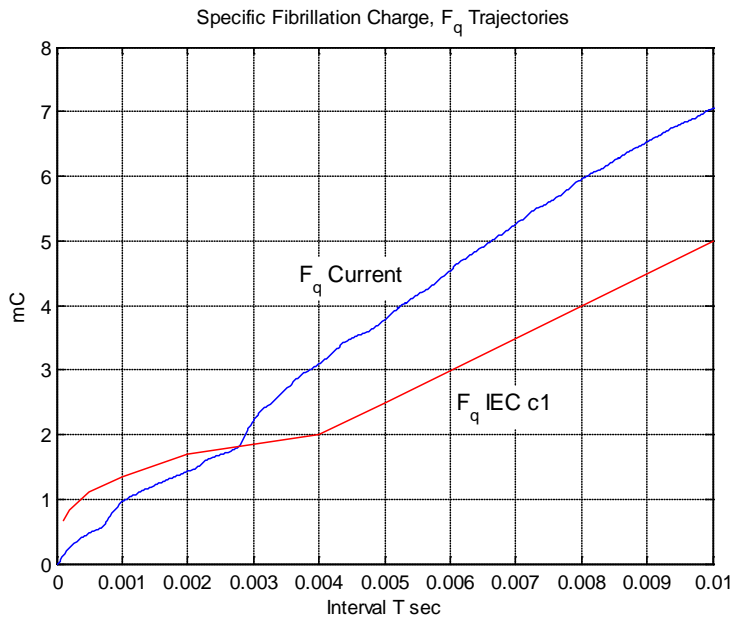


Figure 62 F_q trajectory for path hand to feet (Example 2)